Deciphering the mechanism(s) which limit reovirus spread in resistant lung and HNSCC cancer cells

by

Kevin James

A thesis submitted in partial fulfillment of the requirements for the degree of

Master of Science

in

Virology

Department of Medical Microbiology and Immunology
University of Alberta

ABSTRACT

Reovirus is a naturally benign virus that preferentially replicates in transformed cells and is currently undergoing clinical trials as a promising oncolytic therapy. In normal mouse fibroblasts, transformation by constitutively activated Ras oncogene is sufficient to promote reovirus infection. However, not all tumour cells containing Ras mutations are susceptible to reovirus, and clinical trials show mixed response to reovirus treatment. Accordingly, we aim to discover additional host-determinants important for conferring susceptibility to reovirus infection.

Our first objective was to identify tumorigenic cells that restrict reovirus infection. Reovirus primary infection (at 18 hours post-infection, hpi), and dissemination over two rounds of virus replication (48 hpi) was measured in a panel of lung (H1299, A549, H23, H522, H322) and head and neck (SCC9, A253) carcinoma cells using cell-based ELISA. A549, H322, A253, and SCC9 cells were 8-90 times less permissive to reovirus dissemination relative to highly susceptible H1299 cells. Differences in cell death were observed between cells, notably in H322 and A253 cells which released up to 100-fold less progeny virions within the first 24 hpi. However, it was determined that restricted virion release was not the sole determinant for reduced reovirus cell-cell spread. We next evaluated if antiviral innate signalling contributes a barrier to reovirus dissemination among less-susceptible cells. Multiplex ELISA and qRT-PCR analysis of cell culture media and cellular RNA from reovirus-infected cells showed high levels of IFN-β, IFN-λ, and TNF-α among resistant A549, H322, A253, and SCC9 cells. ShRNA-mediated knock-down of IRF3, IRF7, IFN Type I and III receptors, or IFN-β neutralization in A549 cells had no effect on reovirus dissemination, suggesting that these factors are singularly insufficient to confer resistance in these cells. It remains to be determined if Type I and III IFN responses act together to promote resistance to reovirus, or if alternative antiviral pathways are involved.

DEDICATION

"Once you eliminate the impossible, whatever remains,
no matter how improbable, must be the truth"

- Sir Arthur Conan Doyle

ACKNOWLEDGEMENTS

I would like to thank my supervisor Dr. Maya Shmulevitz for giving me the opportunity to work in her lab. She took on a student who was very curious and excited about translational cancer research but without much previously virology training, and the chance to learn it all from her was greatly appreciated by me.

I would also like to thank the members of my committee Dr. Rob Ingham and Dr. Mary Hitt for all their time over the years and all of the thoughtful suggestions, criticisms and support they have provided me.

I would like to thank my external examiner Dr. Jim Smiley and the chair of my defense Dr. Troy Baldwin for being a part of the process.

A thankyou must also go out to all the members of the Shmulevitz lab that I have shared space and science with over the course of my degree. Adil Mohammed for always being willing to help, late night chats about science that kept me from being too discouraged, and of course debates about optimal NFL Fantasy teams. Wan Kong who was great to share a lab bench bay with and always willing to lend a hand or just our catchphrase “science.” Heather for everything she does for the lab and for always having an ear to listen and something interesting to say. All of the undergrad students that were in the lab with me, but especially the original trio of Georgi Trifonov, Alicia Guenette, David Fast that I was lucky to become close with, and Patricia Chen as well for always being so positive.

I’d also like to acknowledge a few others I have met in the MMI department who made my stay more enjoyable, namely the friendships I enjoyed with fellow Gooner Chris Morcos, conference travel buddy Furkat Mukhtarov, and Lionel Jensen. I’d also like to single out former MMI student

Jenna Wilson for editing parts of my thesis, and helping me speed through crossword puzzles on lunch.

A final and important thankyou must go out to my family for their support during my degree. Hopefully you all missed me while I was halfway across the country and won't mind having me back, I definitely look forward to spending more time with you all.

TABLE OF CONTENTS

LIST OF TABLES

LIST OF FIGURES

LIST OF ABBREVIATIONS

BCIP	5-bromo-4-chloro-3-indolyl phosphate
BSA	bovine serum albumin
DMEM	Dulbecco's modified Eagle's medium
dsRNA	double-stranded RNA
EC50	effective concentration 50%
ECMV	encephalomyocarditis virus
ELISA	enzyme-linked immunosorbent assay
ERK	extracellular signal-regulated kinases
FBS	fetal bovine serum
GFP	green fluorescent protein
HMCV	human cytomegalovirus
HNSCC	Head and neck squamous cell carcinoma
hpi	hours post infection
hr (hrs)	hour (hours)
IFN	interferon
IFNAR	interferon-α/β receptor
IFNλR	interferon lambda receptor; aka. IFNλR1, IL28RA
IRF	interferon regulatory transcription factor
ISG	interferon stimulated gene
ISRE	interferon-sensitive response element
ISVP	infectious subviral particle
JAK	Janus kinase
JAM-A	junction adhesion molecule-A
JNK	c-jun N-terminal kinase
kDa	kiloDalton
MAPK	mitogen activated protein kinase
MEK	MAPK/ERK Kinase
MEM	minimum essential medium
min	minutes
MOI	multiplicity of infection
mRNA	messenger RNA
MV	measles virus
NBT	nitro-blue tetrazolium
NU	neutralizing units
OAS	2′-5′-oligo-adenylate-synthetase
PAMP	pathogen-associated molecular pattern
PBS	phosphate-buffered saline
PBST	PBS, 0.1% Triton X-100
PFU	plaque forming units
PKR	double-stranded RNA-activated protein kinase
PRR	pattern recognition receptor
qRT-PCR	quantitative reverse-transcription polymerase chain reaction
RIG-I	retinoic acid-inducible gene 1
RIPA	radioimmunoprecipitation assay buffer
RPM	revolutions per minute

RPMI	Roswell Park Memorial Institute medium
RT	room temperature
SDS-PAGE	sodium dodecyl sulfate polyacrylamide gel electrophoresis
shRNA	short hairpin RNA
STAT	signal transducer and activator of transcription
TBST	Tris buffered saline, 0.1% Tween 20
TCID	tissue culture infectious dose
TNF	tumour necrosis factor
TRAF	TNF receptor-associated factor
TRAIL	TNF-related apoptosis-inducing ligand
TYK-2	non-receptor tyrosine-protein kinase 2
VSV	vesicular stomatitis virus

CHAPTER 1: INTRODUCTION

1. Reovirus Background

1.1. Discovery, Classification and Structure

Mammalian Reovirus belongs to the *Reoviridae* family, which is comprised of 9 different genera. Four of these genera (Orthoreoviruses, Orbiviruses, Coltiviruses and Rotaviruses) can infect humans and mammals, another 4 genera infect plants and insects, and the remaining genus infects fish. Naturally, members of the family share similar characteristics in morphology, genome composition and replication. *Reoviridae* are defined by their non-enveloped, icosahedral shape and two protein shells that surround a segmented dsRNA genome either 10, 11, or 12 genes in size.[1]

The mammalian orthoreovirus (commonly referred to as reovirus) has an inner protein shell or core that measures 60nm in diameter, and an outer protein shell or capsid measuring 81nm in diameter.[1] The genome is divided into 10 different segments, which are grouped according to their large (L1, L2, L3), medium (M1, M2, M3), or small size (S1, S2, S3, S4) when separated by gel electrophoresis (see **Figure 1.1.1**).[2] However, these 10 genes code for 11 proteins because the S1 components of the mature virion, while the other 3 proteins are non-structural in nature. The non-structural proteins are μNS, σNS, and σ1s, corresponding to the M1, S3, and S1 genes respectively.[4] They reside in the cytoplasm of infected cells and assist in infection but are not part of the mature virion that is packaged and released from host cells.

Reovirus was first isolated in 1951 from human respiratory and enteric tracts, but it was originally misidentified as a variant of echovirus belonging to the *Picornaviridae* family before being re-classified in 1959.[5] It was later deduced that there are 3 distinct serotypes of reovirus; Type 1 Lang (T1L), Type 2 Jones (T2J), and Type 3 Dearing (T3D). T1L was isolated from the

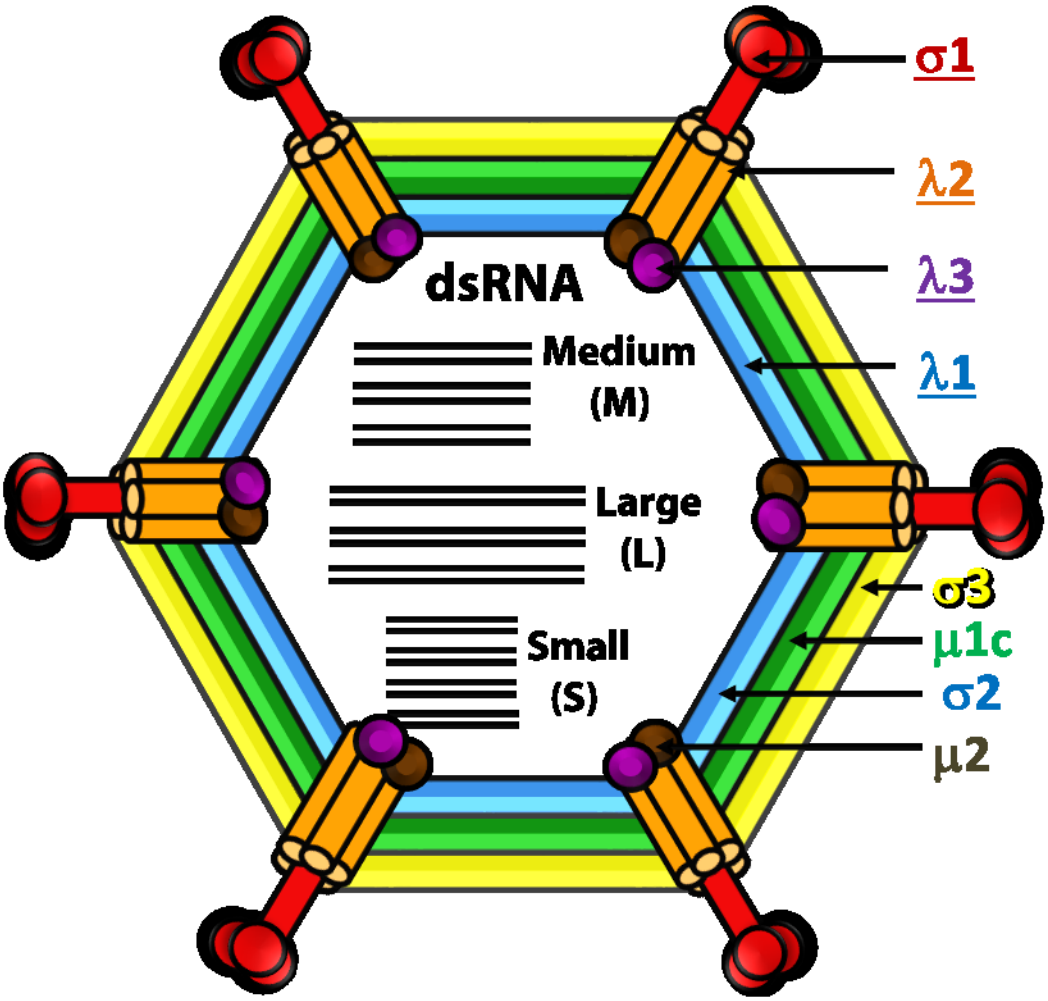

Figure 1.1.1. Reovirus Structure. Mammalian reovirus is dsRNA virus, with genome divided by size into 10 different segments (4 small, 3 medium, 3 large). Reovirus is a non-enveloped virus with a dual protein shell making up an outer capsid and an inner core. (Figure courtesy of Dr. Shmulevitz)

rectal swab of a healthy child, while both T2J and T3D strains were isolated from children with diarrheal ailments.[5, 6] These serotypes are morphologically similar, but they can be differentiated via antibody neutralization assays and hemagglutination inhibition tests as described by Rosen and others.[7, 8, 9] Each serotype has differences in viral spread and affects host cell tropisms in different ways. For example, T1L reovirus has little effect on cellular RNA and protein synthesis, T2J reovirus rapidly inhibits host cell synthesis, and the T3D serotype displays and intermediate phenotype restricting host synthesis later in infection compared to T2J.[10] The reovirus serotype in the Shmulevitz lab, and thus used for this project, was the Type 3 Dearing strain.

1.2. Pathogenesis and Replication

The etymology of "reovirus" has roots in its perception as a benign virus to humans and its isolation from the respiratory and enteric tracts. Reovirus is therefore an acronym for *R*espiratory *E*nteric *O*rphan virus, with the orphan designation referring to the lack of association of infection with the clinical presentation of symptoms.[5] In one study, 27 adult male volunteers were divided into 3 groups of 9 and infected with either reovirus serotype 1, 2, or 3 by intranasal inoculation.[11] Reovirus was recovered from the subjects by isolation from anal swabs, but only 4 of 27, or 15% reported signs of any clinical illness. Symptoms were those associated with the common cold, such as headache, sneezing, cough and malaise. In a larger study, 37% of 185 patients infected with nasal secretions containing reovirus isolated from a patient contracted symptoms matching the common cold.[12] However, patients infected with the same strain of reovirus sourced from cell culture reported no symptoms. A rise in antibodies against reovirus was detected in similar amounts of subjects treated with infectious nasal secretions and those with reovirus from culture, and also between those who developed symptoms and those who did not. Thus it was proven reovirus could infect the volunteers but no link to causation of any clinical illness could be

established. Despite the relatively non-pathogenic nature of reovirus, it is ubiquitous in nature and the prevalence of detectable anti-reovirus antibody serum titers increases in an age dependent manner from early childhood to 5-6 years of age.[13, 14] By adulthood there is a widespread reovirus seropositivity of up to 100%.[15]

As a non-enveloped virus, reovirus is unable to gain entry into host cells via membrane fusion and instead must disrupt the limiting cellular or endosomal membrane to pass into the cell.[16] This is usually accomplished through stimuli such as receptor interactions, low pH and proteases.[17] Reovirus cell-entry has been characterized in detail in L929 mouse fibroblast cells by various groups. First the virion attaches to the junctional adhesion molecule A (JAM-A) receptor, before interacting with the β_1 integrins on the cell surface and uptake through clathrin-mediated endocytosis, or caveolae-mediated endocytosis.[18, 19, 20] Some reovirus strains such as T1L and T3D have also been shown to bind to the sialic acid cellular receptor in addition to JAM-A, enhancing the strength of binding.[21, 22] Once the virion is inside the endosome, enzymes remove the σ3 outer capsid protein converting it into an infectious subviral particle (ISVP).[23, 24] ISVP formation was thought to be dependent on an acidic environment to enable activity of proteases such as cathepsins B and L, although acid-independent infection has been proven possible due to the activity of cathepsin S in more neutral and slightly alkaline environments.[24, 25, 26] During infection by the oral route pancreatic serine proteases remove the capsid in the intestine, and during oncolytic therapy ISVPs can be formed extracellularly as the tumour microenvironment is typically high in proteases.[27, 28, 29, 30] ISVPs then undergo cleavage of the exposed μ1 protein which is capable of penetrating both surface and endosomal membranes.[31] Once into the cytoplasm, the exposed reovirus cores remain intact to conceal virus dsRNA from the host as core proteins internally synthesize and cap viral mRNAs. These mRNAs are subsequently released through λ2 channels

in the core exposed by the release of the σ1 protein.[32] Translation of the viral mRNAs takes advantage of the host's protein synthesis machinery which is gradually taken over.[33, 34] Viral proteins assemble into new cores which amplify the replication process, until mature reovirus virions are assembled with the addition of capsid proteins. Progeny virions are then released by lysis or apoptosis.[35] See **Figure 1.2.1** for an overview of the reovirus replication process.

2. Reovirus as an Oncolytic Therapeutic

2.1. Discovery of Oncolytic Properties

Initial observations of the oncolytic potential of reovirus occurred many decades ago when Bennette isolated a strain of Type 3 reovirus that was destroying ascites tumours in mice.[36, 37] Hashiro *et al.* then determined that transformed mouse cells were more susceptible to reovirus cytotoxicity than primary mouse cells, or normal human and primate cells, amongst other examples.[38] Duncan *et al.* provided further evidence when T3D reovirus was found to exert cytopathic effects and greater infection in SV-40 transformed human fibroblast cells than on the same WI-38 cells that had not been transformed. The un-transformed cells were still productively infected with reovirus but exhibited no cytopathological effects.[39] However, the underlying mechanism(s) leading to the greater susceptibility of transformed cells was still not very well understood at this time.

Major progress on this front was made in the 1990s in the lab of Dr. Patrick Lee when the aberrant signalling pathways of the transformed cells were investigated. Strong *et al.* observed that mouse cell lines that did not express the epidermal growth factor (EGFR) receptor were relatively resistant to reovirus, but when EGFR constructs were transfected into the cells they became reovirus-sensitive.[40] When normal mouse fibroblast NIH3T3 cells, which are not permissive to reovirus infection, were transformed with the v-erbB oncogene (a close homolog to EGFR lacking

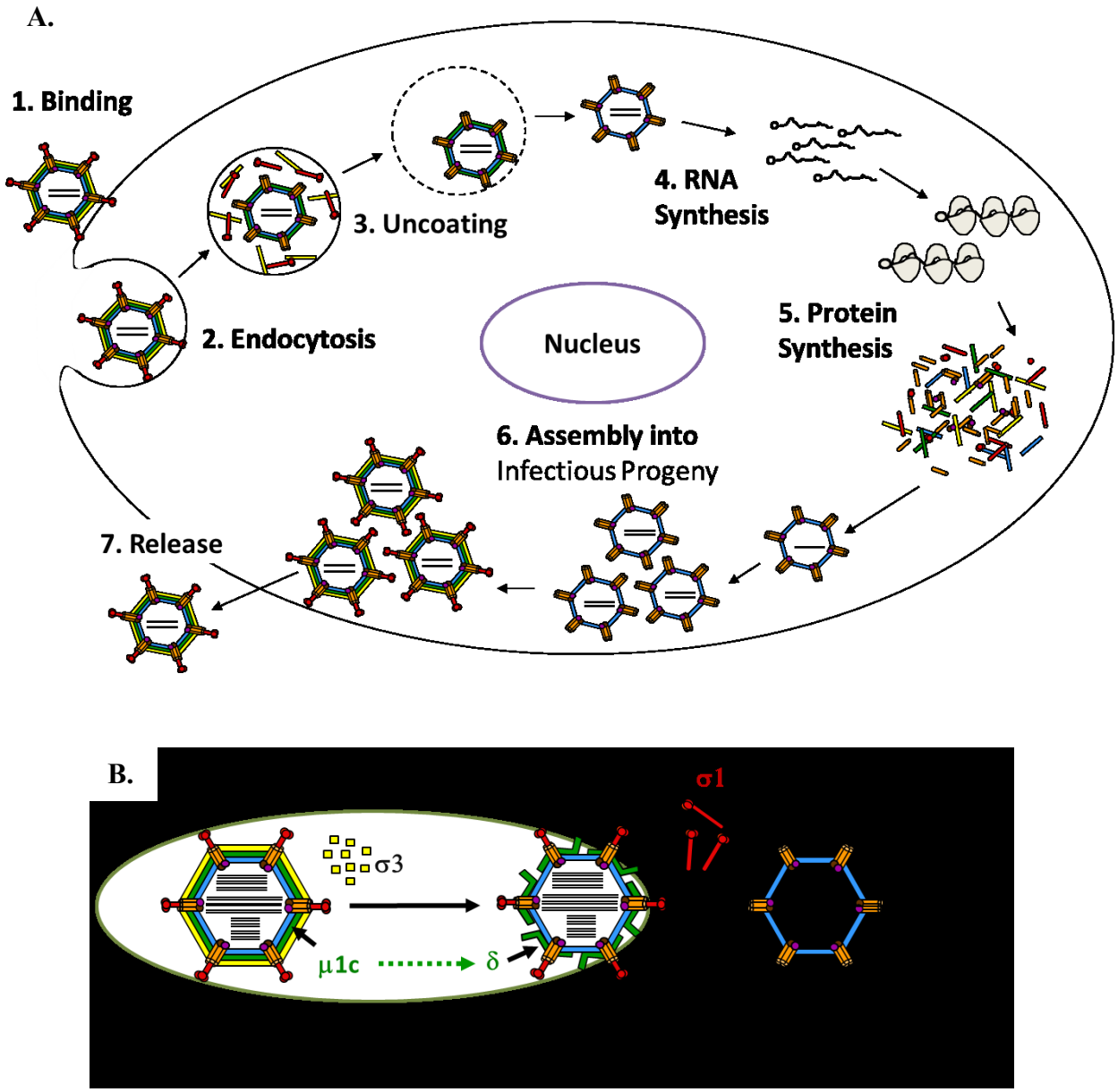

Figure 1.2.1. Reovirus Infection and Replication Process. A) Overview of the infection and replication steps of a reovirus virion. **B)** The uncoating process of a reovirus particle inside a lysosome. The σ3 outer capsid protein is removed, and the exposed, cleaved μ1 protein penetrates the membrane allowing entry into the cytoplasm. The σ1 protein detaches and viral RNA is released from the core. (Figure courtesy of Dr. Shmulevitz)

most of the extracellular binding domain) their susceptibility to reovirus was increased.[41] The conclusion was drawn that the increased efficiency of reovirus infection in EGFR and v-erbB transformed cells was not a result of any reovirus-EGFR binding, but instead was taking advantage of an already activated signalling pathway downstream. The Ras pathway was a candidate central to EGFR downstream signalling, and when NIH3T3 cells were transformed with activated Ras reovirus infection was enhanced as a result.[42, 43] Activating mutations of the Ras gene are frequently attributed to being present in approximately 30% of all human tumours.[44] When taking into account other activating mutations upstream of Ras and its downstream effectors, and also the interconnectivity of the signalling pathway, this number has been put at approximately 80% of all cancers.[44, 45, 46] It was this link between active Ras signalling, cancer, and the reovirus tropism towards Ras-active cancer cells that led to the assessment of reovirus as an oncolytic therapy.

2.2. Clinical Oncolytic Reovirus - Background Details

The Calgary, Alberta, Canada based company Oncolytics Biotech Incorporated has been testing a formulation of the T3D reovirus strain in numerous clinical trials under the trade name Reolysin®.[47] Recently Oncolytics Biotech published the sequence of their proprietary T3D reovirus strain.[48] Shmulevitz Laboratory PhD student Adil Mohamed compared it to the sequence of our lab strain of reovirus and found no amino acid differences between the Shmulevitz and Reolysin® strains, and only 6 silent nucleotide mutations (personal communication, Adil Mohamed). One advantage that reovirus has over other viruses being evaluated for their oncolytic potential is that it is naturally selective for many cancer cells, and does not need to be altered or attenuated in any way. Another attractive consideration of course is its benign nature in healthy humans, such that it has perhaps a more convincing safety profile than other oncolytic virus candidates.

2.3. Results of Reolysin® Clinical Trials

Numerous clinical trails with Reolysin®, 32 in total across North America and Europe, have been undertaken against a variety of different cancers in over 1000 total patients.[49, 50] The safety profile across a range of studies from Phase I to Phase III has been excellent, with adverse effects limited to cold-like symptoms such as headaches, fever, nausea, and diarrhea, with no maximal tolerable dose having been reached.[50, 51] This remains true for clinical trials where reovirus has been administered by intratumoural injection, and also those where reovirus was given intravenously.[51, 52, 53, 54, 55]

Clinical trials have examined Reolysin® both as a monotherapy and in combination with radiation or other drugs that are standard of care such as docetaxel, gemcitabine, carboplatin, pemetrexed and paclitaxel among others.[49, 50] Some early clinical data suggested that reovirus monotherapy was not very effective, likely due to immune clearance of the virus.[50, 56] In a Phase I trial of patients with relapsed multiple myeloma there was efficient cell entry and synthesis of viral RNA but reovirus protein production was limited. Therefore, the authors suggested that combination therapies may be the best anti-cancer approach for Reolysin®.[57] However, that conclusion seems premature when the results of REO 014 are examined, a Phase II study of 55 patients with bone and soft tissue sarcomas metastatic to the lung, in which a clinical benefit rate (complete response + partial response + stable disease/no progression) of 43% was observed.[49] Therefore, oncolytic reovirus monotherapy does have some remedial value. That being said, a combination of reovirus with other therapies seems to have been more effective in most studies, as either additive or synergistic effects have been proven with this approach.[50] Synergy between Reolysin® and a variety of chemotherapeutic agents was observed in a panel of non-small cell lung carcinomas resulting in increased apoptosis.[58] Examples *in vivo* include, but are not limited

to, preclinical studies with Reolysin® in combination with docetaxel in a murine prostate cancer model, or with gemcitabine in a murine ovarian cancer model.[59, 60] In human clinical trials, Reolysin® is frequently used as part of a multi-therapeutic regimen, such as in a recently completed Phase III trial testing intravenously administered Reolysin® in combination with paclitaxel and carboplatin against metastatic head and neck squamous cell carcinomas (HNSCC). In a cohort of over 100 patients, the combination therapy was statistically significantly better than the chemotherapy drugs alone at stabilizing or shrinking metastatic tumours and at increasing the progression free survival time of patients.[49]

Oncolytic reovirus has clear potential for success as anti-cancer treatment, however when objectively looking at the results of the trials it is clear that Reolysin® treatment is not effective for everyone and therefore some improvements can be made. In order to understand the mixed results of the clinical trials, we will need to better understand the mechanisms of reovirus infection and spread in cancer cells.

3. Mechanisms of Reovirus Infectivity in Transformed Cells

3.1. Previously Studied Determinants of Reovirus Oncolysis

As described previously, the discovery of the oncolytic properties of reovirus was linked to selectivity for cells with active Ras transformations.[43] A few different mechanisms have been attributed to cells with constitutively active Ras signalling that result in enhanced reovirus replication.[61, 62, 63] When compared to normal cells, Ras-transformed cells have shown enhanced proteolysis of lysosomal reovirus particles, that progeny virions are more infectious than those produced in non-transformed cells, a greater susceptibility to apoptosis, and a reduced level of PKR activity and IFN-β expression.[43, 61, 62, 63, 64] Firstly NIH3T3 cells have similar levels of reovirus binding and internalization when Ras-transformed vs. untransformed, however within the

first 24 hours 3x more Ras-transformed cells are infected.[63] The differential step was determined to be faster uncoating of the virions into an ISVP that can penetrate the lysosomal membrane and get into the cell cytoplasm. Quantitative PCR, northern blot and western blot analysis determined that transcription and translation rates between Ras-transformed and normal cells were similar. Reovirus titres from transformed cells were greater than could be explained by improved uncoating only, so reovirus was purified from transformed and non-transformed cells for comparison by plaque assay. Despite appearing similar by electron microscopy and SDS-PAGE analysis, progeny virions harvested from transformed cells were 4x more infectious.[63] Additionally, titres of extracellular (released) virus from Ras-transformed NIH3T3 cells indicated a 9x greater efficiency of release. Use of a pan-caspase inhibitor blocked the majority of cell death and release, indicating the importance of apoptosis in augmenting reovirus infection in transformed cells.[63] Fragmentation of golgi bodies in response to reovirus infection in Ras-transformed cells has been linked to increased sequestration of Ras in the golgi bodies, resulting in increased apoptotic signalling.[65] The effects of Ras-transformation on innate immunity and IFN as it relates to reovirus spread will be discussed in the next subsection. Additionally, another group of researchers found a determinant of susceptibility to reovirus oncolysis that is unrelated to the Ras status of the cancer cells both *in vitro* and *in vivo* mouse flank tumour models. When hydroxyurea was used to arrest the cells in S phase before infection, reovirus replication was enhanced and greater oncolysis was achieved in cell culture, and tumour shrinkage was significantly greater.[66] Therefore synchronisation of cancer cells in an advantageous phase of the cell cycle influences susceptibility to reovirus infection and could be exploited in treatment of cancer.

In an attempt to narrow down the field of effectors downstream of Ras, Norman *et al.* observed reovirus infections in transformed NIH3T3 cells with various Ras mutations.[67] Ras-active NIH3T3

cells that were unable to signal through Raf or phosphatidylinositol 3-kinase (PI3-K) were still permissive to reovirus infection, and retained active signalling through Ral. Providing further support, H-Ras active cells switched from a permissive to a reovirus resistant phenotype with a Ral knock out. Downstream of Ral, chemical inhibitors pinpointed the importance of signalling through p38 for reovirus susceptibility, implicating a Ras/Ral/p38 pathway for permissiveness in NIH3T3 cells.

There is growing recognition in the scientific community that susceptibility to reovirus infection is more complicated than being simply conferred by a Ras mutation. In most clinical trials evaluating reovirus, activation state of the EGFR/Ras pathway is not used an entry requirement or biomarker.[68] Although one group found correlation between KRas mutant colorectal cancer cells and greater reovirus oncolysis, other groups have found no link between Ras or MAPK activity and susceptibility to reovirus in a variety of cancer cell lines, and have suggested an alternative pathway may be involved.[30, 69, 70] Twigger *et al*. went more into detail, examining a panel of 15 HNSCC cell lines that were stratified in their permissiveness to reovirus for any biomarkers that correlated to reovirus susceptibility.[68] No correlation was found between the reovirus sensitivity of these cells and the EGFR expression or Ras activation. Inhibitors were used against 3 of the main pathways downstream of Ras: MAPK, PI3-K, and p38MAPK and again no connection to reovirus permissiveness was found. There are at least 18 different pathways downstream of Ras that boost cell growth through the regulation of a variety of cellular processes.[71] It is certainly possible that some of these pathways are being activated upstream or downstream of Ras and triggering factors affecting reovirus oncolysis that are currently unknown.[61]

In addition to signalling throughout the Ras pathway, the 15 HNSCC cell lines were tested for other determinants of susceptibility to reovirus induced cell death. Cell-surface expression of

JAM-A, the cellular receptor for reovirus, did not match the susceptibility of the cells; illustrated by the highest amount of receptor being present on the second most resistant cell line.[68] This observation has been confirmed in a variety of other cancer cell lines where expression of both JAM-A and β1-integrin did not correlate with susceptibility.[30] In contrast to previous reports that Ras activation sensitized cells to reovirus-induced apoptosis, Twigger *et al*. found HNSCC cell death to be unaffected by use of the pan-caspase inhibitor ZVAD, and caspase 3 activation was not observed following reovirus infection.[68, 72] In a different study, increased reovirus-induced cell lysis was linked to greater mRNA expression of the apoptotic gene Noxa, suggesting its importance in the panel tested which included lung, brain, skin, and bladder cancer cells. Interestingly, greater reovirus susceptibility in this cell panel tested by Terasawa *et al*. also matched with increased expression of the cathepsins B and L, which are important for reovirus uncoating.[30] Perhaps it is logical that the incredible heterogeneity among cancer cells would result in many different determining factors that influence reovirus oncolysis.

3.2. Known Antiviral Pathway Deficiencies that Allow for Productive Infection

As mentioned previously, one of the effects active Ras has on transformed cells is to inhibit their antiviral defenses, allowing for greater permissiveness to reovirus infection and spread. Early experiments by Strong *et al*. discovered that during reovirus infection a 65 kDa protein was being phosphorylated in response to reovirus infection and inhibiting protein translation in untransformed cells.[43] The 65 kDa protein was determined to be PKR; knockdown of the gene or chemical inhibition of PKR in NIH3T3 cells resulted in much greater susceptibility to reovirus infection, although more recently inhibition of PKR phosphorylation was observed to have no effect on reovirus susceptibility in HNSCC cells.[43] In Ras-transformed NIH3T3 cells PKR phosphorylation is blocked as a direct result of the usurpation by active Ras signalling, allowing

reovirus protein translation to continue.[43, 68] A decade later, Shmulevitz *et al.* implicated the negative regulation of retinoic acid–inducible gene I (RIG-I) and poor production of and response to IFN-β as main contributors to enhanced reovirus spread amongst Ras-transformed cells.[64] Ras-transformed NIH3T3 cells were limited in their production of ISGs such as ISG15, RIG-I, and 2′-5′-oligo-adenylate-synthetase (OAS) in response to reovirus infection and exogenous IFN-β stimulation, which makes it more difficult to fight off infection. Ras-transformed and normal cells both had comparable levels of RIG-I, so it was determined that reduced signalling of RIG-I was likely regulated through the MEK/ERK pathway to abrogate IFN-β production. Having less IFN-β of course makes cells more vulnerable to reovirus. However, this is not a universal truth as in the panel of HNSCC cells evaluated by Twigger *et al.* there was no correlation between susceptibility to reovirus and basal interferon levels or interferon production in response to reovirus.[68] A selection of brain, skin, bladder and lung cancer cell lines examined by Terasawa *et al*. also exhibited no correlation between susceptibility to reovirus and the induction of IFN-β mRNA.[30]

While IFN-β is typically the most prevalent Type I IFN, IFN-α also mediates important antiviral activity.[73] Ras/MEK signalling in the model Ras-transformed NIH3T3 cells was found to inhibit the IFN-α antiviral response by blocking phosphorylation of STAT1 and STAT2, and reducing STAT2 production at the transcriptional level.[74] In HCT116 colorectal cancer cells, which are K-Ras mutated, active signalling through the PI3-K/AKT pathway was also found to reduce STAT1 and STAT2 levels, along with inhibiting expression of IRF1 and IRF9.[75] Lower levels of STATs and IRFs would logically make cells more susceptible to infection by reducing the effectiveness of the IFN response, however, other researchers implicated active signalling through the PI3-K/AKT pathway as a positive factor in determining cell permissiveness to

reovirus.[76] Transient activation of signalling was seen in A549 lung cancer cells when infected with T3D reovirus, and when PI3-K activation of AKT was blocked, reovirus RNA synthesis and yield was increased.[76, 77] The signalling through PI3-K/AKT led to phosphorylation of transcriptional repressor EMSY, relieving suppression of the interferon response element (IRSE) and upregulating ISG activation namely Viperin, IFITM1, and ISG15.[76, 78] Viperin and ISG15 actively reduced reovirus infection levels once activated.[76] In a different study, reovirus infection in a selection of cancer cell lines found no correlation between levels of ISG56, OAS, and PRRs RIG-I and MDA5 and susceptibility to reovirus.[30]

The inhibited innate antiviral responses observed in some Ras-transformed cells provide support for further investigation in order to gain a deeper understanding of how they influence reovirus infection in human cancer cells. Research completed to date indicates there are multiple weaknesses in cancer cell antiviral responses that are capable of influencing susceptibility to reovirus infection and spread. Given the complexity of the signalling pathways involved and the sheer number and diversity of cancer cells, we should not be surprised when different cells exhibit different traits or possess conflicting properties. It is also likely that there are many more mechanisms of reovirus susceptibility still to be uncovered. My thesis will be focusing on the diversity of antiviral signalling in a selection of lung cancer and HNSCC cells in response to reovirus infection, so for this reason I will briefly introduce some important components of the innate antiviral signalling pathway.

4. Overview of Relevant Innate Antiviral Signalling

4.1. Sensors of Reovirus dsRNA

In order to elicit an appropriate response against a viral infection, the immune system first needs to detect the presence of a pathogen. As such, immune cells are equipped with a plethora of

pattern recognition receptors (PRRs) to detect the diverse range of pathogen associated molecular patterns (PAMPs) they may encounter.[79] In the context of viral infections, common PAMPs include viral nucleic acids. More specifically, dsRNA of RNA viruses can be detected by PRRs including retinoic acid-induced gene (RIG)-I, melanoma differentiation-associated gene 5 (MDA5), and protein kinase RNA-activated (PKR). Thus, upon pathogen detection with these receptors downstream signalling can result in the induction of cytokines, such as IFNs, important for facilitating an antiviral response.

RIG-I is a cytoplasmic pathogen recognition receptor important for the detection of RNA viruses and some DNA viruses by recognizing 5' phosphates on single- or double-stranded RNA.[80, 81] RIG-I as well as MDA5 are two RIG-I-like receptors (RLRs) which recognize and are activated by viral dsRNA. They both contain a DExD/H-box helicase domain, and N-terminal caspase activation and recruitment domains (CARDs).[81, 82, 83] Following the activation of either RIG-I or MDA5, CARDs interact with the mitochondrial activator of virus signaling (MAVS) CARD, resulting in downstream signaling and activation of TBK1 and IKKε protein kinases. Activation of these two kinases results in the phosphorylation and activation of interferon regulatory factor (IRF)-3 and NF-κB. IRF-3 and NF-κB are transcription factors that upon activation translocate into the nucleus and promote the transcription of various genes for the innate immune response including interferons.

PKR is an interferon induced, RNA-activated serine/threonine protein kinase which is ubiquitously expressed.[84, 85, 86] It is characterized by two functional domains including an N terminal dsRNA binding domain containing two dsRNA binding motifs, and a C terminal catalytic domain. Following PKR activation by dsRNA binding, autophosphorylation and subsequent substrate phosphorylation occurs.[86] The downstream signalling following PKR activation results

in NF-κB and Type I IFN induction, as well as the phosphorylation of elf-2α which subsequently inhibits viral protein translation and propagation.[84, 87, 88]

4.2. Interferon Regulatory Factors

A key family of antiviral cytokines induced by viral infections are the Type I and Type III IFNs. The cellular mediators of this induction are the interferon regulatory factors (IRFs) which are thus critical in antiviral defence.[89]

There are nine human cellular IRF genes that have been identified.[90, 91, 92] While the IRFs share significant homology, they differ functionally based on the cell type of expression, intrinsic transactivation potential, and ability to interact with transcription factors, co-factors or other members of the IRF family.[93] Viral infections induce the expression of the tightly regulated Type I IFN and Type III IFN genes via IRF family members.[89, 94]

In the 5' region of IFN-α and IFN-β genes there is a sequence domain designated the virus responsive element (VRE); this element contains conserved GAANN repeats, with which IRF family members interact.[89, 95, 96, 97, 98] For the transcriptional induction of IFN-β genes, IRF-3, NF-κB, activating protein 1 (AP-1), JUN, and the high mobility protein HMG-1 come together to form an enhanceosome at the IFN-β VRE and subsequently recruit cAMP responsive element binding (CREB) and histone transacetylases.[99, 100] In contrast, the IFN-α VRE does not have the NF-κB binding site, but contains AANNGAAA repeats which bind many IRF family members.[92, 101, 102] Accordingly, the transcriptionally active enhanceosome for the IFN-α genes requires IRF-1, IRF-3 and IRF-7 along with histone transacetylases.[103] The promoter sequences of Type III interferon genes also contain binding sites for the transcription factors NF-κB, IRF-3, IRF-7, and AP-1, suggesting co-expression with Type I IFN genes.[94, 104, 105]

During a reovirus infection, RIG-I is the primary sensor of reoviral genomic dsRNA, and is necessary for IRF-3/7 activation along with mitochondrial antiviral-signaling (MAVS) protein.[106, 107] In this context, IRF-3 is required for both the induction of IFN-α and IFN-β following reovirus infection resulting in restriction of viral growth.[106] It should be noted that while at low MOI IRF-3 signalling induces expression of Type I IFNs, while at high MOI IRF-3 signalling along with IPS-1 enhances reovirus-induced apoptosis.[106]

4.3. Type I Interferon

Type I interferons are key cytokines for the antiviral immune response. The two most highly studied type I IFNs include IFN-α, a class encoded by 13 homologous genes in humans, and IFN-β, encoded by a single gene, *IFNB1*.[108, 109] These cytokines are produced by many cell types in response to their recognition of PAMPs, such as cytosolic or extracellular nucleic acids, with PRRs.[110] These cytokines signal through either the homo-dimeric IFN-α/β receptor 1 (IFNAR1) which has an especially high affinity for IFN-β, or through the heterodimeric IFNAR1-IFNAR2 receptor which is capable of binding all type I IFNs.[108] The activation of these receptors promotes downstream signalling resulting in transcription of IFN-stimulated genes (ISGs) which elicit immunostimulatory and antiviral effects via the JAK/STAT pathway.[111, 112, 113]

4.4. Type III Interferon

Type III IFNs, also known as IFN-λs, consist of four family members in humans: IFN-λ1 (IL-29), IFN-λ2 (IL-28A), IFN-λ3 (IL-28B), and IFN-λ4.[114, 115] Like Type I IFNs, IFN-λs promotes the transcription of ISGs to induce an antiviral state.[116, 117] However, while Type I IFNs act globally, IFN-λs act primarily on epithelial cells located in tissues and mucosal barriers which are at higher risk for viral exposure and infection. Thus, IFN-λs induce an antiviral response in these cells to combat this high risk for viral infection. The IFN-λ receptor is composed of two chains,

the specific IFN-λ receptor-chain 1 (IFN-λR1) and the shared IL-10 receptor chain 2 (IL-10R2). Upon receptor binding to any of the 4 IFN-λ family members, the JAK/STAT pathway is activated leading to the induction of ISGs.[116]

4.5. JAK/STAT

The tyrosine kinases of the Janus family (JAK Kinases) and the tyrosine phosphorylation and activation of the signal transducers and activators of transcription (STAT)-proteins is a key Type I IFN downstream signalling pathway.[118] JAK-1 and TYK-2 Janus family tyrosine kinases are in constitutive association with IFNAR1 and IFNAR2 subunits of the Type I IFN receptor respectively.[119, 120, 121] Binding of Type I IFNs to the receptor results in JAK-1/TYK-2 activation and subsequent tyrosine phosphorylation of the associated type I IFN receptor subunits.[122, 123, 124, 125] Following activation, JAK kinases tyrosine phosphorylate several STAT-proteins (STAT-1, STAT-2, STAT-3 and STAT-5) which then homo- and heterodimerize and translocate into the nucleus.[126, 127, 128, 129, 130] Additionally, phosphorylated STATs recruit IRF-9 to form the IFN-stimulated gene factor 3 (ISGF3) and translocate into the nucleus. In the nucleus these transcription factors regulate transcription of ISGs by binding to sequences within the promoters.[129, 130, 131]

4.6. Interferon Stimulated Genes (ISGs)

The JAK/STAT signalling pathway regulates the transcription of interferon-stimulated genes (ISGs).[132] ISGs reinforce the IFN response and can control bacterial and viral infections by directly targeting the pathogen life cycle. There are various functions resulting from ISG induction, including IFN-induced pathogen-sensing sensitization and antiviral effector functions.[133]

IFN-induced pathogen-sensing sensitization is a function of ISGs that primes cells to respond to an imminent pathogenic threat.[133] In the absence of infection, PRRs and IRFs are expressed at a basal level. Upon PAMP recognition, activated IRF-3, IRF-7 and NF-κB translocate to the

nucleus and induce IFN genes. Additionally, these transcription factors also bind the promoters of a subset of ISGs including those for IRFs and PRRs. Thus, ISGs reinforce the IFN signalling and enhance pathogen detection even prior to IFN release and JAK/STAT pathway activation.[133]

ISGs also carry out antiviral effector functions targeting various stages in the viral life cycle, including viral entry, translation and replication, and viral egress. Known ISGs that target viral entry include myxovirus resistance (Mx) proteins, cholesterol-25-hydroxylase (CH25H), the IFN-inducible transmembrane family (IFITM) family, and the tripartite motif (TRIM) family of proteins.[133, 134]

In the context of reovirus, various ISGs have been demonstrated to interfere in infections including MxA and PKR which restrict infection by targeting post-entry events including protein synthesis.[135, 136, 137] IFITM3 also restricts reoviral infection by targeting late endosomal cell entry mechanisms.[138] IFITM3 expression is induced by type I IFNs, such as IFN-α, and has two transmembrane domains with both the N and C termini localized in the ER and endosomal lumen, and thus localizes to late endosomes.[138, 139, 140, 141] In late endosomes, reovirus is uncoated by the action of acid-dependent cathepsin proteases.[19, 25] IFITM3 delays the kinetics of acidification in these compartments altering the dynamics of endosomal uncoating. This leads to either inefficient membrane penetration or lysosomal degradation of viral particles, therefore hampering reoviral infection and replication by restricting entry.[138] Reovirus infection increased transcripts of the ISGs IFITM1, ISG15, and Viperin in A549 cells. However, only ISG15 and Viperin overexpression reduced reovirus replication, and shRNA knockdown increased reovirus replication. These effects were not observed with IFITM1.[76] An overview of an IFN response to reovirus infection can be seen in **Figure 1.4.6.**

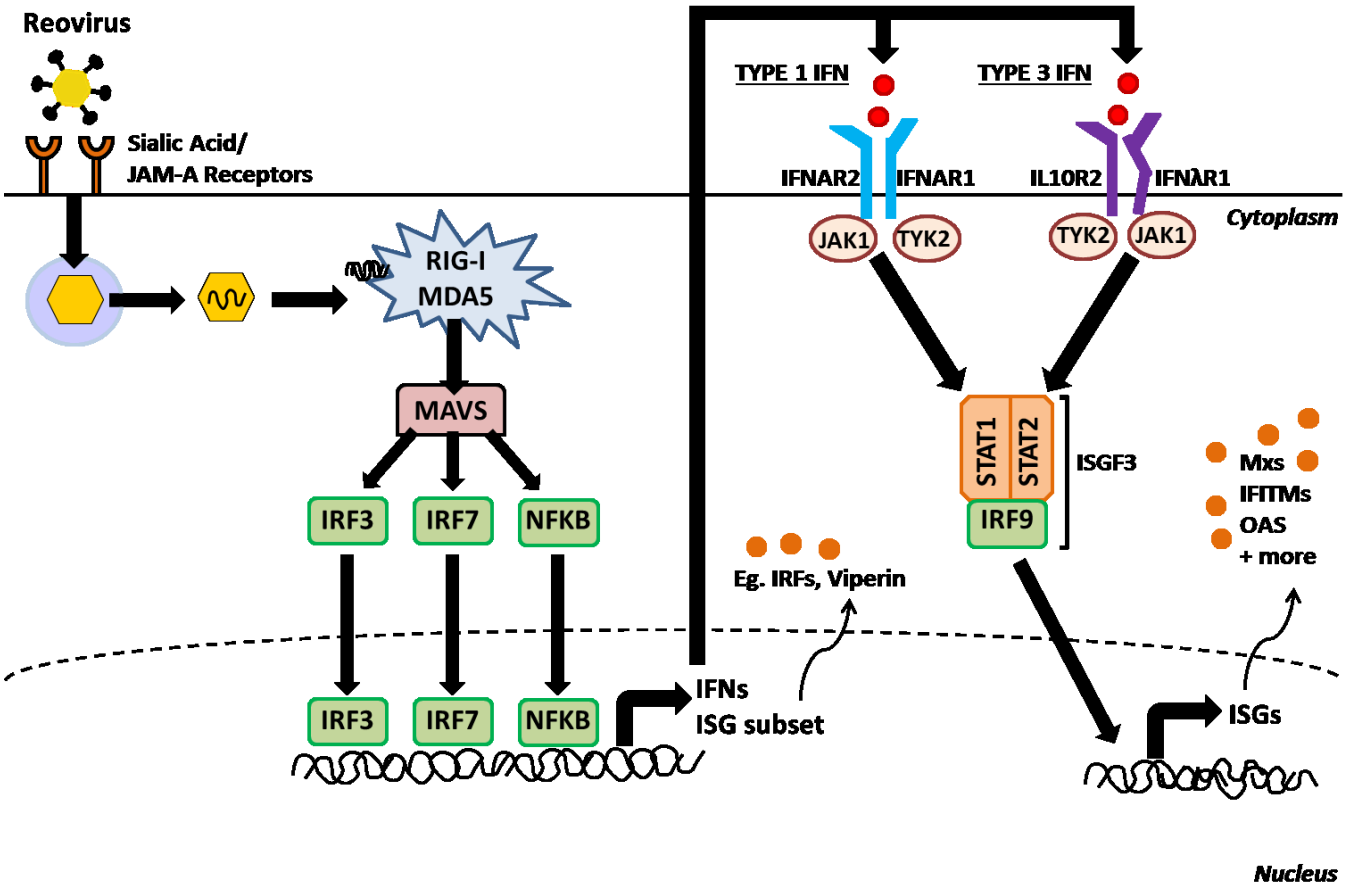

Figure 1.4.6. Simplified Rendering of an Interferon Response Pathway to a Reovirus Infection.

4.7. Tumour Necrosis Factor (TNF)

The tumor necrosis factor superfamily (TNF SPF) of cytokines has a significant role in the host defense via the regulation of cellular survival and death.[142] TNF secretion is induced by PKR recognition of dsRNA activating the NF-κB pathway.[143] Members of this superfamily include TNF-α, TNF-β and TNF-related apoptosis-inducing ligand (TRAIL).[142] Their function is dependent on the cytosolic signaling domain of the TNF receptors (TNFRs) with which they interact.[144, 145] There are two types of TNFRs based on the cytosolic signaling domain: the TNF receptor associated factors (TRAFs) and the death domain (DD) receptors.[142] Upon TNF binding, the TRAFs recruit factors promoting NF-κB activation. In contrast, upon activation with TNF DD receptors interact with DD-containing adaptor proteins promoting caspase activation and resulting in apoptosis.[142]

In the context of viral infections, TNF-α and TNF-β induce selective killing of infected cells and resistance in uninfected cells. Additionally, TNF potentiates antiviral effects of IFNs and inhibits viral replication in HSV-2, EMCV, VSV & Adenovirus-2.[146] Reovirus is known to induce the expression of TNF-α, which further induces the expression TRAIL.[147, 148] TRAIL mediates apoptosis of virus infected cells in HCMV and reovirus infections, via the crosslinking of TRAIL with death domain receptors TRAIL-R1 and TRAIL-R2.[148, 149, 150, 151, 152] The consequent downstream signaling recruits adaptor proteins resulting in the activation of caspases and inducing apoptosis.[148] A simplified rendering of the TNF-α response pathway following reovirus detection can be seen in **Figure 1.4.7.**

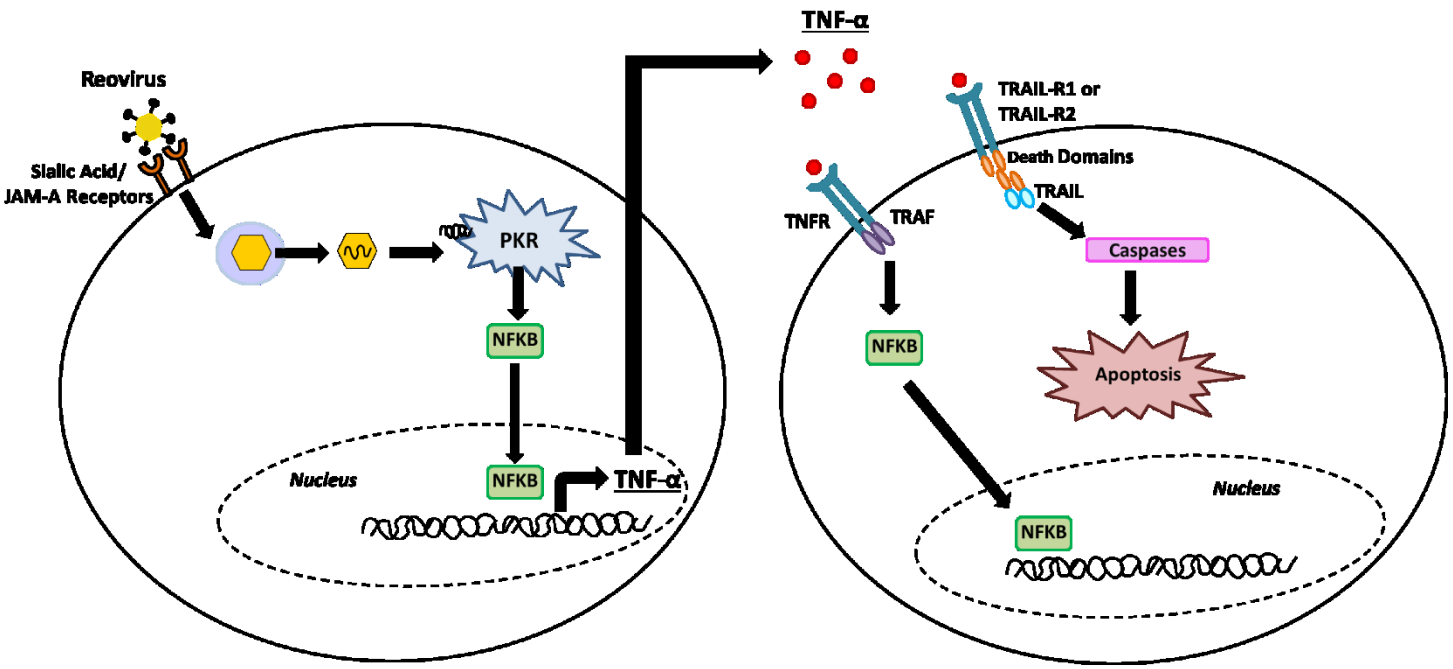

Figure 1.4.7. Simplified Overview of a TNF-α Response Pathway to a Reovirus Infection.

5. Antiviral Signalling and other Oncolytic Viruses

There are many viruses currently undergoing basic research and clinical trials due their potential as oncolytic therapeutics. A modified adenovirus, under the trade name Oncorine, was approved for use as a head and neck cancer treatment in 2005, albeit only in China not worldwide.[153] The first oncolytic approved for use in a western jurisdiction just passed FDA review in 2015 for use against advanced melanoma; Amgen's T-Vec, a modified HSV-1 virus. Examples of other viruses currently in clinical trials come from 9 different virus families: the Adenoviridae, Picornaviridae, Herpesviridae, Paramyxoviridae, Parvoviridae, Reoviridae, Poxviridae, Retroviridae, and Rhabdoviridae.[154] For some of these viruses, in order to increase their effectiveness at cancer cell killing, the effects of modulating the innate antiviral response in the targeted cancer cells has been evaluated. I have highlighted a few below for comparison with oncolytic reovirus.

5.1. Vesicular Stomatitis Virus (VSV)

VSV is a single stranded RNA virus with oncolytic activity in many different types of cancer. VSV is naturally quite sensitive to IFN, and novel variants have been synthesized which induce IFN production upon infection, boosting its safety profile in normal cells while still retaining its oncolytic properties.[155] Since some cancer cells maintain functional IFN production and response capabilities, this can provide an obstacle for effective VSV oncolysis. VSV has been tested quite frequently against both HNSCC and pancreatic ductal adenocarcinoma (PDA) cell panels and a stratified variation in oncolytic response was observed.[156, 157, 158, 159, 160] Screening the cells for up to 33 different antiviral genes linked to the Type I IFN response found most cells had at least a small increase in IFN-α or IFN-β production, but a combination of MxA, OAS1, IRF-7 and IRF-9 genes was highly expressed in the most resistant cells only. Exogenous IFN-2α or IFN-β was

used as a pre-treatment to see if it conferred protection from VSV infection.[160] Both IFN-2α or IFN-β blocked VSV infection of normal cells, but only IFN-β protected the JSQ-3, SQ20B, and SCC61 HNSCC cells from infection. The addition of extrinsic IFN-β was also able to confer resistance to VSV upon the previously susceptible RKO colon cancer cells and MiaPaCa2 pancreatic cancer cells.[156, 160] Researchers also tested up to 16 different small molecule inhibitors of the Type I IFN signalling pathway in different experiments to see if they would make VSV-resistant cells more permissive to infection. PI3-K and STAT3 inhibitors proved ineffective, however the JAK1/2 inhibitor ruxolitinib was highly effective as an enhancer of VSV replication in previously resistant HNSCC and PDA cells resulting in 100-1000 fold-greater progeny yield.[158, 159, 161] Use of ruxolitinib decreased expression of the ISGs MxA and OAS1. TPCA-1, an IKK-β and JAK1 inhibitor, also replicated this effect in resistant PDA cells.[161] Thus, VSV is an interesting example of an oncolytic virus where the attenuation of the Type I IFN response in target cancer cells can render susceptibility to cancer cell killing in previously resistant cells.

5.2. Measles Virus (MV)

The measles virus is an RNA virus that is highly pathogenic to humans. However, attenuated strains of MV have shown promising oncolytic potential.[162] Infection with wild-type MV is characterized by its ability to limit the host cells' IFN-α and IFN-β responses.[163] MV non-structural C and V proteins have been found to inhibit STAT signalling as well.[164, 165, 166] In the attenuated MV strain this functional capability is lost making the virus susceptible to Type I IFN antiviral defenses.[162] Panels of prostate cancer, sarcoma, and malignant pleural mesothelioma (MPM) cell lines have shown a mixed susceptibility to MV.[162, 163, 167] In a panel of 22 MPM cell lines and some normal primary cells, MV was unable to productively infect the primary cells or 7 MPM cell lines that had functional Type I IFN responses, including IFN-α and IFN-β production and Mx1

expression.[163] Of the 15 susceptible cell lines to MV, the addition of exogenous IFN-α and IFN-β was able to induce resistance in 11. Similar results were seen in the testing of the sarcoma cell panel, where inhibition of MV replication was linked to strong expression of STAT1, IFITM1, and viral sensor RIG-I.[167] In 3 of 5 susceptible sarcoma cell lines, the addition of extrinsic IFN-β resulted in a switch to a more resistant phenotype. Thus, just like with VSV, attenuated MV provides another example of an oncolytic virus whose ability to replicate in cancer cells is determined by the strength of their Type I IFN response.

5.3. Adenovirus

Adenoviruses are DNA viruses which also have shown promise in oncolytic therapeutics. Selective tumor replication of adenoviruses has been shown possible by exploiting the PKR downstream inhibition of viral protein translation and replication.[88] PKR is an upregulated ISG upon IFN-α and IFN-β stimulation, and can detect adenoviral dsRNA which is produced following infection via bidirectional transcription. Adenovirus counteracts the activation of PKR by producing small virus-associated (VA) RNAs, such as VAI, which bind without activating PKR, thus acting as a dsRNA antagonist.[168] Downstream effectors of the Ras pathway can also block activation of PKR by dsRNA, hence viruses unable to revert PKR activation can still replicate normally in cells with an activated Ras pathway.[169] VAI mutant adenovirus was found to propagate poorly in normal human cells, but regain their replication ability in human pancreatic tumor cells, with an activated Ras-pathway.[88] Therefore, this provides an approach for selective replication of attenuated adenovirus in Ras-activated cells through exploitation of limited antiviral function of PKR.

5.4. Influenza A Virus

The influenza A virus is a well known, highly contagious single stranded RNA virus.[170] Influenza A synthesizes a non-structural protein (NS1) that inhibits the Type I IFN response of cells.[171] Recombinant influenza lacking NS1 exhibit attenuated pathogenesis in normal cells, but are able to replicate in cells with defective Type I IFN pathways such as Ras-transformed cancer cells.[172, 173] Again, this provides an example of how exploiting the Type I IFN response can lead to successful oncolytic actions that are safe against normal cells.

5.5. Implications for Oncolytic Reovirus

There are numerous viruses currently being optimized as an oncolytic therapeutic. I highlighted a selection of these which were included genetically modified or naturally selective viruses against cancer cells. The common thread linking the activity of these viruses was they exploit defective Type I IFN pathways to replicate in cancer cells. This would suggest that the Type I IFN response should be considered a major candidate as an unknown restriction factor limiting reovirus spread between some types of cancer cells.

CHAPTER 2: HYPOTHESIS AND APPROACH

Based upon the previous review of the current knowledge of reovirus dissemination in cancer cells, the following project rationale, hypothesis and objectives were proposed:

1. Rationale

There is an understanding of why model Ras-transformed cells are susceptible to reovirus infection. However, we know that cancer cells in clinical trails are not always susceptible to reovirus infection and killing. We DO NOT KNOW why this is the case because of the vast heterogeneity and complexity of different cancers and host immune responses.

2. Hypothesis and Thesis Objectives

It was hypothesized that the cancer cells which are most resistant to reovirus dissemination possess active antiviral mechanism(s) that more susceptible cancer cells do not have. In an effort to determine what differentiating antiviral mechanisms are active in cancer cells that resist the spread of reovirus infection, the following objectives were proposed for my MSc. project:

1.1. Screen a panel of lung cancer and head and neck squamous cell carcinoma (HNSCC) cell lines for susceptibility to reovirus infection

1.2. Determine if cell death and/or antiviral factors play a dominant role in restricting reovirus spread among more resistant cancer cells

1.3. Inhibit specific parts of the antiviral signalling pathway in an attempt to identify the main factor(s) responsible for restricting reovirus infection

CHAPTER 3: MATERIALS AND METHODS

For reference please refer to:

Table 3.1. List of Cell Lines and Culture Media Used in this Project

Table 3.2. List of Antibodies Used in this Project

Table 3.3. List of shRNA Constructs Used in this Project

Table 3.4. List of Primers Used in this Project

1. Cells and Cell Culture

Cell lines were sourced from the American Type Culture Collection (ATCC). Cells were incubated at 37°C with 5% CO_2 and subcultured when confluent. Cell line descriptions, seeding information, and appropriate culture media can be seen in **Table 3.1**. All media used for cell culture was supplemented with 5 ml antibiotic/antimycotic (Sigma), 5 ml of non-essential amino acids (Sigma), 5 ml of sodium pyruvate (Sigma), 10 ml of 200 mM L-glutamine (Sigma), and 10% fetal bovine serum (Invitrogen/Gibco) per 500 ml bottle (aka. complete media).

2. Reovirus

2.1. Reovirus Production

Reovirus stock was grown in L929 spinner cultures at 37°C without CO_2 in suspension culture medium (JMEM powder 11 g, $NaHCO_3$ 2.2 g, HEPES Sodium Salt 1.3 g, Glucose 1 g, in 1 L of H_2O at pH 7.2). When cell density reached $1x10^6$ cells/ml they were infected at an MOI of 0.1. When 80-90% death was observed cells were pelleted (1500 xg for 15 min) and frozen at -20°C or processed immediately, and the medium was discarded. Purification of reovirus from the pellets was performed as previously described.[174]

2.2. Infections

Reovirus infections were carried out in serum-free MEM medium with no additional supplements. Cells were infected for 1 hr and were incubated at 37°C with 5% CO_2. During this incubation, viral infection medium was swished every 5 min to facilitate distribution of virus particles throughout each well. Following the 1 hr infection, viral infection medium was removed and fresh medium was applied to cells. Cells were subsequently incubated at 37°C with 5% CO_2 until their collection at the respective time points indicated by individual experiments.

3. 96well Reovirus Infectivity Assay

Cells were seeded 125 µl/well at a density optimized to achieve confluency next-day in 96-well flat-bottom plates (Greiner Cellstar; see **Table 3.1** for cell seeding information). Approximately 24 hrs post-seeding, health and density of cells was confirmed by microscopy. Following visual confirmation, 1:4 serial dilutions of reovirus infection medium was applied to cells in 50 µl of medium according to the infection protocol previously described (**Methods 2.2**; reovirus titre). At 18 hrs and 48 hrs after infection, medium was discarded and cells were rinsed once with 1x PBS. Cells were then fixed with methanol for >5 min at RT, before another wash with 1x PBS. After removal of the wash, Blocking Solution (1x PBS, 0.1% Triton X-100, 3% BSA) was added at 200 µl/well for either 1 hr at RT, or 4°C overnight. Blocking solution was then removed, and 50 µl of rabbit anti-reovirus (Shmulevitz laboratory in-house stock) was added at a 1:5000 dilution in Blocking Solution. Before adding secondary antibody, cells were washed 3x quickly with PBST (PBS, 0.1% Triton X100), incubated for 5 min at RT, and repeated 2 more times. Wash was discarded and 50 µl of goat anti-rabbit alkaline phosphatase (Jackson Immunoresearch) was added at 1:4000 in Blocking Solution. Both the

primary and secondary antibodies were incubated on a rocker either for 1 hr at RT or 4°C overnight. Again, the plates were washed with PBST as described above following antibody incubation. Finally, the substrate mixture was made by adding pNPP (VWR) to Diethanolamine Buffer (97 ml diethanolamine, 100 mg $MgCl_2$, pH 9.8 in 1 L of H_2O) at 1 mg/mL and pipetted onto cells at 200 µl per well. The plate was then incubated in the dark at RT and scanned at 20, 40, and 60 min on the Perkin Elmer plate reader with Wallace Envision Manager software at 405 nm. The timepoint where absorbance values were not fully saturated was chosen for data analysis. $TCID_{50}$ was measured by plotting absorbance values vs. reovirus dilutions, and interpolating the midpoint of the curve to a specific reovirus concentration.

4. Cell Staining

4.1. For Reovirus Protein (BCIP/NBT substrate)

Following infection and removal of medium from the cells, cells were rinsed with 1x PBS. Cells were then fixed with methanol for >5 min at RT, before another wash with 1x PBS. After removal of the wash, Blocking Solution (1x PBS, 0.1% Triton X-100, 3% BSA) was added at 200 µl/well for either 1 hr at RT, or 4°C overnight. Blocking solution was then removed, and 50 µl of rabbit anti-reovirus (Shmulevitz laboratory in-house stock) was added at a 1:5000 dilution in Blocking Solution. Before adding secondary antibody, the plates were washed 3x quick with PBST (PBS, 0.1% Triton X-100), incubated for 5 min at RT, and repeated 2 more times. Wash was discarded and 50 µl of goat anti-rabbit alkaline phosphatase antibody (Jackson Immunoresearch) was added at 1:4000 in Blocking Solution. Both the primary and secondary antibodies were incubated on a rocker either for 1 hr at RT or 4°C overnight. Again, the plates were washed as previously described following antibody incubation. Wells were soaked with AP Buffer (100 mM Tris-HCl pH 9.5, 100 mM NaCl, 5 mM MgCl in H_2O) at RT

for 5-10 min before staining with a mixture of BCIP and NBT substrates (both Sigma, diluted 1:100 in AP Buffer). Staining was done at RT in the dark, and took approximately 20 min for the reovirus infected cells to stain a distinct purple as visualized under a microscope. The reaction was quenched by removing the substrate and adding 1x PBS with 5 mM ethylenediaminetetraacetic acid (EDTA). After incubating in 1x PBS with 5mM EDTA for approximately 15 min at RT the solution was replaced with 1x PBS and stored at 4°C for imaging with the EVOS FL Auto microscope (Life Technologies).

4.2. Hoescht

Prior to staining with Hoescht 33342 dye (50 mg/ml), monolayers of cells were rinsed once with 1x PBS and fixed with methanol for >5 min at RT, before another wash with 1x PBS. Hoescht stain was diluted 1:7500 in 1x PBS and incubated on cells for 20 min at RT. Following the incubation, the dye was removed and replaced with 1x PBS. Cells were imaged with the EVOS FL Auto microscope (Life Technologies).

5. Plaque Assays

5.1. Technique

Samples were titred on confluent monolayers of L929 cells that were seeded on 24well plates. 100 µl of sample was used to infect each well, as previously described (**Methods 2.2**). Typically, a dilution series of 10^{-5}–10^{-10} was applied across each row of 6 wells. After 1 hr, infectious medium was removed from the wells, and a 0.75 ml agar plug was added and allowed to solidify over approximately 30 min. The plugs consist of a mixture containing 2x JMEM powder medium (Sigma; add 2x the normal supplements), agar, and normal MEM culture medium in a 1:1:2 ratio. Once the agar solidified, the plates were incubated upside-down at 37°C for 96 hpi. Following the incubation period, 1 ml of 4% paraformaldehyde

(Shmulevitz laboratory in-house stock) was used to soak each well for 1-4 hrs. Paraformaldehyde was poured off into waste and the agar plugs were removed from the plates with a quick flick of the wrist. Wells were fixed with methanol for 5 min, and then stained with crystal violet (1% diluted in 50% Ethanol, 50% H_2O solution) for 5 min. Distinct, visible clearings among the purple stained monolayer were counted as plaques.

5.2. Lysate/Total Titre vs. Media/Released Titre

When assessing the percentage of virus released by cells, a total titre sample and released-into-media sample was collected. The sample for released virus in media is a simple collection of 100 µl of the infected cell media at the desired time point. To collect a sample representing the total amount of virus, the infected cell media is reduced to 90 µl, and 10 µl of 10X RIPA (10% NP4O, 5% sodium deoxycholate) is added to make a total volume of 100 µl. The RIPA will lyse the cells after mixing by pipetting up and down, and the volume is collected.

6. Simulated Virus Release Assay

Confluent monolayers of cells in 12well plates were infected to an initial TCID of 20%. At 18 hpi some wells were fixed and stained for reovirus protein with BCIP/NBT substrate (**Methods 4.1**) as a measure of initial infection. In other wells, infection was allowed to progress to 48 hpi before fixing the cells and staining for reovirus protein. Some of these wells had additional reovirus spiked into the culture media at the 24 hpi timepoint to simulate a greater release of virus by the cells. The amount of virus added as the spike was an MOI specific to each cell line sufficient for a TCID of 50%. Wells were fixed 48 hpi and stained for reovirus protein. All wells were also stained with Hoescht dye to enable a total cell count. Cells were imaged with the EVOS FL Auto microscope (Life Technologies).

7. Media Transfer Experiments

The cell lines of the cancer panel were infected to an initial TCID of 20%, and at 18 hpi the culture media were collected and frozen at -80°C. To remove infectious virions from the media it was spun in an ultracentrifuge at 100,000 xg for 60 min, and then run through 2 cycles of 2:30 on the UV Crosslinker (100 μJ/cm^2; Ultra-Violet Products). This treatment media was then added to cells in 1:2 dilutions, topped up to a 100 μl final volume with fresh culture medium. The media pre-treatment was left on the cells for 18 hrs and then removed from the cells. Cells were then infected with a 1:500 dilution of reovirus (3.7x10^9 pfu/ml). At 18 hpi cells were fixed with methanol, blocked, and stained for reovirus protein (as described **Methods 4.1**) and imaged with the EVOS FL Auto microscope (Life Technologies).

8. Multiplex ELISA

Cells were infected to a TCID of 20% in 6well plates and incubated in 1.5 mL of medium. At 18 hpi, the media of infected and corresponding uninfected cells was collected and flash frozen in liquid nitrogen before storage at -80°C. This was repeated for 3 independent experiments in total. Samples were thawed for testing with the Human IFN 9-Plex ELISA Kit (PBL Assay Sciences). Samples were added in duplicate to wells of the 96well ELISA plate at 50 μl each, and the instructions of the ELISA kit were followed exactly. The plate was imaged in the GE ImageQuant LAS 4000, and the results were analyzed with the Quansys Biosciences Q-View software.

9. RNA Assay Techniques

9.1. RNA purification

Prior to harvesting with Lysis Buffer, cell monolayers were washed with 1x PBS. Lysis Buffer was added to wells (100 µl/well to 12well plates, 200 µl/well to 6well plates) and the plate was swirled for 5 min prior to collection by pipette. Lysis Buffer was from the GenElute Mammalian Total RNA Miniprep Kit or the GenElute 96well Total RNA Purification Kit (both Sigma). Instructions from the kit were followed for purification of the lysates into RNA. RNA was eluted in RNAse-free water and quantified on a BioDrop scanner (MBI Lab Equipment).

9.2. cDNA synthesis

25 µl of pure RNA was diluted out to 100 µg/ml for each sample. For each reaction 2.5 µl of RNA was mixed with an initial master mix (0.5 µl random primers [150 ng/µl], 0.5 µl 10 mM dNTP mix, 2.5 µl H_2O) and incubated at 65°C for 5 min. Samples were then buried under ice for 1 min and spun down, before addition of a new master mix (2 µl 5x First Strand Buffer, 1 µl 0.1 M DTT, 0.5 µl H_2O, 0.5 µl MMLV RT). Samples were run on T100 Thermal Cycler (BioRad) for 12 min at 25°C, 50min at 37°C, and 15 min at 70°C. When the cycle was complete the cDNA product was diluted with 30 µl of H_2O and frozen at -20°C for future use.

9.3. Primer Generation and Testing

The RefSeq mRNA code for the specific target was entered into a PubMed nucleotide search. The complete nucleotide sequence for the target was then entered into the Primer3web free online software (v.4.0.0, http://bioinfo.ut.ee/primer3/) to generate sets of primers. Two primer sets were selected for each target, from different segments of the sequence if possible. Primer sets were tested against a 1:2 dilution series of reovirus infected A549 cell cDNA. Primers sets

with the best standard curves were selected for use (efficiency near 100%, slope between 3.2-3.6).

9.4. qRT-PCR protocol

qRT-PCR was performed using a CFX96 Real-Time System (BioRad). Samples 20 µl in volume were run on the "QPCRandMelt" protocol (steps below, time is min:sec). Each 20 µl sample consisted of 3 µl cDNA, 2 µl specific primer, 5 µl H_2O, and 10 µl SYBR Select Master Mix (Applied Biosystems). Analysis of data was performed with the BioRad CFX Manager software.

a) 95°C for 5:00
b) 95°C for 0:15
c) 60°C for 0:40
d) Plate read
e) Go to b) 39x
f) 55°C for 0:31
g) 55°C for 0:05 + 0.5°C/cycle, ramp 0.5°C/sec
h) Plate read
i) Go to g) 80x

10. Gene Knockdown Techniques

10.1. Plasmid Purification

A "stab" of bacteria containing the desired stock shRNA plasmid was taken with a toothpick and incubated in 200 µl of lysogeny broth (LB) for 1 hr at 37°C. Next, this 200 µl culture was added to 5 ml of LB + ampicillin (100 µg/ml) in 14 ml snap-cap tubes (Falcon) to allow some air circulation. The tubes were incubated for 20-22 hrs in a shaker at 200 RPM and 37°C. Post-incubation 1.5 ml was frozen down in a 10% glycerol mixture, and the remaining volume was purified according to the instructions of the GenElute HP Plasmid Miniprep Kit (Sigma).

10.2. Lentivirus Production

6well tissue culture plates were seeded with HEK 293T cells in complete medium (DMEM, 10% FBS and all supplements) to be 80-90% confluent the next day (approximately $2.3x10^5$ cells/well in 2 ml of medium). 30-60 min prior to transfection the culture medium was replaced with 500 µl of fresh complete medium. In one set of tubes, aliquots of 4.6 µl of packaging mix (Sigma), 0.5 µg of the desired shRNA construct DNA, and 20 µl complete medium was arranged. In a separate tube, per construct, 29.4 µl of complete medium and 3.6 µl of LipoD293 InVitro DNA Transfection Reagent (SignaGen Laboratories) were mixed together. The DMEM/LipoD293 mixture was added to the plasmid construct tubes and mixed by pipetting up and down. Mixtures were incubated for 15 min at RT, and then the entire transfection cocktail was added dropwise to the 6well plate of cells (directly into the medium). Plates were gently swirled every hour to homogenize the mixture and maximize contact with cells. At 5 hrs post-transfection, the medium was aspirated and replaced with 1 ml of pre-warmed complete medium. 24 hrs post-transfection, and every approximately 6 hrs thereafter, medium was collected and stored at 4˚C. After every 6 hr collection, 1 ml of pre-warmed complete medium was used to replace sample collection, and 2 ml was used for longer overnight incubations. Collections were stopped when 72 hrs post-transfection was reached or if cells appeared unhealthy. The pooled media were centrifuged at 250 x g for 10 min to remove any cells. Final pooled lentivirus media were run through a 0.45 um filter (Millipore) and stored at -80˚C.

10.3. Stable Cell Line Generation

To transduce target cells, 8 µg/ml sequabrene (Sigma) was added to the lentivirus pooled media, and then 500 µl of lentivirus/sequabrene mixture was added to each 12well of cells at

50-70% confluency. Cells were incubated for 4-6 hrs, gently swirling every hour. Then transduction mixture was replaced with complete cell medium. 48 hrs post-transduction, cells were subjected to selection with puromycin (Sigma) at 2.5 μg/ml in medium. Any subsequent culture of cells was performed with medium containing puromycin (2.5 μg/ml) to maintain selection pressure.

11. Gels and Blotting

11.1. Sample Collection

Before the total protein was harvested, cell monolayers were washed with 1x PBS. Following the wash step, a RIPA lysis buffer (1% NP4O, 0.1% SDS, 50 mM Tris, 150 mM NaCl, 0.5% Na Deoxycholate, 1 mM EDTA, pH 7.4) with added protease inhibitor (1:100; Invitrogen) was applied to the cells for 15-20 min on ice (100 μl for a 12well monolayer, 200 μl for a 6well monolayer). A 1:5 volume of protein sample buffer (PSB) was added to the total cell lysates, and the mixture was boiled for approximately 10 min at 100°C. Samples were then either run on an SDS-PAGE gel or stored at -20°C.

11.2. SDS-PAGE Gels

Protein lysates were fractionated on SDS-PAGE gels (8-12%). Gels were made in-house and stored at 4°C for up to two weeks, at which point any remaining unused gels were discarded. The gels were run at 100 V until samples passed through the stacking layer, at which point the settings were adjusted to 140 V for the duration of the electrophoresis.

11.3. Western Blotting

Proteins from the SDS-PAGE gels were transferred onto a nitrocellulose membrane (GE Healthcare 0.45 μm) using a Trans-Blot Turbo apparatus (BioRad). Following the transfer, membranes were rinsed in Tris-Buffered Saline (35.0 g NaCl, 24.2 g Tris Base, pH 7.5 in 1 L

water) with 0.1% Tween 20 (TBS-T) for 5 min and then treated with blocking buffer for 30-60 min. Blots were stained with a primary antibody for 60 min at room temperature or overnight at 4°C. Following the primary antibody staining, the membrane was washed three times with TBS-T for 5 min each and then stained with an appropriate secondary antibody for 60 min at room temperature (see **Table 3.2** for antibody concentrations). The membrane was then washed again in TBS-T three times for 5 min, before being scanned in a GE ImageQuant LAS 4000. If an HRP secondary antibody was used, 1.5 ml of substrate per blot was applied for 5 min before scanning in the ImageQuant under the CY2 wavelength.

12. Flow Cytometry

Cell monolayers were washed with 1x PBS, suspended in 100 µl of Trypsin (Invitrogen), and quenched with 1 ml of culture medium for collection by pipette. Cells were pelleted by centrifugation, washed in 1x PBS, pelleted again and then fixed by suspension in 4% paraformaldehyde for 45 min - 2 hrs at 4°C. Fixed cells were rinsed with 1x PBS and then suspended in blocking solution (PBS-T, 3% BSA) for 60 min at room temperature. Following blocking, the primary anti-reovirus antibody was added for 60 min at RT or overnight at 4°C. Cells were washed with 1x PBS following this step, and then secondary antibody was added for 60 min at RT. Cells were again washed with 1x PBS, pelleted, and then re-suspended in 500 µl of 1x PBS before processing with a BD LSR Fortessa. Data was analyzed using FCS Express software.

13. Cytokine Addition Assay

Cells were seeded on 96well plates. The next day the culture medium was removed from the confluent monolayer and dilutions of cytokines in culture medium was applied for 18 hrs. Cytokines were sourced from PBL Assay Sciences, and the dosages of cytokines were derived

from the maximal value quantified by multiplex ELISA (**Figure 4.4.1**; IFN-β 3,000 pg/ml, TNF-α 1,000 pg/ml, IFN-λ 12,000 pg/ml – equal 3-part mixture of IFN-λ1, IFN-λ2, IFN-λ3). Cytokines were added in 1:2 serial dilutions of that maximal value, down to 1:8 final dilutions. After 18 hrs of this treatment, the cytokine medium was removed from the cells and they were infected with a reovirus dosage specific to each cell line targeting a TCID of 50%. At 18 hpi medium was removed from the cells, and they were fixed and stained for reovirus protein (as described in **Methods 4.1**). Images of the cells were taken with a EVOS FL Auto microscope (Life Technologies).

Table 3.1. List of Cell Lines and Culture Media Used in this Project

Cell Line	Description	Culture Medium	Seeding Density (cells/ml) for confluency in 24 hrs
HEK 293T	human embryonic kidney cells with SV40 T-antigen and adenovirus type 5 E1A and E1B	DMEM	$2.5x10^5$
L929	normal mouse fibroblast	MEM	$2.0x10^5$
H522	lung epithelial adenocarcinoma; non-small cell lung cancer	RPMI	$4.0x10^5$
H1299	lung epithelial adenocarcinoma; non-small cell lung cancer	RPMI	$2.5x10^5$
H23	lung epithelial adenocarcinoma; non-small cell lung cancer	RPMI	$2.5x10^5$
A549	lung epithelial adenocarcinoma; non-small cell lung cancer	RPMI	$2.5x10^5$
H322	lung epithelial adenocarcinoma; non-small cell lung cancer	RPMI	$4.0x10^5$
SCC9	tongue squamous cell carcinoma	RPMI	$2.0x10^5$
A253	submaxillary salivary gland epidermoid carcinoma	RPMI	$2.5x10^5$

Volume of cell suspension (trypsinized cells in medium) used for seeding:

6well plate – 2 mL

12well plate – 1 mL

96well plate - 125µl

Table 3.2. List of Antibodies Used in this Project

Primary Antibodies				
Antibody	**Species**	**Source**	**Catalog #**	**Dilutions**
Primary Antibodies				
IFNλR1	rabbit	Abcam	ab83865	WB 1:500
IRF3	rabbit	Santa Cruz	sc-9082	WB 1:200
IRF7	mouse	Santa Cruz	sc-74471	WB 1:500
Mx1	rabbit	Santa Cruz	sc-5059	WB 1:200
P-IRF3	rabbit	Cell Signalling	4947	WB 1:1,000
P-STAT1	rabbit	Cell Signalling	9167	WB 1:1,000
STAT1	rabbit	Cell Signalling	9172	WB 1:1,000
α-Reo	rabbit	Shmulevitz Lab stock	n/a	WB, FCyt 1:10,000
β-Actin	mouse	Santa Cruz	sc-47778	WB 1:1,000
Secondary Antibodies				
α-rabbit HRP	goat	Jackson Immunoresearch	111-035-144	WB 1:10,000
α-mouse HRP	goat	Jackson Immunoresearch	115-035-146	WB 1:10,000
α-rabbit CY2	goat	Jackson Immunoresearch	111-545-144	FCyt 1:2,500
α-mouse CY2	goat	Jackson Immunoresearch	115-545-146	FCyt 1:2,500
α-rabbit CY5	goat	Jackson Immunoresearch	111-495-144	WB 1:3,000 FCyt 1:2,500
α-mouse CY5	goat	Jackson Immunoresearch	115-175-166	WB 1:3,000 FCyt 1:2,500
α-rabbit Alkaline Phosphatase	goat	Jackson Immunoresearch	111-055-144	IC 1:4,000
Neutralizing Antibodies				
IFN-β	sheep	PBL Assay Science	31400-1	600 NU/ml

WB = Western Blot

FCyt = Flow Cytometry

IC = Immunocytochemistry

Table 3.3. List of shRNA Constructs Used in this Project

Target Gene	Designation	Chosen As Best (Y/N)	The RNAi Consortium #
IFNAR1	IFNAR1-1	N	TRCN0000059013
IFNAR1	IFNAR1-2	N	TRCN0000059014
IFNAR1	IFNAR1-3	N	TRCN0000059015
IFNAR1	IFNAR1-4	Y	TRCN0000059016
IFNAR1	IFNAR1-5	Y	TRCN0000059017
IFNAR2	IFNAR2-1	N	TRCN0000058784
IFNAR2	IFNAR2-2	N	TRCN0000058785
IFNAR2	IFNAR2-3	N	TRCN0000058786
IFNAR2	IFNAR2-4	N	TRCN0000058787
IFNAR2	IFNAR2-5	Y	TRCN0000058783
IL28RA	IFNλR1-1	N	TRCN0000058988
IL28RA	IFNλR1-2	N	TRCN0000058989
IL28RA	IFNλR1-3	Y	TRCN0000058990
IL28RA	IFNλR1-4	N	TRCN0000058991
IL28RA	IFNλR1-5	Y	TRCN0000058992
IRF3	IRF3-1	Y	TRCN0000005919
IRF3	IRF3-2	N	TRCN0000005920
IRF3	IRF3-3	N	TRCN0000005921
IRF3	IRF3-4	Y	TRCN0000005922
IRF3	IRF3-5	N	TRCN0000005923
IRF7	IRF7-1	N	TRCN0000014859
IRF7	IRF7-2	N	TRCN0000014860
IRF7	IRF7-3	N	TRCN0000014861
IRF7	IRF7-4	Y	TRCN0000014858
IRF7	IRF7-5	Y	TRCN0000014862

Table 3.4. List of Primers Used in this Project

Target	Forward		Reverse	
	Position	Sequence	Position	Sequence
GAPDH	--	cgaccactttgtcaagctca	--	aggggagattcagtgtggtg
Reovirus S4	--	ggaacattgtgagagcagca	--	gcaagctagtggaggcagtc
IFN-λ1 (IL29)	124	ggtgactttggtgctaggct	256	ggccttcttgaagctcgcta
IFN-λ2/3 (IL28A/B)	448	tatcctctcccagttccggg	595	gttgaaggtgacagaggcct
TNF-α	--	ctgggcaggt--ctactttggg	--	gagccagaagaggttgaggg
IFN-β	--	cctgaaggccaaggagtaca	--	cagcatctgctggttgaaga
IL28RA (IFNλR1)*	--	cacgggccctggacttttct	--	ctgcaaggtccttcttccatctt
IFNAR1	--	atcggtgctccaaaacagtc	--	gtgctctggctttcacacaa
IFNAR2	--	cccttaaaatgcaccctcct	--	tcaagactttggggaggcta
IRF3	--	tcagggccttggtagaaatg	--	gcaggtaggccttgtactgg
IRF7	--	taccatctacctgggcttcg	--	tgctgctatccagggaagac
Viperin (RSAD2)	589	cgtgagcatcgtgagcaatg	731	tcttctttccttggccacgg
IFITM3	464	catcgtcatcccagtgctga	580	agggcgaggaatggaagttg
Mx1	2681	agctcggcaacagactcttc	2808	ccgtacgtctggagcatgaa
OAS2	--	ggtgaacaccatctgtgacg	--	taccatcggagttgcctctt
Ifi44	64	agacagagcagctaccctca	198	ctaagccgcttccctccaaa
TRIM22	--	ctgtgcctccctgtcgtatt	--	ctccgtggtttgtgacattg
PLEKHA4	--	ggcttcataagcaggacagc	--	gacgctgcctaggacactct

* this primer sequence was kindly shared with me by Dr. Deanna Santer

CHAPTER 4: RESULTS

Contribution of others: Data for the spread of infection of A253 and SCC9 cells (**Results Section 1.2, Figure 4.1.2**) was the work of undergraduate project student David Fast and medical student Timothy Cooper. All other results are my own work.

1. Characterization of reovirus infection in lung and head and neck cancer cells reveals a stratification of susceptibility to the virus

Prior to commencement of this project, it had been established in the Shmulevitz lab that A549 lung cancer cells were less susceptible to reovirus infection than H1299 lung cancer cells or L929 mouse fibroblasts. My first goal was to establish the extent of susceptibility to reovirus in additional HNSCC and lung cancer cells that were included to form a larger panel of cell lines to study and compare with each other.

1.1. Higher MOIs are required to establish initial infection in A549, H322, SCC9 and A253 cells

To pinpoint the amount of reovirus needed to achieve specific initial TCIDs for future experiments, the cell lines of the panel were exposed to various doses of reovirus (doses are provided as an MOI based on titres obtained on highly permissive L929 mouse fibroblasts), stained for reovirus protein expression, and quantified by flow cytometry at 18 hpi. H522 and H1299 lung cancer cells had the greatest susceptibility to initial infection, they reached 20% infection at MOIs of 0.5 and 1.2 respectively, similar to known susceptible L929 cells. The 4 other cancer cell lines (A549, H322, SCC9, A253) required a higher initial dose of virus to reach 20% infection, notably so for A549 and SCC9 cells. The infection curves of these 4 cell lines also began to taper off and plateau as MOIs increased rather than progressing towards complete infection as was seen with infected cells like L929, H522, and H1299 cells (**Figure 4.1.1**). This suggests that some cell lines (L929, H522, H1299) are more permissive to

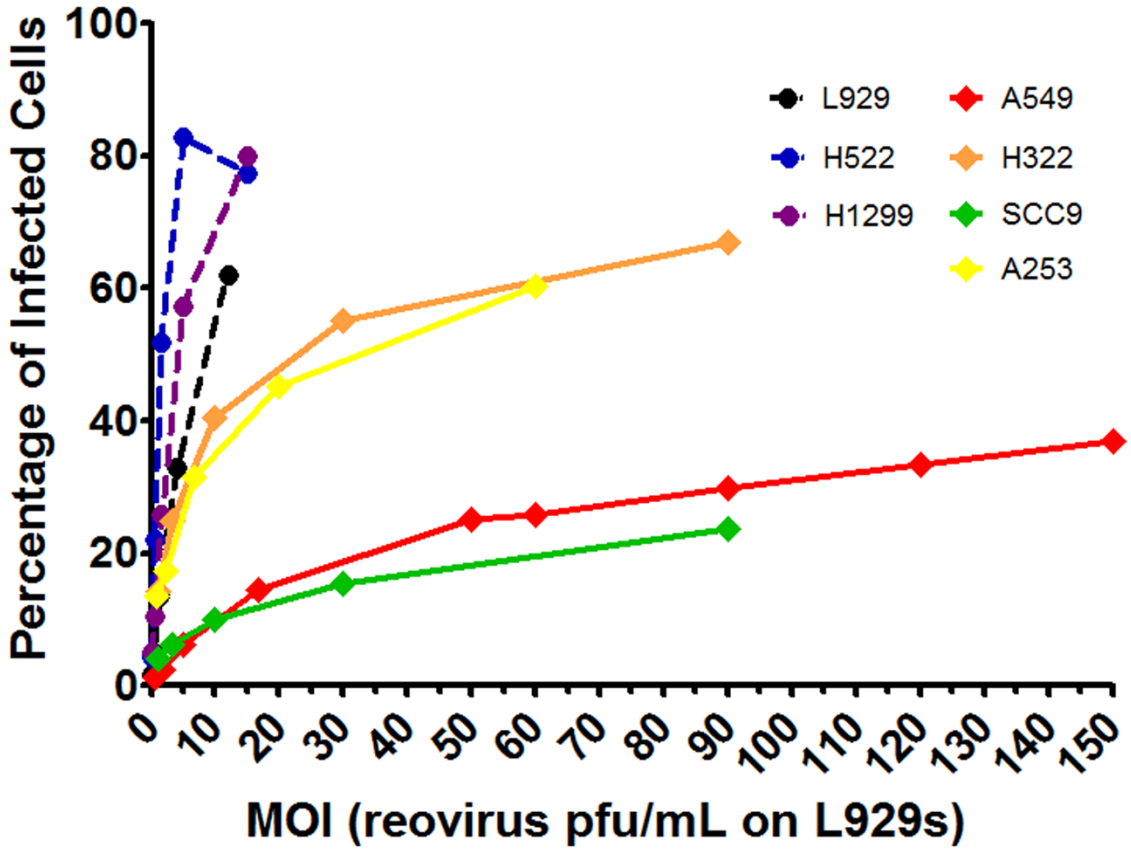

Cell Type	MOI (pfu/cell) resulting in a 20% TCID
L929	2.2
H522	0.5
H1299	1.2
A549	31.0
H322	2.2
SCC9	56.0
A253	3.5

Figure 4.1.1. The amount of reovirus virions required to establish infection varies greatly between cell lines. Cells were exposed to 1/3rd serial dilutions of reovirus. At 18 hpi, cells were fixed and stained with reovirus-specific antiserum and fluorescence-conjugated secondary antibodies to detect productively infected cells by flow cytometry. Multiplicity of infection (MOI) was calculated from titers obtained on the highly permissive L929 mouse fibroblast cell line. Data above represents one experiment.

productive infection with reovirus, while other cell lines (H322, A253, A549, SCC9) may have methods of limiting reovirus infectivity.

1.2. Decreased spread of infection as measured by reovirus protein levels was observed in A549, H322, SCC9 and A253 cells

To check for differences in the cell-cell spread of reovirus infection following the initial round of replication, a cell-based ELISA assay was used to quantify reovirus protein levels in the panel of cell lines (as described in methods section). All cell lines were exposed to the same ¼ serial dilutions of reovirus and assessed for reovirus protein levels at 18 hpi (representing initial infection) and 48 hpi (following the second round of infection). Dose-response curves were used to calculate EC50 values, defined as the effective concentration of reovirus needed to produce 50% of maximal reovirus protein for a given cell line. Dividing the 18 hpi EC50 by the 48 hpi EC50 gave a 'coefficient of spread' for each cell line, with a value of 1 representing no spread of infection occurring from 18 hpi to 48 hpi (**Figure 4.1.2**). The HNSCC cell lines had the lowest values, meaning they were the most resistant to reovirus spread of the panel tested. The spread coefficient for SCC9 cells was 1.4 ± 0.12, and for the A253 cells it was 0.4 ± 0.06, indicating that A253 cells remarkably had lower levels of reovirus protein at 48 hpi than they did at 18 hpi. A549 and H322 lung cancer cells both had values of 4.6 (A549 ± 1.3; H322 ± 2.5), and were classified as resistant to the spread of reovirus. That is because the values were much higher for H1299 and H522 lung cancer cells, 33.3 ± 8.9 and 80.5 ± 30.0 respectively. Those two cell lines were classified as susceptible to reovirus spread, in addition to the positive control L929 mouse fibroblasts, which were known to be susceptible and had a spread coefficient of 70.8 ± 2.4. H23 cells were also tested and had a spread coefficient of 9.9 ± 3.6, fitting a more intermediate phenotype between cells that are resistant to spread and those that are very susceptible.

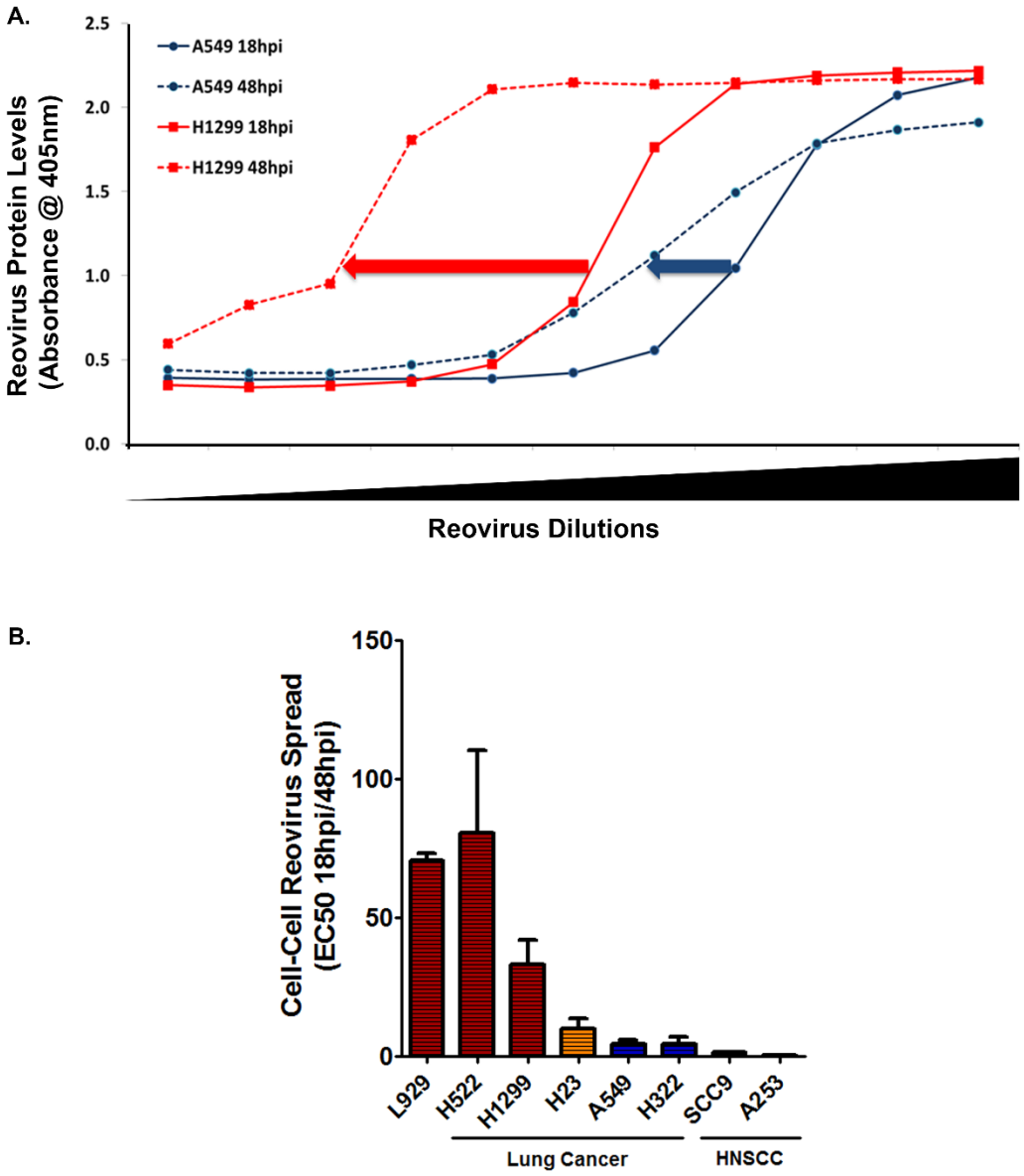

Figure 4.1.2. Cancer cell lines show varied susceptibility to reovirus dissemination. Cells were exposed to 1/4th serial dilutions of reovirus. At 18 hpi (initial infection) and 48 hpi (secondary infection), cells were fixed and subjected to cell-based ELISA to quantify reovirus protein levels. **A)** Representative data of reovirus dose-response curves for two lung cancer cell lines. A greater distance between the solid (18 hpi) and dashed (48 hpi) curves indicates greater cell-to-cell reoviral spread as is visible in H1299 cells (red) relative to A549 cells (blue). **B)** EC50 analysis of lung cancer and HNSCC cell lines reveals that L929, H522, and H1299 cells (shown in red) are significantly more susceptible to secondary cell-to-cell spread of reovirus than the other cells. Reovirus does not spread as effectively between A549, H322, SCC9, and A253 cells (blue), while H23 cells (orange) are intermediate in phenotype. Each cell line was tested in a minimum of 4 independent experiments, error bars represent standard deviation.

2. Differences in early progeny virion release following initial infection in cells are not solely responsible for differing susceptibility to reovirus infection

Reovirus is an oncolytic virus that spreads between cells when new virions are released following cell death.[175] Therefore, it made sense to assess the role and importance of cell death in the differences in reovirus susceptibility observed across the cancer cell panel.

2.1. All cancer cell lines in the tested panel have the capacity to establish a productive reovirus infections

Screening the panel of cancer cell lines revealed that they possess differing susceptibilities to reovirus infection, however it was important to demonstrate that reovirus was capable of establishing a productive infection in all cell lines so that comparisons between cell lines are valid.

To verify that the cell lines could support productive reovirus infection, cells were infected with reovirus sufficient for an initial TCID of 75% as previously determined by cell staining. It was decided to infect a high amount of cells initially because the goal was not to examine cell-to-cell spread of virus, but to see if infection would successfully take hold of the cells and if infectious virions were produced. Cell lysates were harvested at 18, 24, 30, and 40 hpi and plaque assays were performed (as described in methods section). Reovirus titres (pfu/mL on L929 cells) for all cell lines reached at least $1x10^7$ by 18 hpi, and at the end of the time-course titres had plateaued in the $1x10^8$-10^{10} range (**Figure 4.2.1 panel A**). Therefore, all cell lines are capable of sustaining a productive reovirus infection.

2.2. H322 and A253 cancer cells restrict early release of the progeny virions

Sampling the media of infected cells over the 40 hour time-course described above (section 4.2.1) and titrering it on L929 cells enabled quantification of the amount of virus being released by the cells. Comparing released virus from media samples with the titres calculated from total

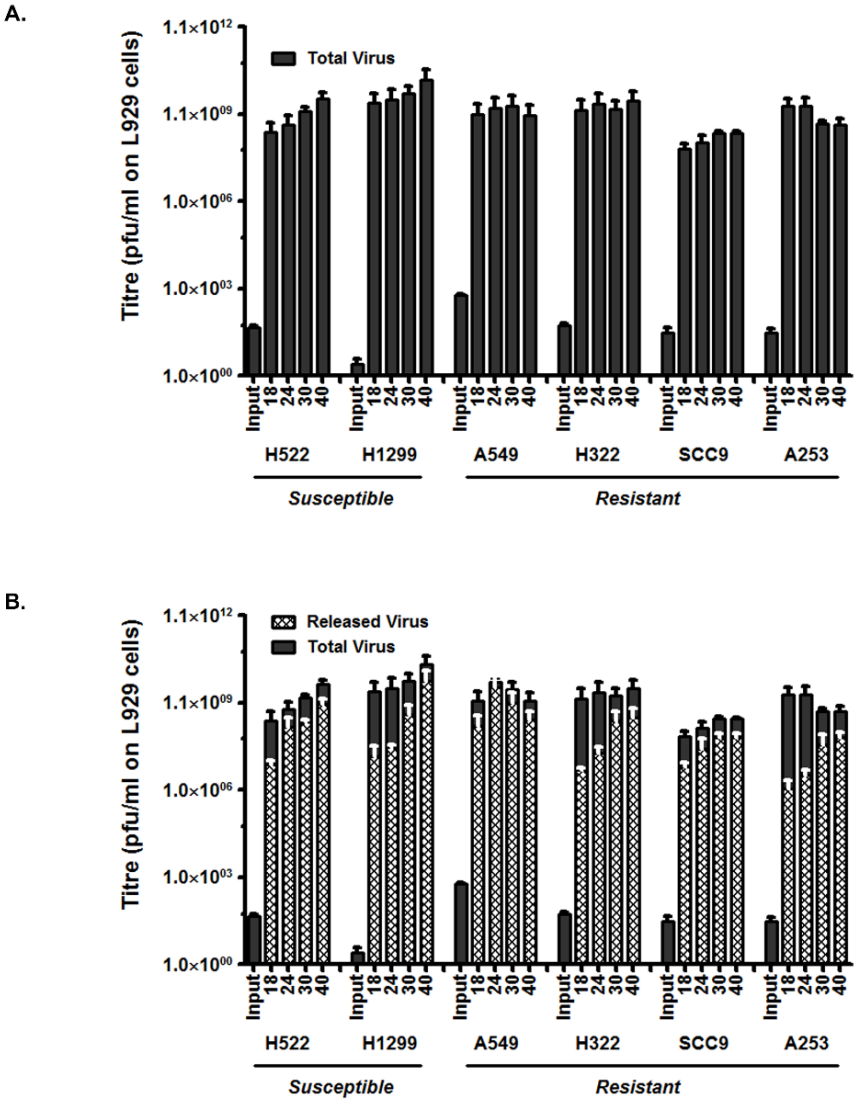

Figure 4.2.1. All cell lines can sustain productive reovirus infection, but H322 and A253 cells restrict the release of progeny virions in comparison to other resistant cells. Cells were infected with a TCID of 75% and samples of lysate and media were collected and titred on L929 cells. Data represents 2 independent experiments, titred in quadruplicate. Graphs are log2 scaled. **A)** Titres of lysate collected from cell lines over a time-course from 18 hpi to 40 hpi, representing the total virus produced by the cells. All cell lines in the panel sustain productive infections and saturate the system. **B)** Titres of the virus released into the cell culture media are shown as white bars overlaid on top of the total titres (in black). Among the four less susceptible cell lines, H322 and A253 cell show reduced release of infectious progeny virions, especially over the first 24 hpi.

lysates (combined cell lysate and media; results section 4.2.1) representing the complete amount of virus in the system, enabled calculation of the percentages of virus being released by the different cell lines.

As can be seen in **Figure 4.2.1 panel B**, of the four cell lines that were resistant to reovirus dissemination, H322 and A253 cells show the lowest titres of virus released into media within the first 24 hpi. The titre of reovirus released into media by H322 cells is ~2% of the total virus in the system at 18 hpi, and ~3% at 24 hpi. For A253 cells the titre of the released virus is less than 1% at both 18 hpi and 24 hpi. In comparison, the percentage of infectious virions released by A549 and SCC9 cells at 18 hpi is in the 9-10% range, and is even higher at 24 hpi. This means H322 cells release 5-6 fold less infectious reovirus virions and A253 cells release over 100 fold less.

2.3. Restriction of early progeny virion release is not solely responsible for H322 cell and A253 cell resistance to spread of reovirus infection

To determine if the reduced virion release over the first 24 hpi by H322 and A253 cells in comparison to A549 and SCC9 cells was the main mechanism for limited spread of infection, an assay was designed to simulate a greater virion release by H322 and A253 cells (see methods section). Following initial infection at a TCID of 20%, additional reovirus was spiked into the culture media at 24 hpi to simulate a permissive release of virus, but this did not result in a corresponding equivalent increase in infection when the cells were stained at 48 hpi (**Figure 4.2.2 panel A**). To calculate the percent of infected cells, Hoechst nuclear staining was used to obtain a total cell count and immunocytochemistry staining was used to identify infected cells. The A253 cells, which have a profile of clearing reovirus by 48 hpi, were initially 19% infected and the reovirus spike added at 24 hpi was sufficient to infect 29% of cells on its own.

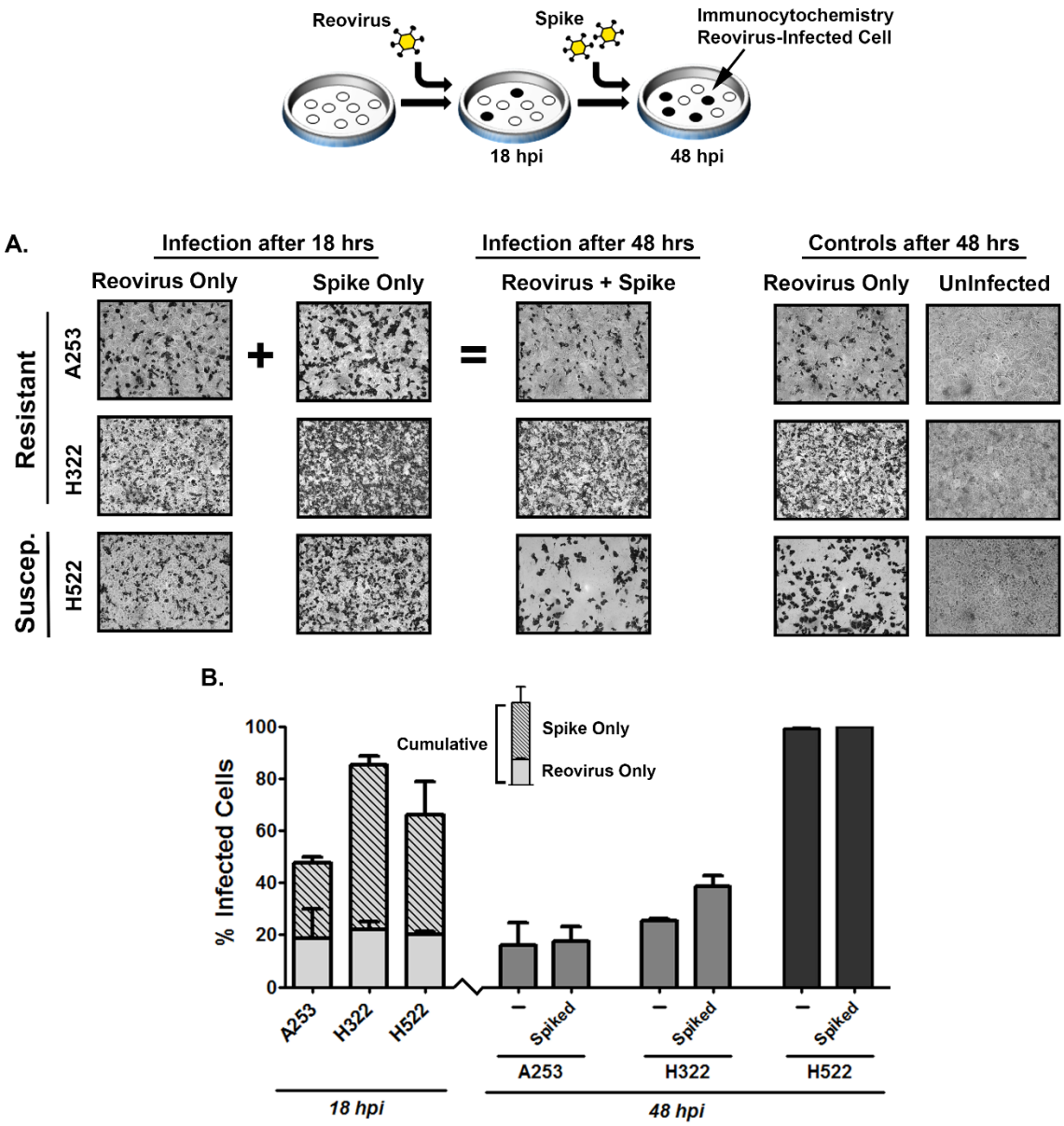

Figure 4.2.2. Simulating a more permissive virion release had minimal effect on increasing the final infection in A253 and H322 cells. Cells were infected to an initial TCID of 20% and allowed to progress to 48 hpi before staining for reovirus protein expression. Additional reovirus was spiked into the media of some samples (Spiked) at 18 hpi to simulate a greater release of virus. **A)** Immunocytochemistry staining shows reovirus infection (black). Unstained space is filled with confluent healthy cells, except in the case of H522 cells at 48 hpi where all cells are either infected or dead, leaving empty space. Images are representative of 2 independent experiments. **B)** Cells were stained with Hoechst to obtain a total cell count; percent infection was quantified by comparing reovirus-infected cells versus total cells. The addition of an extra reovirus spike did not result in an increase in A253 cell infection, and only a small increase in H322 cell infection. Bars represent SD from 2 the separate experiments.

Therefore, at 48 hpi it would be expected that at least a combined 48% of A253 cells would be infected with reovirus. However, only 18% of cells were infected 48 hpi even with the added reovirus meant to simulate a more permissive release; that was a marginal increase on the 16% infection observed in A253 cells that did not receive extra reovirus spiked into culture media (**Figure 4.2.2 panel B**). H322 cells, which allow a very limited spread of infection, were initially 22% infected and the amount of reovirus added in as a spike was able to infect 63% of cells on its own. Therefore, when the initial infection and spike of reovirus were combined you would expect approximately 85% of cells to be infected, yet when the cells were stained at 48 hpi only 39% were reovirus infected, although still an increase from 26% of cells infected at 48 hpi with no spike added. The permissive H522 cells, acting as a positive control were 99% infected by 48 hpi off an initial 20% infection, so the additional reovirus spike only served to ensure 100% of cells were infected at endpoint and to increase cell death. We had expected that when additional reovirus was spiked into the media of H322 and A253 cells the amount of infected cells would increase. Conversely, when we saw infection increase only minimally in proportion to the amount of extra virus added, we concluded that limited cell death was not responsible for reducing reovirus spread.

3. Cell culture media from infected cells possesses antiviral properties

With differences in cell death among the cell lines being ruled out as the sole determinant for resistance to reovirus spread, it was hypothesized that the resistant cells were producing some sort of antiviral factors that could be detected in culture media. To test this possibility, the working panel of cancer cell lines was infected to a TCID of 20-50% (twice; and once at a TCID of 50%) and then the media samples were collected at 18 hpi. Reovirus particles were removed and inactivated using ultracentrifugation and UV treatment before medium was

transferred onto A549 cells as a pre-treatment prior to reovirus infection. A549 lung cancer cells are known to respond to soluble antiviral factors such as, but not limited to, IFN-α, IFN-β and TNF-α.[176, 177, 178] Following an 18 hr pre-treatment with transferred media, the A549 cells were exposed to a standard dose of reovirus and stained for infected cells 18 hrs later. As can be seen in **Figure 4.3.1**, media pre-treatments that came from the resistant cell lines had a greater protective, anti-reovirus effect on the A549 cells in comparison to media from the more susceptible H1299 and H522 cell lines.

4. Cancer cell lines that are more resistant to reovirus produce greater amounts of antiviral cytokines and mRNA transcripts than more susceptible cells

Following the observation that culture media from reovirus infected cells potentiates an anti-reovirus response in A549 cells, it was decided to profile the cytokines present in the media of infected cells. Cells were infected at a TCID of 20%, and at 18 hpi the cell culture media and cell lysates were collected separately for storage at -80°C. Media and lysates were collected in this manner from 3 independent experiments. The media samples were analyzed by a multiplex ELISA assay that detected various antiviral cytokines. The lysates were used to make cDNA from which levels of various antiviral transcripts were measured by quantitative reverse-transcription polymerase chain reaction (qRT-PCR).

4.1. Cytokine Levels are highest in media of infected resistant cells

The multiplex ELISA assay used to profile the cell culture media detected various well known antiviral molecules such as the Type I, II, and III IFNs, TNF-α and other cytokines such as IL-6, IL-1α and IP-10. Analytical focus was narrowed onto Type I and III IFN and TNF-α because of their known antiviral properties.[108, 146] Type II IFN (IFN-γ) production is limited to

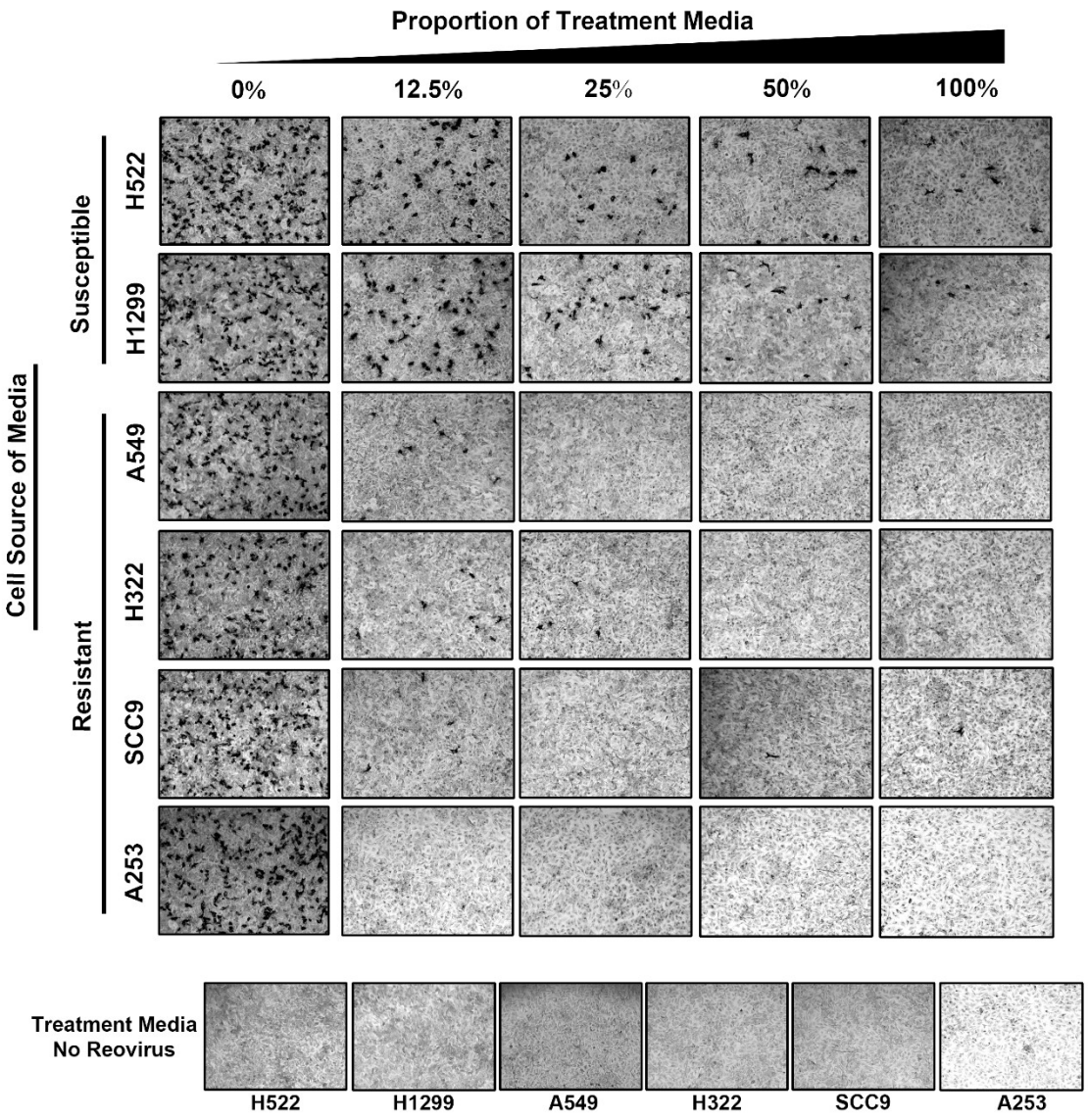

Figure 4.3.1. Transfer of cell culture media from resistant cell lines confers greater anti-reovirus protection on A549s than media from more susceptible cell lines. Cell lines were infected with reovirus and culture media was collected at 18 hpi. Media was depleted of reovirus particles by UV-treatment and ultracentrifugation. The media was then applied as a pre-treatment on A549 cells for 18 hours prior to infection with reovirus. Reovirus stained cells appear black. This image is representative of results from 3 independent experiments.

T cells and NK cells and was therefore excluded from my data analysis.[179] Data profiling the amounts of IFN-γ, IL-6, IL-1α and IP-10 detected can be seen in **Appendix A**.

The overall trend observed by multiplex ELISA was that the cell lines most resistant to reovirus infection produced the greatest amount of antiviral cytokines. The exception to this group was the H322 lung cancer cells, which have a cytokine profile that is more similar to the susceptible H1299 and H522 cells than to the other resistant cell lines (**Figure 4.4.1 panel A**). This was surprising and interesting because media transferred from infected H322 cells was observed conferring an anti-reovirus state in A549 cells (**Figure 4.3.1**), and the limitation of cell death had already been ruled out as the reason H322 cells resisted reovirus spread (**Figure 4.2.2. panel B**).

As seen in **Figure 4.4.1 panel B**, IFN-β was the most highly secreted Type I IFN, approximately 5 times more concentrated in media than levels of IFN-α, which itself was detected in greater levels in media than IFN-ω. Overall, the most abundant cytokines detected in cell media were the Type III IFNs (IFN- λ1/2/3), followed by IFN-β, and then TNF-α (**Figure 4.4.1 panel C**). A549 cells secreted the greatest amount of IFN-β and IFN-λ, 10x the amount released by the most susceptible H522 and H1299 cells. SCC9 cells secreted the greatest amount of TNF-α, 8.5x the amount secreted by H522 cells (**Table 4.4.1**). IL-1α was also detected in smaller quantities, and was induced the most by the resistant HNSCC cell lines in response to reovirus (**Figure 4.4.1 panel A**).

4.2. mRNA expression of cytokine transcripts is highest in the more resistant cells

Expression of cytokine mRNAs showed higher production in cells that are resistant to reovirus spread, broadly matching the trend that was observed in the ELISA that detected the cytokines present in culture media. The resistant cells all produced greater levels of IFN-λ and

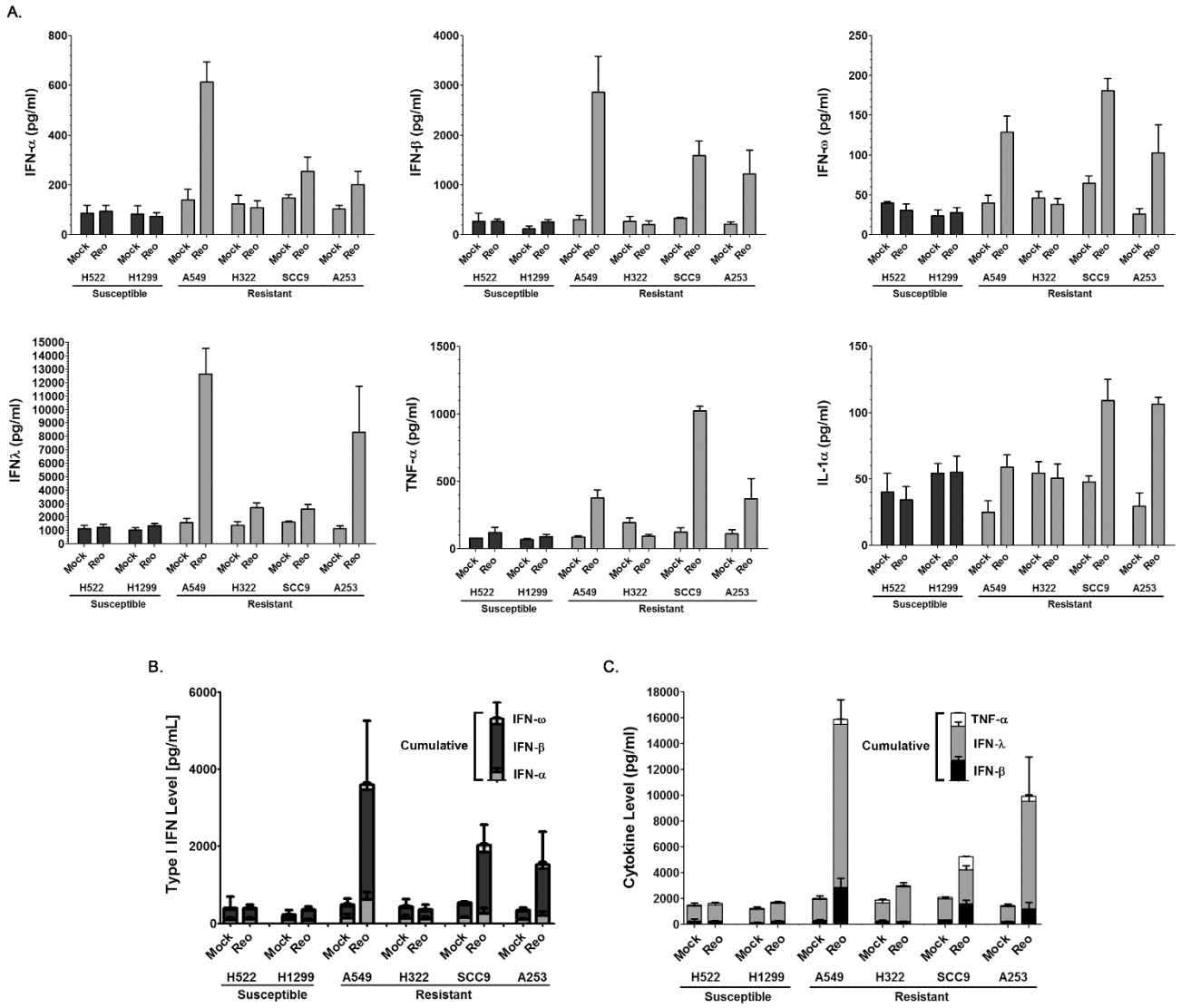

Figure 4.4.1. Resistant cell lines A549, SCC9 and A253 secrete the most cytokines in response to reovirus infection. Cell lines were infected with reovirus and culture media was collected 18 hpi for quantification of cytokine content by multiplex ELISA. Data are from 3 independent experiments, with samples tested in duplicate. **A)** Basal levels of cytokines in uninfected cells were similar across the panel, however, post-infection the resistant cells secreted higher amounts of Type I and III IFNs, TNF-α, and IL-1α. The H322 cell line is the exception from the group of resistant cells, secreting cytokines in amounts similar to the susceptible cells. Cells susceptible to reovirus spread are represented by black bars, cells more resistant to spread are represented by grey bars. **B)** For easy comparisons, Type I cytokines values were re-plotted together in one graph. IFN-β is the most plentiful of the Type I IFNs; it is secreted by all cells in much greater amounts than IFN-α or IFN-ω. **C)** The 3 cytokines secreted into media in the highest quantity were IFN-λ, IFN-β, and TNF-α respectively. This was consistent across all cell types in the panel.

TNF-α transcripts than the susceptible cell lines (**Figure 4.4.2**). IFN-β mRNA expression was higher in 3 of 4 resistant cell lines (A549, SCC9, A253), but strong induction in H1299 cells coupled with low transcription in H322 cells meant it did not apply to every resistant cell line.

Levels of mRNA expression were compared relative to H522 cells which are the most susceptible to reovirus spread (**Table 4.1.1**). While H322 cells had 10x less IFN-β mRNA than H522 cells, H1299 cells did generate a markedly stronger IFN-β mRNA response to infection than their susceptible counterpart (128x > H522 cells). This is in contrast to the low IFN-β secretion profile of H1299 cells, which matches the H522 cells, and suggests some defect(s) may be present downstream of the transcription step in H1299 cells. TNF-α mRNA expression was 2-8 fold greater than H522 cells in the A549, H322, and A253 cells. The resistant SCC9 cells had by far the most TNF-α mRNA (34x > H522 cells), which correlates to the ELISA results where SCC9 cells secreted the most TNF-α. Levels of IFN-λ mRNA were ~200-1800x greater in resistant cells than H522 cells, although this only translated into a 2-10x increase in cytokine secretion. A similar disparity was seen between levels of IFN-β mRNA and cytokines.

4.3. mRNA expression of Type I and III IFN receptors does not correlate with a cell's susceptibility to reovirus infection

Production of cytokines is one aspect of a cell's innate antiviral defenses, but an equally important part is the ability to detect and respond to antiviral cytokines. Therefore, cell lines in the cancer panel were screened for levels of both IFNAR1 and IFNλR1 transcripts by qRT-PCR. Receptor mRNA levels did not correlate with susceptibility as the two cell types with the highest expression were H522 cells and A253 cells, which are susceptible and resistant to reovirus respectively (**Figure 4.4.3 panel A**). Induction of the two receptors in response to reovirus infection was typically not observed, with the exception of A549 and A253 cells

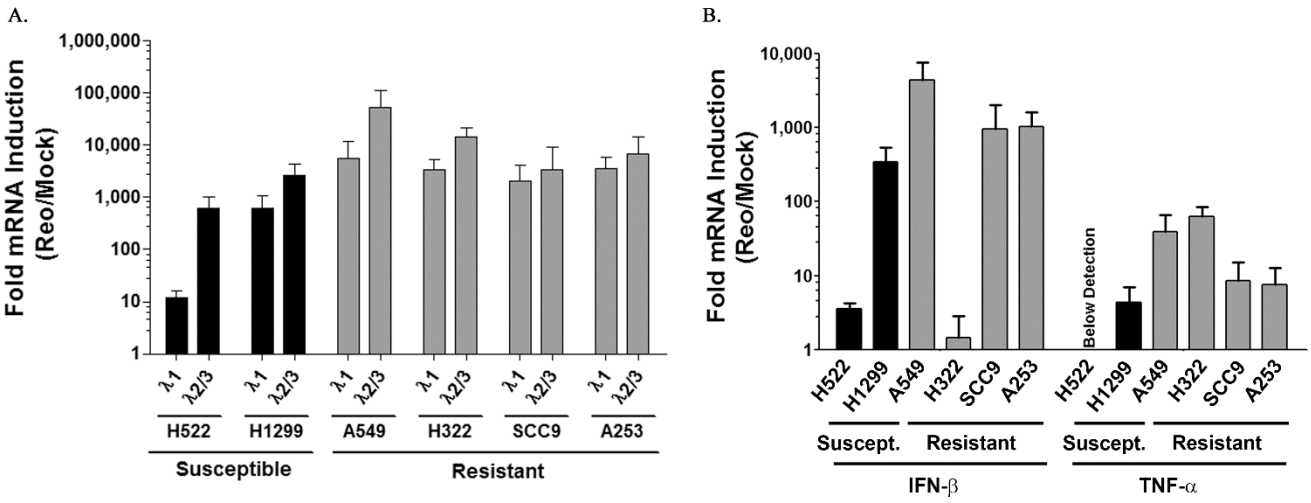

Figure 4.4.2. Cells that are more resistant to reovirus produce greater amounts of mRNA transcripts for antiviral cytokines. Cell lines were infected with reovirus and lysates were collected 18 hpi for RNA purification and subsequent qRT-PCR analysis. Cells susceptible to reovirus spread are represented by black bars, cells more resistant to spread are represented by grey bars. Data measured the induction of mRNA post-infection from 3 independent experiments, error bars represent SD. **A)** Levels of IFN λ1, λ2/3 transcripts are highest in the cells that are resistant to reovirus. **B)** IFN-β induction was highest in the resistant cell lines, except for H322 cells, which were less responsive than susceptible H1299 and H522 cells. TNF-α was mRNA was upregulated the most in all resistant cells, and no value was calculated for susceptible H522 cells as mRNA levels were below detection in uninfected cells.

Table 4.4.1. Fold-Difference of Reovirus Induced mRNA Transcripts and Soluble IFN-β, IFN-λ, and TNF-α. mRNA transcript levels (detected by qRT-PCR) and soluble cytokine amounts (detected by ELISA) from reovirus infected samples (TCID 20%) were collected 18 hpi in 3 independent experiments. Values are displayed are averages of those 3 experiments, relative to the most susceptible H522 cells.

Cell Type	IFN-β		IFN-λ		TNF-α	
	mRNA	Cytokine	mRNA	Cytokine	mRNA	Cytokine
H522	1.0	1.0	1.0	1.0	1.0	1.0
H1299	127.7	1.0	43.0	1.1	0.2	0.8
A549	1554.8	10.5	1705.9	10.2	8.4	3.1
H322	0.1	0.8	204.5	2.2	2.6	0.8
SCC9	2585.4	5.8	171.8	2.1	34.0	8.5
A253	517.0	4.5	757.7	6.7	2.3	3.1

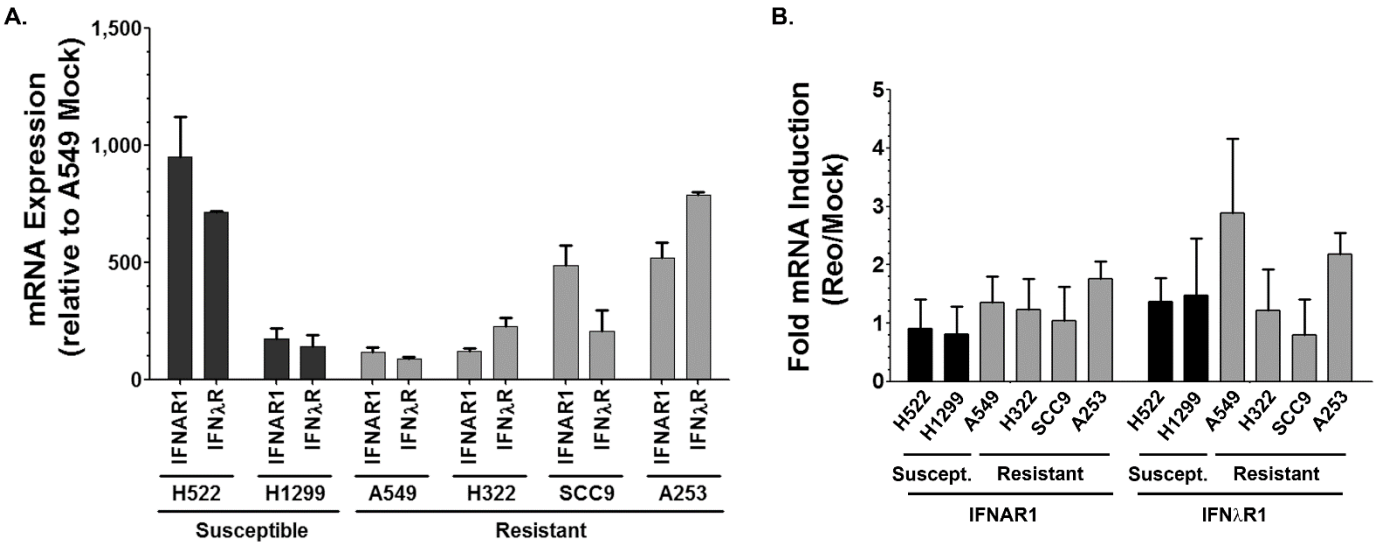

Figure 4.4.3. The expression of Type I and Type III IFN receptor mRNA does not correlate with cell susceptibility to reovirus. Cell lines were infected with reovirus and lysates were collected 18 hpi for RNA purification and subsequent qRT-PCR analysis. Cells susceptible to reovirus spread are represented by black bars, cells more resistant to spread are represented by grey bars. Data are from 3 independent experiments, error bars represent SD. **A)** Within each cell line the mRNA levels of the IFNAR1 and IFNλR receptor subunits are similar to each other. The exception is SCC9 cells, which have 2x the expression of IFNAR1. Highest receptor expression was surprisingly seen in the most susceptible H522 cells. **B)** Receptor levels of IFNAR1 remained stable in response to reovirus infection. There did appear to be some induction of the IFNλR receptor in A549 cells (~3-fold) and A253 cells (~2-fold).

where the levels of IFNλR1 mRNA approximately doubled (**Figure 4.4.3 panel B**). It should be noted though that the levels of the IFNAR and IFNλR1 receptors expressed on the cell surface is unknown.

4.4. mRNA expression of ISGs and other select genes of interest varies between a few different phenotypic profiles

The cell lines in the cancer panel were tested for mRNA expression of known antiviral ISGs and other genes of interest such as PLEKHA4 that had been previously identified by Dr. Shmulevitz by microarray (personal communication, Dr. Shmulevitz) as potentially correlating with susceptibility to reovirus infection. In total, 7 different genes were analyzed for expression via qRT-PCR (**Figure 4.4.4**). A few different trends in mRNA expression were observed; the most common trend was the HNSCC cell lines SCC9 and A253 had higher basal levels of transcripts prior to infection than all the lung cancer cell lines did, both resistant and susceptible. This was observed with expression of OAS2, Ifi44, Viperin, and TRIM 22 (**Figure 4.4.4 panel A**). IFITM3 and PLEKHA4 display a similar phenotype, but interestingly, along with high expression in the HNSCC cells the it is the susceptible H1299 and H522 cells which also showed higher basal transcript levels, and not the resistant A549 and H322 cells like one might expect (**Figure 4.4.4 panel B**). Finally, expression of Mx1 had its own pattern, resistant H322 and SCC9 cells had the lowest expression (**Figure 4.4.4 panel C**). Reovirus infection induced notably higher transcript expression of all 7 genes in all resistant cells except for Mx1 in SCC9 cells. Interestingly, reovirus infection also induced greater mRNA expression of all 7 genes in the susceptible H1299 cells as well, which was not observed in H522 cells.

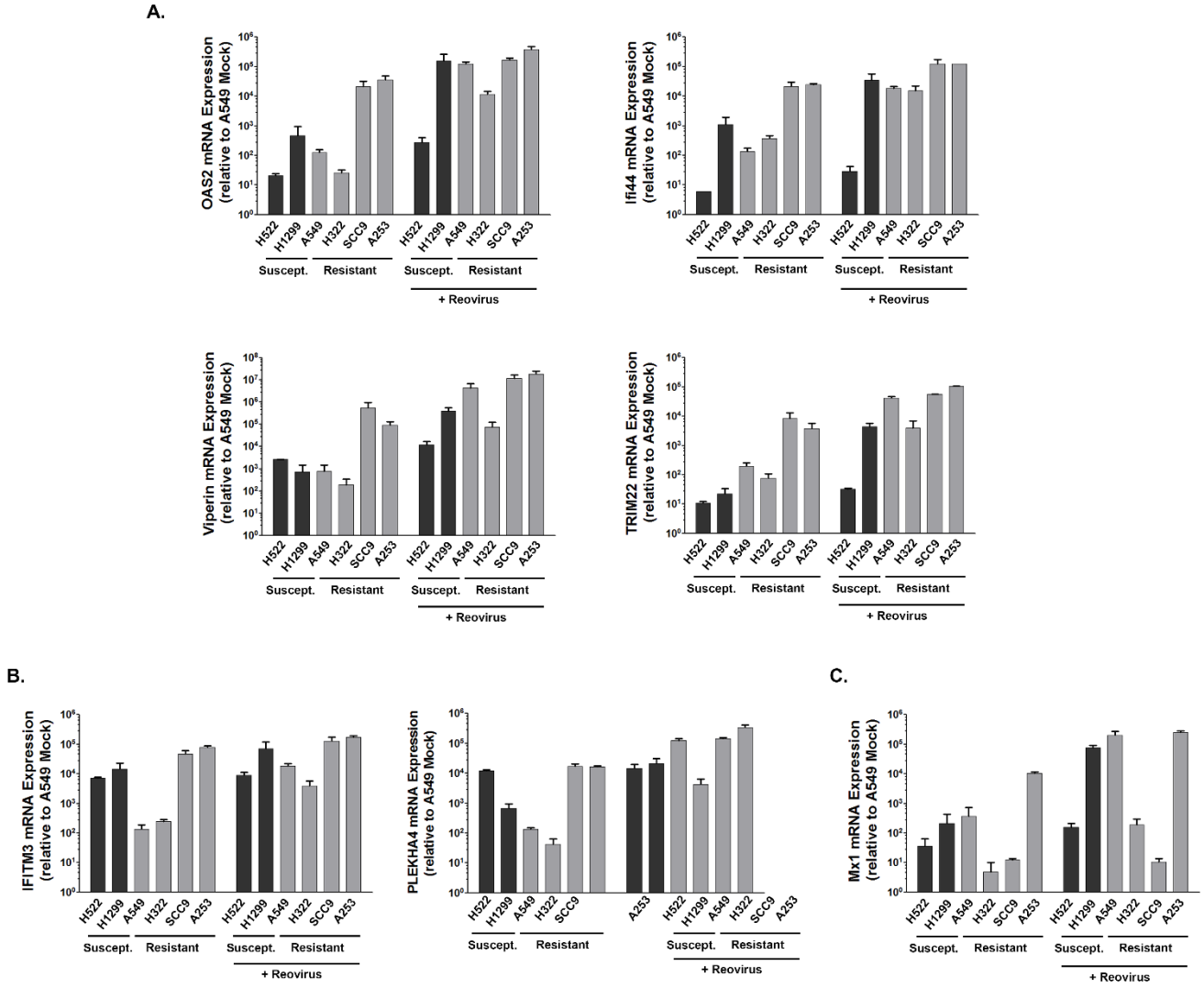

Figure 4.4.4. mRNA expression of ISGs and other genes of interest varies between a few select phenotypes. Cell lines were infected with reovirus and lysates were collected 18 hpi for RNA purification and subsequent qRT-PCR analysis. Data are from 3 independent experiments; error bars represent SD. Cells susceptible to reovirus spread are represented by black bars, cells more resistant to spread are represented by grey bars. Upregulation of mRNA expression in response to reovirus was generally strong in the resistant cell lines, as well as in the susceptible H1299 cells. **A)** Basal expression of OAS2, Ifi44, Viperin, and TRIM22 mRNA is highest in the SCC9 and A253 HNSCC cell lines. **B)** Basal expression of IFITM3 and PLEKHA4 mRNA is high in the SCC9 and A253 HNSCC cell lines, and similarly high in the H522 and H1299 susceptible lung cancer cells. **C)** Mx1 exhibits an mRNA expression profile that is more unique, with H322 and SCC9 cells possessing lowest transcript levels.

5. Inhibition of the Type I and Type III IFN Pathways is insufficient to confer susceptibility to reovirus in model system A549 cells

A549 cells were selected as the model for a reovirus dissemination-resistant cancer cell as a result of their limitation of reovirus cell-cell spread, production of antiviral cytokines, and response to media transfer (**Results Sections 1, 3, 4**). Neutralizing antibodies and shRNA knockdowns were used to inhibit segments of the Type I and Type III IFN pathway to see if the A549 cells became more susceptible to reovirus as a result. If normally resistant A549 cells could be reverted to susceptible, it would implicate the signalling pathway that was inhibited as key in establishing resistance.

5.1. IFN-β neutralizing antibodies effectively inhibit STAT1 signalling in A549 cells

A549 cells were used to test the effectiveness of IFN-β neutralizing antibodies. IFN-β activates STAT1 after binding to the IFNAR receptor, resulting in JAK-1/TYK-2 stimulation and phosphorylation of STAT1, and ending in the consequent activation of the ISRE. It is evident by western blotting that stimulating A549 cells with recombinant IFN-β (r-IFN-β) results in activation of the STAT1 pathway as demonstrated by the increased detection P-STAT1 (**Figure 4.5.1**). Increased doses of neutralizing IFN-β antibodies caused a dose-dependent reduction in r-IFN-β induced P-STAT1 levels. P-STAT1 protein levels were heavily reduced by a dosage of 100 NU/mL of IFN-β neutralizing antibody. To ensure complete neutralization, a dosage of 600 NU/mL of IFN-β antibody was selected for use in future experiments.

5.2. IFN-β neutralizing antibodies do not confer susceptibility to reovirus infection in A549 cells

Resistant A549 cells and susceptible H1299 cells were infected with reovirus at a TCID of 20% for 1 hour. Antibodies neutralizing to IFN-β were added to culture media immediately

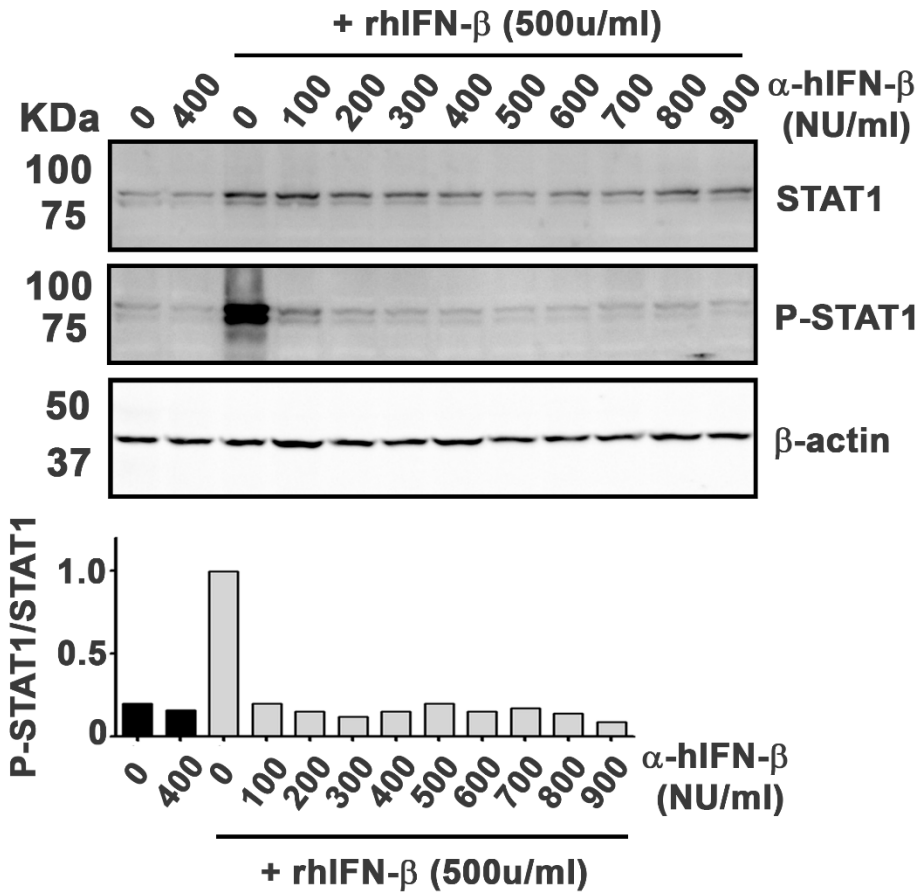

Figure 4.5.1. IFN-β induced STAT1 signalling is effectively inhibited by IFN-β neutralizing antibodies. A549 cells stimulated with 500 units/mL of recombinant IFN-β show strong STAT1 signalling activation through high levels of P-STAT1 at 18 hrs. Simultaneous addition of IFN-β neutralizing antibodies with the recombinant IFN-β effectively reduced activation of the STAT1 pathway. Bands were quantified by densitometry (relative to β-actin) and displayed in the graph below the blot.

following infection and additionally every 24 hrs thereafter to compensate for any degradation and quench increasing levels of IFN-β. It was surmised that neutralization of the IFN-β response to reovirus may be enough to enable permissive spread between A549 cells. Infection was evaluated at 18, 48, and 72 hpi by immunocytochemistry staining. As can be seen in **Figure 4.5.2** the H1299 cells increase in infection during the time course and were almost completely infected by 72 hpi. In contrast, the A549 cells had a reduced infection at 72 hpi when compared to 18 hpi and appeared to be actively clearing the reovirus. In comparison to their counterpart cells that were infected but untreated with IFN-β neutralizing antibodies, the H1299 and A549 cells appeared marginally more infected at 72 hpi when IFN-β was neutralized. Importantly, treating the A549 cells with IFN-β antibodies did not induce notable susceptibility to reovirus comparable to the susceptibility seen in H1299 cells, suggesting that IFN-β is not the sole mediator of resistance in A549 cells.

5.3. shRNA knockdown of IFNAR1/2 mRNA and signalling pathway in A549 cells

IFN-β is not the only major Type I IFN, IFN-α signals though the same IFNAR receptor potentiating similar antiviral effects. Therefore, as a complement to IFN-β neutralization A549 cells were separately transduced with 5 different shRNA constructs against either the IFNAR1 or IFNAR2 subunit of the Type I IFN receptor. An initial screen of stable cells under selection was tested by qRT-PCR and found the most effective knockdowns were constructs 4 and 5 against the IFNAR1 subunit (**Figure 4.5.3)**.

The best IFNAR1-4 and IFNAR1-5 knockdowns in the stably transduced cells were used for reovirus spread analysis in two independent experiments. Knockdown of the cells used for those experiments was quantified by qRT-PCR and revealed a 93% and 88% transcript knockdown with constructs 4 and 5 respectively (**Figure 4.5.4 panel A**). The IFNAR

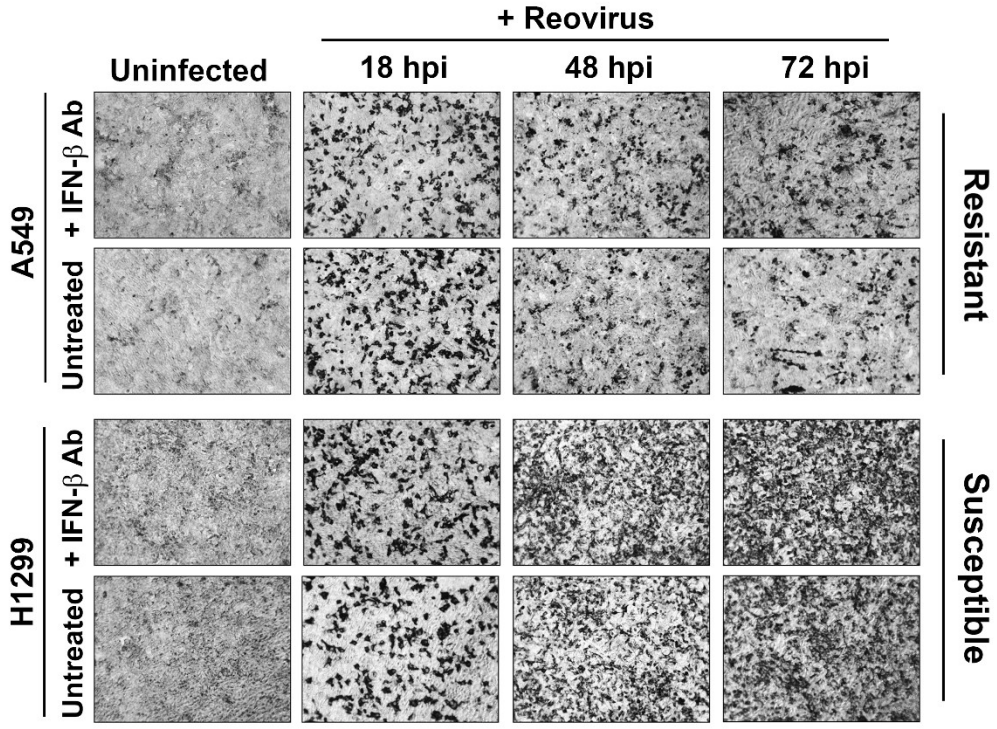

Figure 4.5.2. IFN-β neutralizing antibodies do not confer susceptibility to reovirus infection on A549 cells. A549 and H1299 cells were infected with reovirus to an initial TCID of 20%. IFN-β neutralizing antibodies (300 NU/mL) were added to media immediately following infection and every 24 hrs thereafter. Cells were fixed and stained for reovirus (black) at 18 hpi, 48 hpi, and 72 hpi. Infection at 72 hpi was increased in H1299 cells but decreased in A549 cells. IFN-β neutralizing antibodies did not make the A549 cells notably more susceptible to reovirus dissemination.

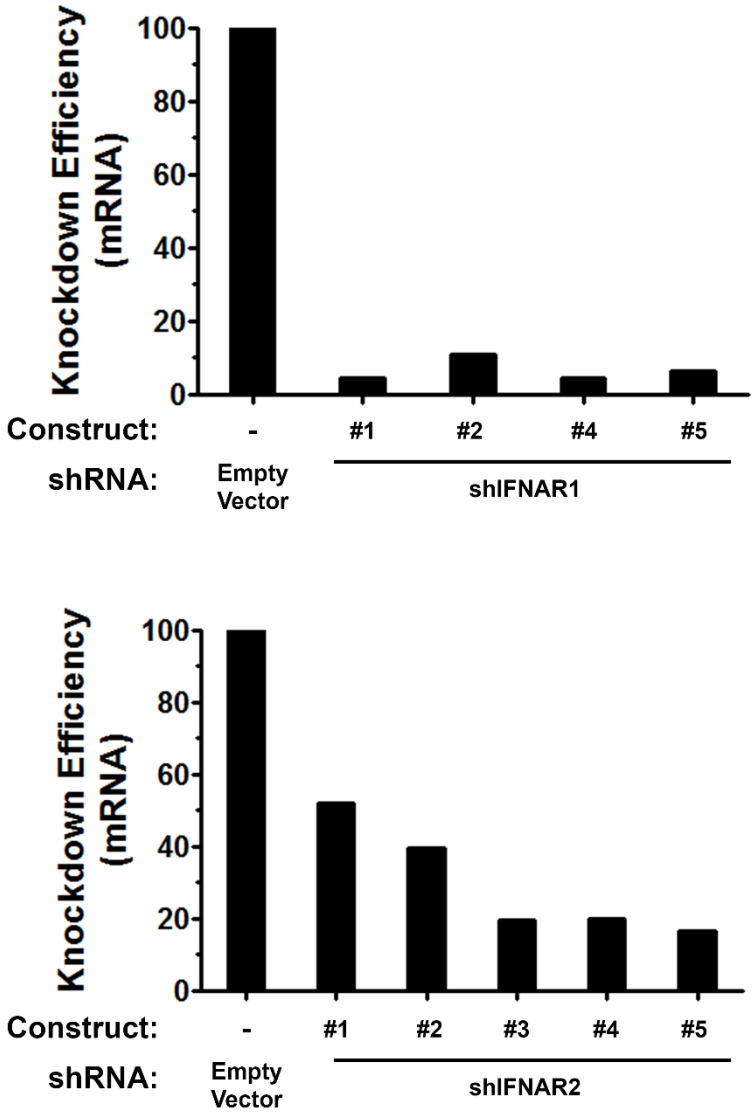

Figure 4.5.3. Various shRNA constructs against the IFNAR1 and IFNAR2 subunits of the Type I IFN receptor were tested for knockdown efficiency. Stable cell lines were generated from A549 cells and different shRNA constructs against the IFNAR1 and IFNAR2 subunits of the IFNAR receptor. Purified RNA was used to test for knockdown efficiency by qRT-PCR. This experiment was done once to identify the best candidate constructs to proceed with for future experiments. IFNAR1 knockdowns were more effective than IFNAR2 knockdowns.

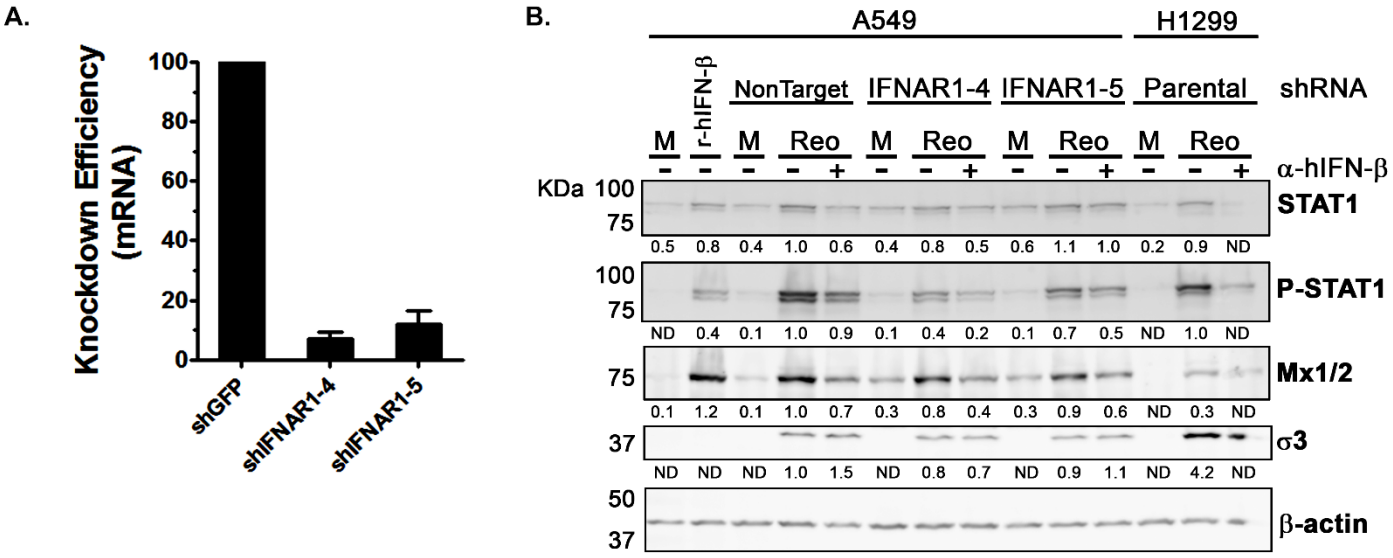

Figure 4.5.4. Knockdown of IFNAR1 in A549 cells was effective. Stable cell lines were generated from A549 cells and the 2 best shIFNAR1 constructs. **A)** Knockdown efficiency was tested relative to a shGFP control by qRT-PCR. mRNA levels were reduced by roughly 90%; shIRNAR1-4 was slightly more effective than shIFNAR1-5. Error bars represent standard deviation between 2 independent experiments. **B)** Samples were collected for Western Blotting at 18 hpi, either mock or reovirus infected with a 20% infectious dose. Bands were quantified by densitometry; values displayed are relative to β-actin and normalized to the reovirus infected NonTargeting shRNA control. The IFNAR1 knockdown cells had reduced levels of P-STAT1 protein when compared to A549 cells transduced with a non-targeting control construct. Again, construct 4 was more effective than construct 5. The use of IFN-β neutralizing antibodies had an inhibitory effect on STAT1 signaling and Mx1 expression. The image shown is representative of 2 independent experiments.

knockdowns were infected with a reovirus TCID of 20% and collected at 18 hpi for western blotting. The IFNAR1-4 and IFNAR1-5 knockdowns both had reduced levels of PSTAT1 signalling following infection with reovirus when compared to Non-Targeting control A549 cells (**Figure 4.5.4 panel B**). The IFNAR1-4 knockdown had less P-STAT1 protein than IFNAR1-5; 40% and 70% expression relative to Non-Targeting cells was observed, respectively. The knockdowns of IFNAR did not result in substantial decrease of Mx1, or an increase of reovirus σ3 protein, which is not surprising as the aim was to infect the cells to equal amounts initially. The use of IFN-β antibodies in complement to the knockdown resulted in a further 20% reduction of STAT1 signalling, and also reduced levels of Mx1. However, neither response was fully limited suggesting reovirus infection activates alternate sources of stimulation.

5.4. shRNA knockdown of IFNλR1 mRNA and protein in A549 cells

The IFN-λs were the highest secreted cytokines detected by ELISA analysis of my cell panel, so it made sense to inhibit their function in an effort to make A549 cells more susceptible to reovirus spread. A549 cells were selectively transduced with different shRNA constructs against IFNλR1, the receptor subunit specific to Type III IFNs. The most effective 2 shRNA constructs of 5 possible selections had been previously determined by PhD student Adil Mohamed in Huh-7.5 human hepatoma cells. In the model reovirus spread-resistant A549 cells I used, IFNλR1 knockdowns of 98% by mRNA were achieved with both constructs among stable cells under selection in two independent experiments (**Figure 4.5.5 panel A**). Receptor protein levels assessed by western blot analysis were reduced by 72% with shIFNλR1-3 and by 67% with shIFNλR1-5 (**Figure 4.5.5 panel B**). However, observed reductions in P-STAT1 and Mx1 protein seemed to be a result of the IFN-β antibody activity rather than the IFNλR1

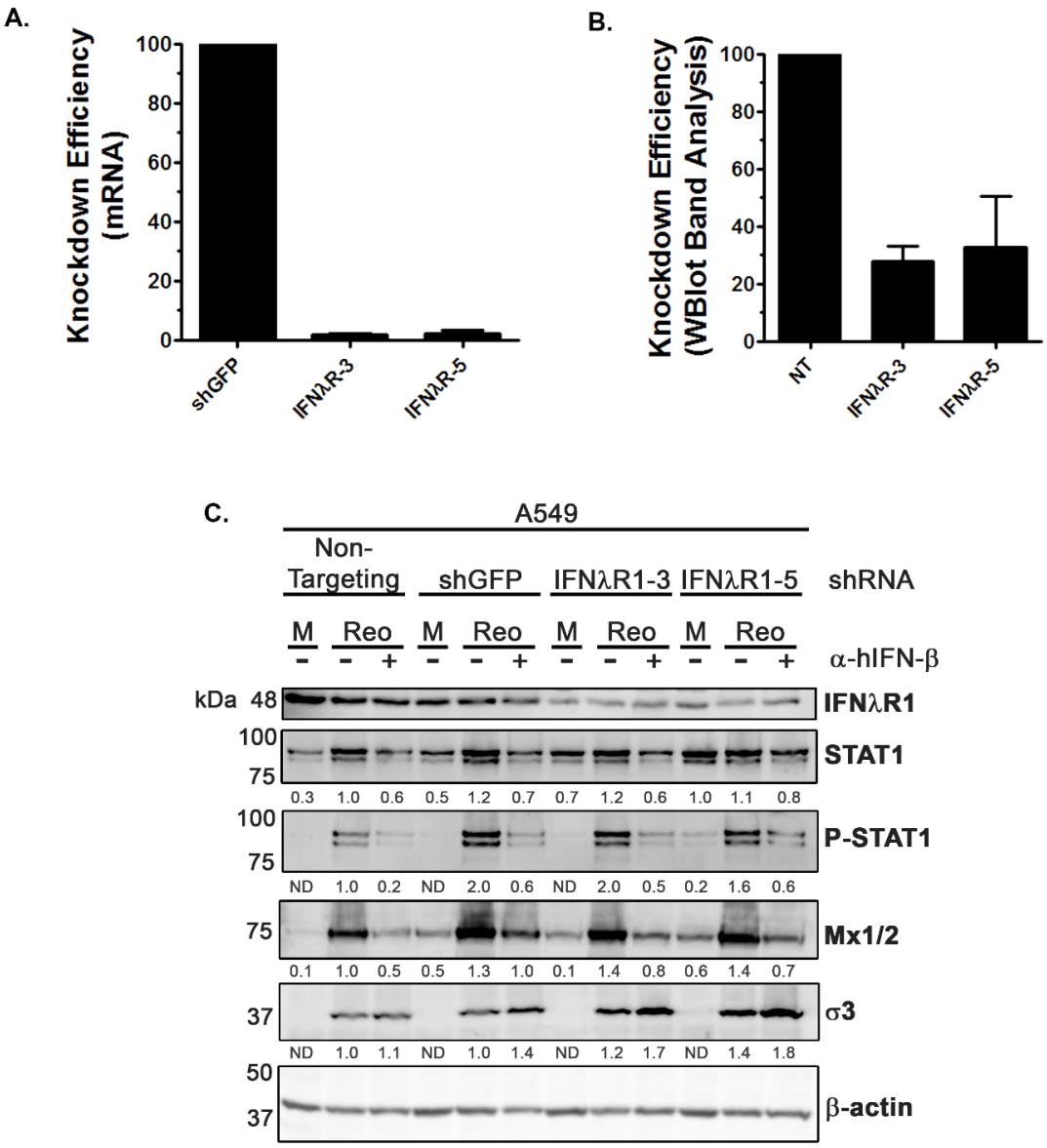

Figure 4.5.5. The IFNλR1 was knocked down in A549 cells but any effect on STAT1 signalling was minimal. Stable cell lines were generated from A549 cells and the 2 best shIFNλR1 constructs. **A)** Knockdown efficiency was tested by qRT-PCR. mRNA levels were reduced by 98% with each construct when compared to the shGFP control. Error bars represent standard deviation between 2 independent experiments. **B)** Band analysis put IFNλR1 protein knockdown at 72% and 67% for constructs 3 and 5 respectively. Error bars represent standard deviation between 2 independent experiments. **C)** Samples were collected for Western Blotting at 18 hpi, either mock or reovirus infected with a 20% infectious dose. Bands were quantified by densitometry; values displayed are relative to β-actin and normalized to the reovirus infected NonTargeting shRNA control. The IFNλR1 knockdown cells had no noticeable reduction in levels of PSTAT1 or Mx1 as a result of the knockdown. Reduction of PSTAT1 or Mx1 was mediated by IFN-β neutralizing antibodies instead. The blot is representative of 2 independent experiments.

knockdown (**Figure 4.5.5 panel C**). Thus, instead of stimulation with reovirus, the cells were stimulated with 15 000 pg/mL of IFN-λ to test for cytokine-specific effects. Cells were collected 18 hrs post-stimulation for western blot analysis. As a result of the knockdown of the Type III IFN receptor, the cells had 30% less STAT1 signalling than A549 cells with the non-targeting sequence construct (**Figure 4.5.6**). Therefore, one could assume that the residual levels of IFNλR1 remaining on the cell surface following knockdown are still sufficient for ~70% of typical STAT1 signalling to occur.

5.5. Combination of IFN-β neutralizing antibodies and shRNA knockdown of IFNAR1 or IFNλR1 has minimal effect on increasing reovirus spread in A549 cells

Stable A549 knockdowns of the IFNAR1 receptor were infected by a TCID of 20% and the percentage of reovirus infected cells was monitored at 18 hpi and 64 hpi by flow cytometry. The spread of reovirus over this time-course in the IFNAR1 knockdown cells was compared to negative control knockdowns that are non-targeting and parental A549s, as well as positive control H1299 cells. While the susceptible H1299 cells showed a 3-4 fold increase in infection from 18 hpi to 64 hpi, A549 cells with IFNAR1 knockdown did not become more susceptible to reovirus than the other A549 cells that had unaltered levels of the Type I IFN receptor. As shown in **Figure 4.5.7 panel A**, all A549 cells were able to reduce their levels of reovirus infection by 64 hpi. The additional use of IFN-β neutralizing antibodies following infection had minimal-to-no effect on the percentage of infected cells, whether they were controls or IFNAR1 knockdowns (**Figure 4.5.7 panel B**).

Stable shIFNλR1 knockdowns of A549 lung cancer cells were infected with a target TCID of 20% at 18 hpi, and the percentage of reovirus infected cells was monitored at 18 hpi and 64 hpi by flow cytometry. The spread of reovirus in the shIFNλR1 cells was also compared to

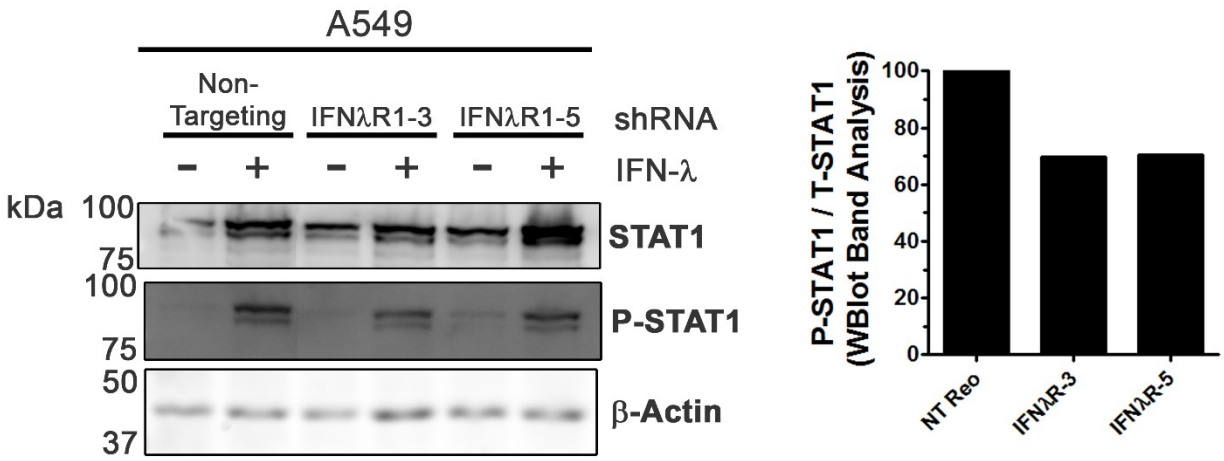

Figure 4.5.6. A549 cells stimulated with recombinant IFN-λ show reduced STAT1 signalling in IFNλR knockdowns compared to Non-Targeting control cells. Stable cell lines were generated from A549 cells and the 2 best shIFNλR1 constructs. Samples were stimulated with 15 000 pg/mL of recombinant IFNλ and collected for Western Blotting after 18 hours. The IFNλR1-3 knockdown cells had 30% less P-STAT1 and the IFNλR1-5 knockdown cells had 29% less. shGFP control cells were contaminated and should be disregarded.

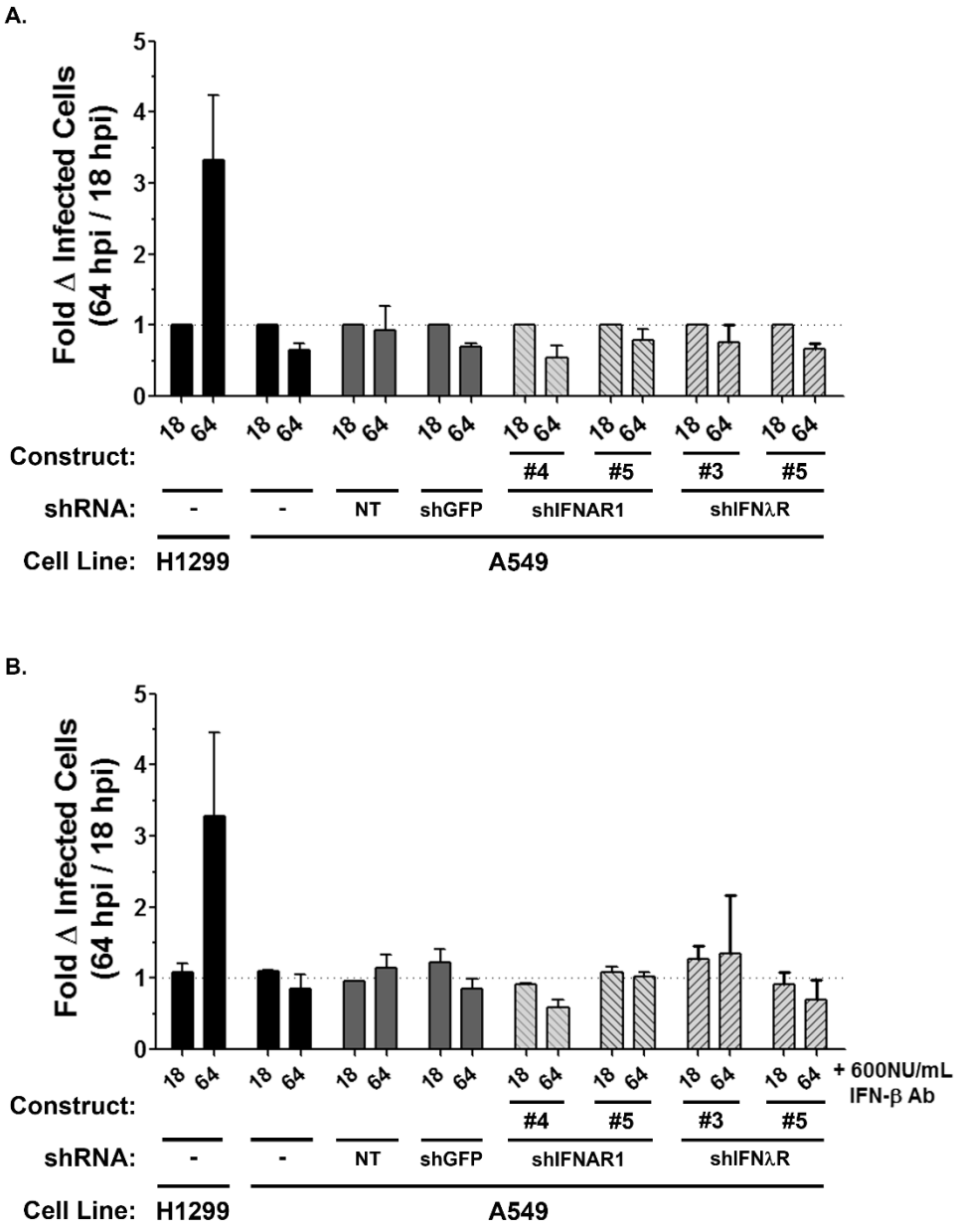

Figure 4.5.7. Knockdown of the Type I or Type III IFN receptor does not make A549 cells susceptible to reovirus dissemination, even with the addition of IFN-β neutralizing antibodies. All cells were infected to an initial TCID of roughly 20% at 18 hpi, as quantified by flow cytometry. Cells were also collected 64 hpi to check if reovirus infection had spread. Fold difference in infection was calculated relative to the percent infected cells at 18 hpi; error bars represent standard deviation over 2 independent experiments. **A)** Reovirus infection decreases in all the A549 cells by 64 hpi despite the knockdown of the IFN receptors. A 3-4 fold-increase in infection was observed in susceptible H1299 cells over the same period of time from 18 to 64 hpi. **B)** 600 NU/mL of IFN-β neutralizing antibodies was added to the media of all cells post-infection and again every 24 hrs. This did not make the A549 cells susceptible to reovirus dissemination.

negative control non-targeting knockdowns and parental A549s, as well as positive control H1299 cells. The susceptible H1299 cells had closer to a 3-fold than a 4-fold increase in infection from 18 hpi to 64 hpi this time as one replication was accidentally over-infected to begin with. The shIFNλR1 knockdowns did not become more susceptible to reovirus than the other A549 cells that had unaltered levels of the Type III IFN receptor. All A549 cells were able to reduce their levels of reovirus infection by 64 hpi (**Figure 4.5.7 panel A**). IFN-β neutralizing antibodies were used to inhibit the antiviral signalling of the cells in complement to the IFNλR1 knockdown, thus jointly inhibiting both the Type I and Type III IFN pathways. This had minimal-to-no effect on increasing the percentage of infected cells by 64 hpi, as the A549 cells remained resistant to reovirus spread (**Figure 4.5.7 panel B**).

6. Inhibition of the IFN pathway through interferon regulatory factor knockdown is insufficient for conferring susceptibility to reovirus in model system A549 cells

Knockdowns of the IFN receptors proved ineffective at conferring susceptibility on A549 cells so various experiments shifted the focus upstream in the innate interferon response to target key interferon regulatory factors. These transcriptional factors, specifically IRF3 and IRF7, were targeted for shRNA knockdowns to see if the A549 cells became more susceptible to reovirus when IRF functions were impaired. Neutralizing antibodies against IFN-β were again used in complement with the shRNA technique as a mechanism of quenching residual IFN signalling.

6.1. shRNA Knockdown of IRF3 mRNA and protein in A549 cells

A549 cells were transduced with 5 different shRNA constructs that targeted IRF3; 4 of these constructs were able to generate stable cell lines. Lysates of these infected cells underwent blotting for both IRF3 and P-IRF3, and results indicated the most effective

knockdowns were achieved with constructs shIRF3-1 and shIRF3-4 (**Figure 4.6.1 panel A**). When the shIRF3-1 and shIRF3-4 knockdowns were quantified by qRT-PCR, mRNA levels of IRF3 were knocked down by 79% and 65% respectively in comparison to shGFP control cells (**Figure 4.6.1 panel B**). Despite equal or greater reduction in the actual protein levels of IRF3 and P-IRF3, STAT1 signalling and levels of Mx1 protein did not appear to be affected by the knockdown in comparison to negative control A549 cells (**Figure 4.6.1 panel C**).

6.2. shRNA Knockdown of IRF7 mRNA and protein in A549 cells

A549 cells were transduced with 5 different shRNA constructs targeting IRF7; the best 2 constructs selected were shIRF7-4 and shIRF7-5. Knockdown effectiveness as quantified by levels of mRNA transcripts compared to the shGFP control was a 92% reduction in IRF7 with construct 4 and a 77% reduction in mRNA with construct 5 (**Figure 4.6.2 panel A**). IRF7 bands were not present in uninfected samples on western blots so differences in IRF7 protein were assessed using the infected knockdown samples and negative controls (**Figure 4.6.2 panel B**). Band analysis from two different experiments showed an average reduction in IRF7 protein of 85% and 11% for constructs shIRF7-4 and shIRF7-5 respectively (**Figure 4.6.2 panel C**). However, the knockdown of IRF7 was not enough to reduce levels of the antiviral ISG Mx1 or to reduce the reovirus-induced STAT1 signalling relative to the negative control samples.

6.3. Independent knockdown of IRF3 and IRF7 has minimal to no effect on increasing reovirus spread in model resistant A549 cells

The shIRF3 knockdowns were infected by an initial 18 hpi TCID of approximately 20% and sampled at 64 hpi to quantify the dissemination of reovirus infection by flow cytometry. The spread of reovirus in the knockdowns was compared to parental A549 cells and A549 cells

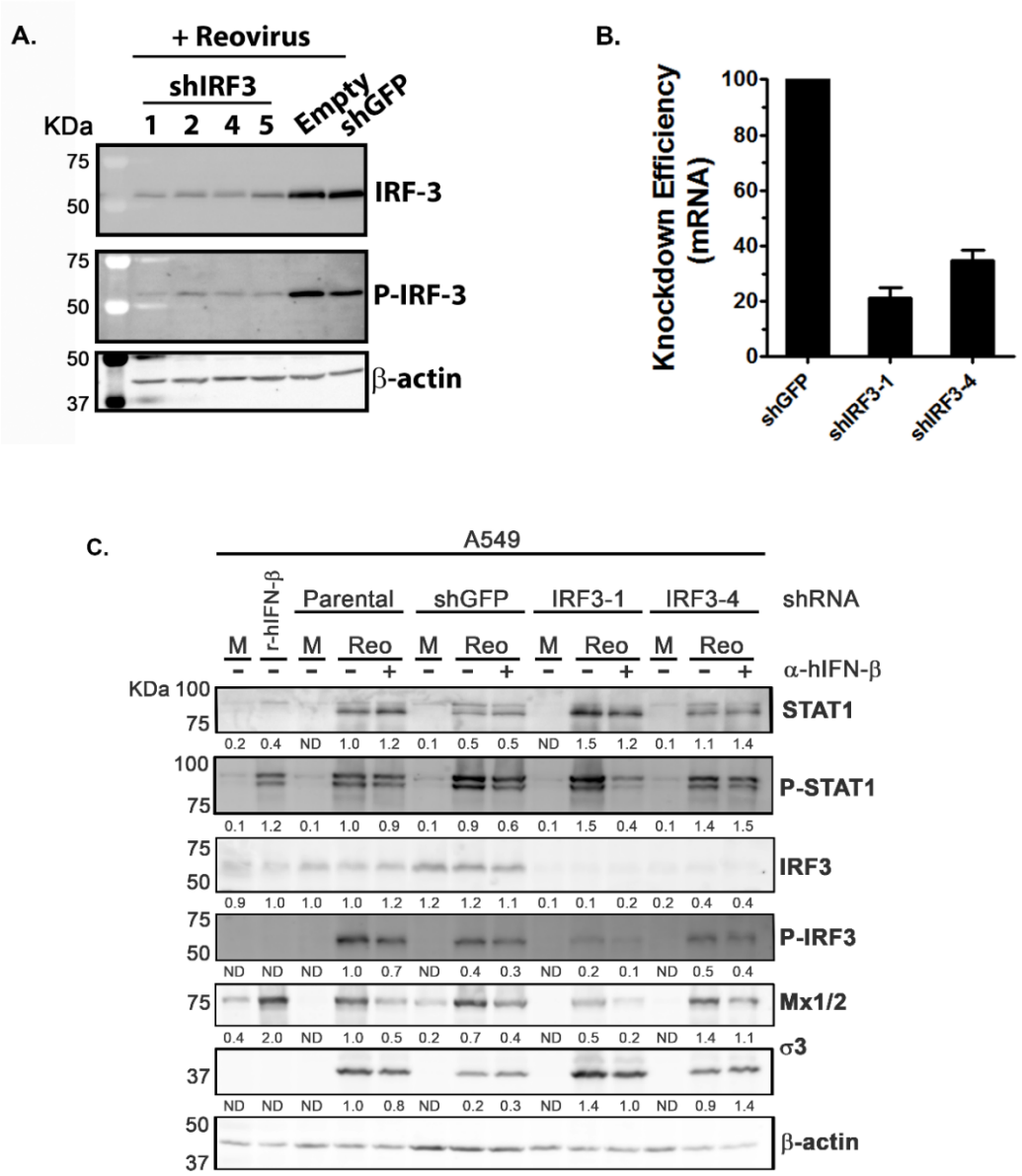

Figure 4.6.1. Knockdown of IRF3 mRNA and protein was achieved in A549 cells. Stable cell lines were generated from A549 cells transduced with IRF3 constructs and kept under selection. **A)** Western blotting of reovirus infected cells collected at 18 hpi indicated IRF3 constructs 1 and 4 gave the best knockdown. **B)** Quantification of IRF3 knockdown at the mRNA level was done by qRT-PCR. Knockdown with IRF3-1 was 79% and with IRF3-4 knockdown was 65%; error bars represent standard deviation from 2 separate experiments. **C)** Samples were collected for Western Blotting at 18 hpi, either mock or reovirus infected with a 20% infectious dose. Bands were quantified by densitometry; values displayed are relative to β-actin and normalized to the reovirus infected parental A549 cells. Less total and phosphorylated IRF3 protein is present in both the knockdowns compared to parental and shGFP A549 cells. Knockdown with shIRF3-1 is more effective than shIRF3-4 and results in reduced Mx1 protein and increased reovirus protein, but does not inhibit STAT1 signalling. Blot is representative of 2 independent experiments.

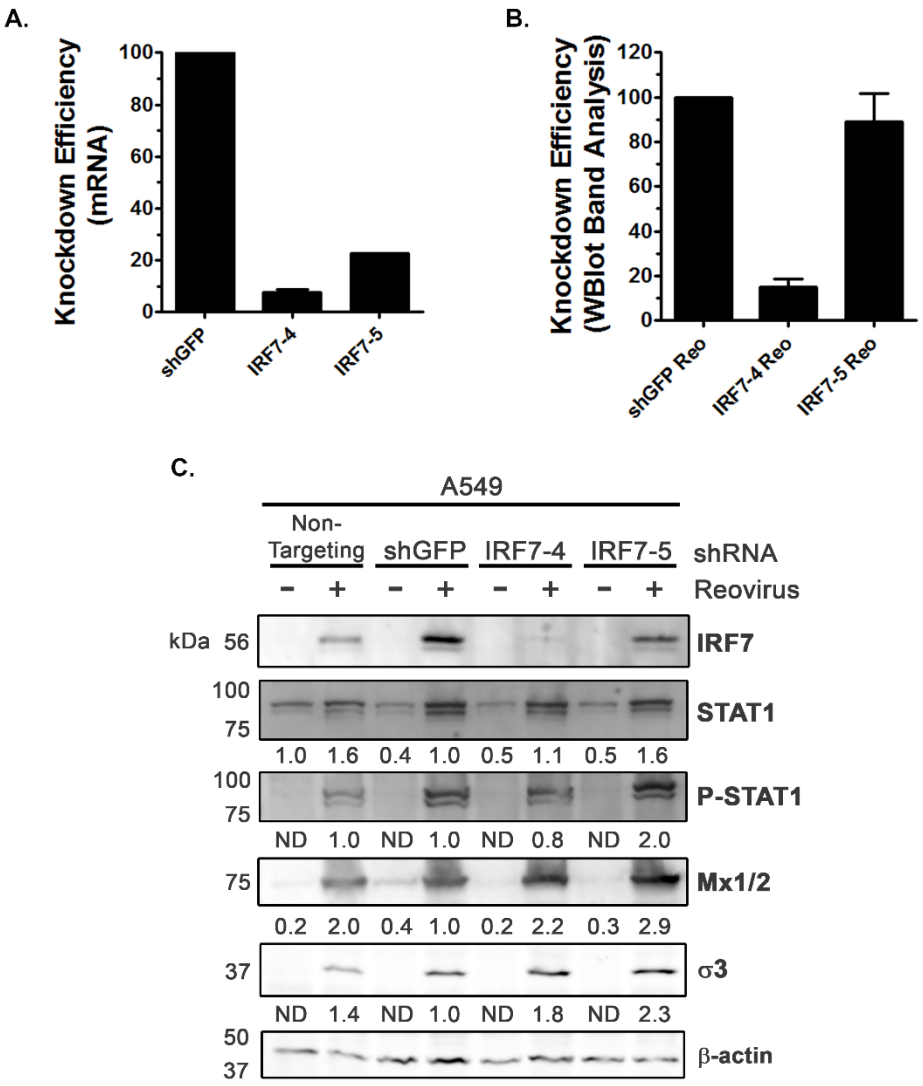

Figure 4.6.2. Knockdown of IRF7 mRNA and protein was achieved in A549 cells. Stable cell lines were generated from A549 cells transduced with IRF7 constructs and kept under selection. Error bars represent standard deviation from 2 independent experiments, and the western blot is representative of 2 experiments as well. **A)** qRT-PCR analysis of the best 2 constructs showed knockdown at the mRNA level of 92% and 77% for IRF7-4 and IRF7-5 respectively. **B)** Band analysis of IRF7 protein gave an 85% knockdown for IRF7-4 compared to shGFP, and an 11% knockdown for IRF7-5. **C)** Mock or reovirus infected samples were collected for Western Blotting at 18 hpi. Band analysis values are relative to β-actin expression and normalized to the reovirus infected parental A549 cells. IRF7 knockdown was not enough to abrogate STAT1 signalling compared to controls, and high levels of Mx1 protein were observed.

with shGFP and random, non-targeting constructs to see if the loss of some IRF3 function made the cells more permissive to reovirus spread (**Figure 4.6.3 panel A**). H1299 cells were the positive control; reovirus infection increases approximately 4-fold from 18 hpi to 64 hpi as they are a permissive cell line. The shIRF3 A549 cells did not become permissive like the H1299 cells as a result of the knockdown. The shIRF3-4 A549s mimicked the results of the negative controls as the reovirus infection began to clear by 64 hpi. The more effective shIRF3-1 knockdown did show an increase in infection from 18 hpi to 64 hpi, although this was a 1.6 fold-increase so not enough to classify the cells as truly permissive like H1299 or H522 cells. This is likely linked to the increased initial infection observed in these cells; in both experiments the shIRF3-1 construct A549s were 45-50% infected at 18 hpi despite being treated with an MOI of virus the same as the other A549 controls and shIRF3-4 knockdown.

The knockdowns of IRF7 were compared to reovirus susceptible H1299 cells and negative control A549 cell lines to see if it increased their permissiveness to the spread of reovirus infection. After two independent experiments it was clear that the shIRF7 knockdown A549 cells were not more permissive to reovirus as the infection began to clear by 64 hpi just like in the parental A549s or those transduced with shGFP or non-targeting constructs (**Figure 4.6.3 panel A**).

6.4. Use of IFN-β neutralizing antibodies in combination with shRNA knockdown of IRF3 does not result in a reovirus susceptible phenotype in A549 cells

As a complement to the effective, yet not 100% knockdown of IRF3, IFN-β neutralizing antibodies were added to culture media immediately following infection and every 24 hrs thereafter to help any quench residual IFN-β signalling. As can be seen in the corresponding graph (**Figure 4.6.3 panel B**) the addition of the antibodies did not result in a susceptible

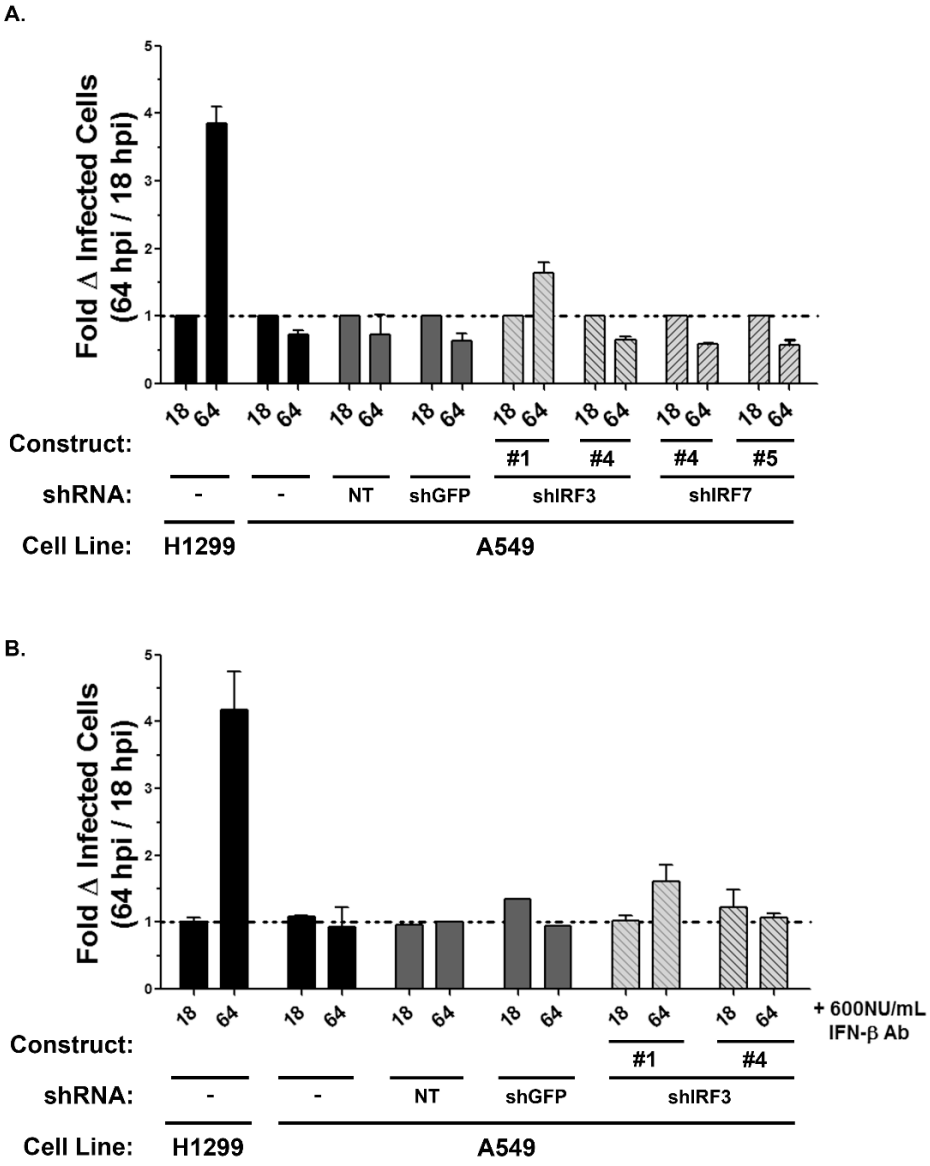

Figure 4.6.3. Knockdown of IRF3 or IRF7 in A549 cells does not result in susceptibility to reovirus dissemination. All cells were infected to an initial TCID of roughly 20%, as quantified by flow cytometry at 18 hpi. Cells were then collected at 64 hpi to check if reovirus infection had spread. Fold difference in infection was calculated relative to the percent infected cells at 18 hpi; error bars represent standard deviation over 2 independent experiments. **A)** Reovirus infection decreases in the A549 cells by 64 hpi despite the knockdown of IRF3 and IRF7. One knockdown, the IRF3-1 construct, did show a 1.6 fold-increase in infection; this construct was more susceptible to initial infection as the same amount of reovirus resulted in ~2x the infection at 18 hpi. A 4 fold-increase in infection was observed in susceptible H1299 cells over the same period of time from 18 to 64 hpi. **B)** 600 NU/mL of IFN-β neutralizing antibodies was added to the media of the IRF3 knockdowns and control cells immediately post-infection and again every 24 hrs. There was no increase in reovirus spread in any of the cells as a result of this treatment.

phenotype being conferred upon the A549 cells as the results matched the lack of spread seen in the cells with knockdown only.

7. Treatment of the cancer cell panel with antiviral cytokines IFN-β, IFN-λ, and/or TNF-α prior to reovirus infection had varying levels of antiviral efficacy

The cell lines of the cancer panel were tested for their response to the 3 main antiviral cytokines previously detected by ELISA in culture media (Results section 4.1). Although secretion levels had been established, it was unknown how each cell line responded to the cytokines. IFN-β, IFN-λ, and TNF-α were added to the cells prior to infection in concentrations corresponding to those detected by ELISA. Following cytokine pre-treatment and subsequent reovirus infection, the cells were stained for reovirus protein and imaged at 18 hpi. If any cytokines primed the cells to prevent subsequent reovirus infection, then it would reveal the importance of that particular antiviral molecule.

7.1. Treatment with individual cytokines can reduce infection but does not fully protect the cells from reovirus

The pre-treatment of the cell panel with antiviral cytokines in culture media had varying effectiveness at reducing the ability of reovirus to infect the cells depending on cytokine and cell type. The most effective cytokine at inducing an anti-reovirus state was IFN-β (**Figure 4.7.1**), followed by IFN-λ in terms of its potency (**Figure 4.7.2**). Cells appeared to respond only minimally to TNF-α, even the SCC9 cells which as previously shown secreted TNF-α into media in the greatest quantity (**Figure 4.7.3**). The A549 cells had the greatest reduction in infection in response to the cytokine treatments, and a less pronounced reduction in infection was seen in H322, H522, and H1299 cells. SCC9 cells only showed some response to IFN-β and not much of a protective effect was observed on A253 cells as a result of any cytokine. Therefore, interestingly, response to the cytokines did not correlate to resistance to spread. For

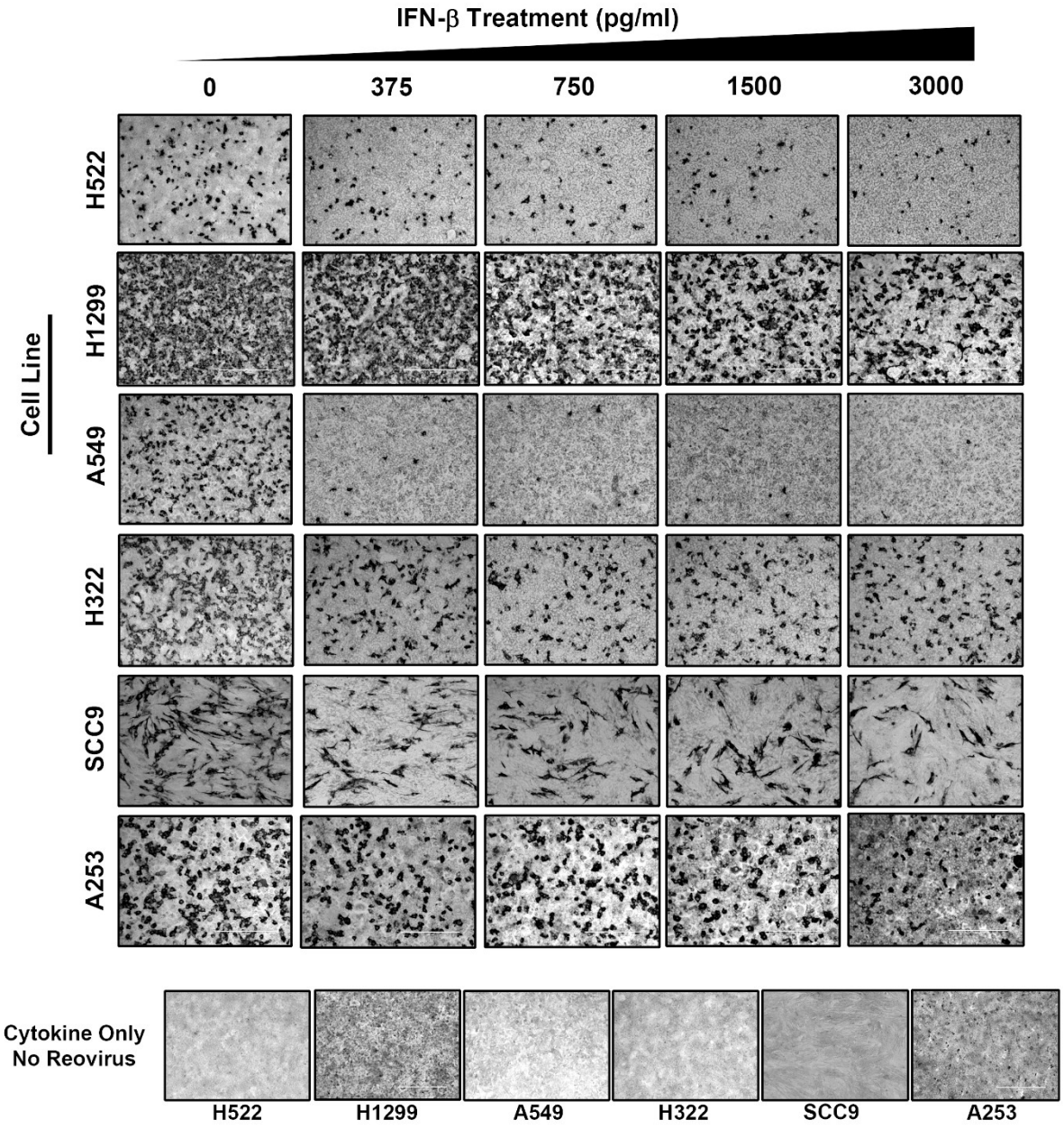

Figure 4.7.1. Pre-treatment of cells with IFN-β has some protective effect against reovirus infection, especially for A549 cells. All cells were seeded for confluency and then treated with ½ dilutions of recombinant IFN-β in media for 18 hrs. The media was then removed and cells were given an initial reovirus TCID of roughly 50%; H522 cells were under-infected and H1299 cells over-infected compared to the other cells. At 18 hpi, cells were fixed and stained for reovirus protein (black). A549 cells responded the most to IFN-β treatment, as infection was almost completely prevented at the lowest cytokine dilution. Infection was also reduced in other cell lines, although the effect was not as strong, even when compared to 8x the amount of IFN-β treatment (A549 at 375 pg/ml vs. H322 at 3000 pg/ml).

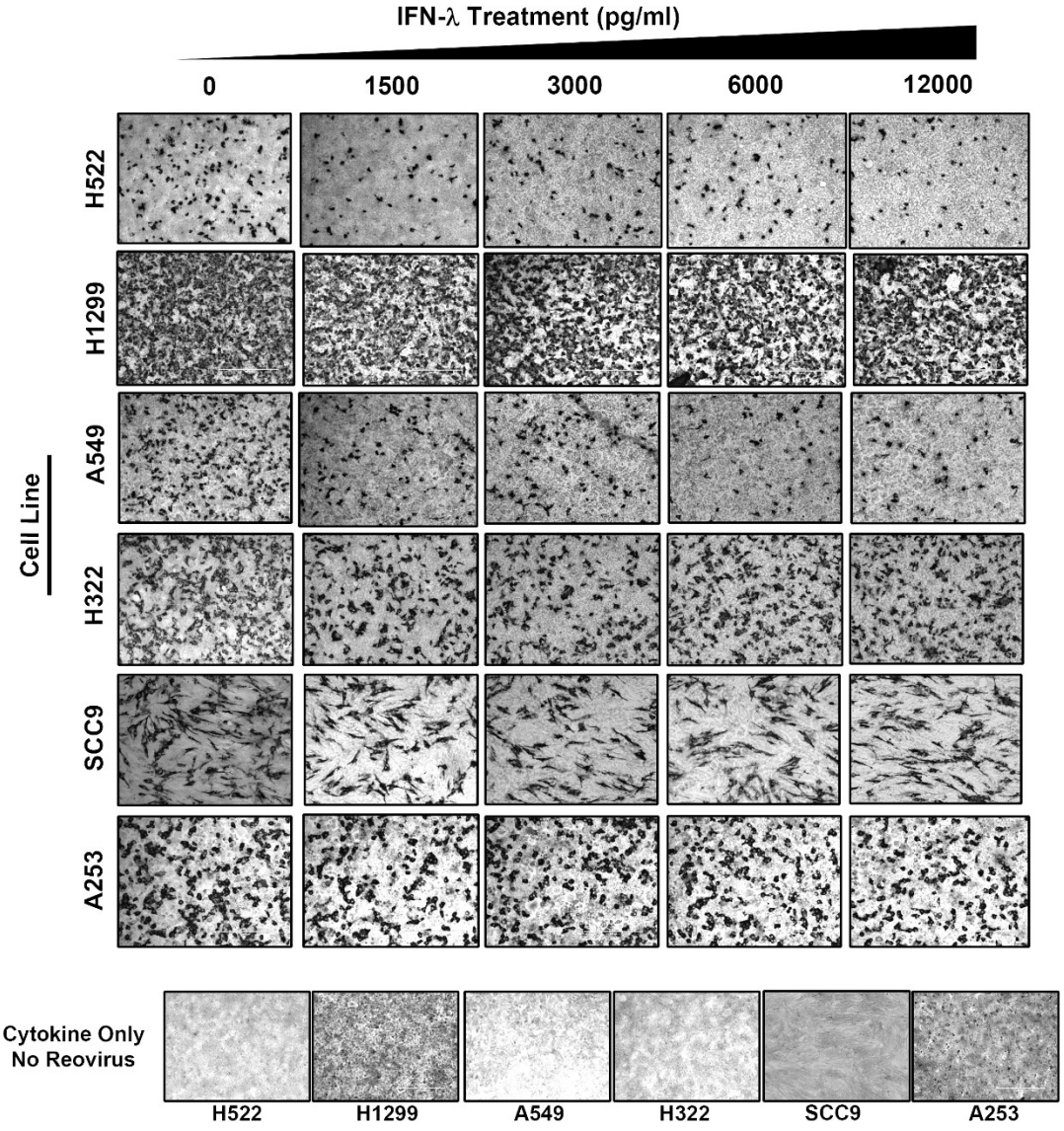

Figure 4.7.2. Pre-treatment of cells with IFN-λ has some protective effect against reovirus infection, especially for A549 cells. All cells were seeded for confluency and then treated with ½ dilutions of recombinant IFN-λ in media for 18 hrs. The media was then removed and cells were given an initial reovirus TCID of roughly 50%; H522 cells were under-infected and H1299 cells over-infected compared to the other cells. At 18 hpi, cells were fixed and stained for reovirus protein (black). A549 cells again responded the most to the cytokine treatment, although infection was still present at the highest concentration of IFN-λ. Infection was not drastically reduced in any of the other cell lines.

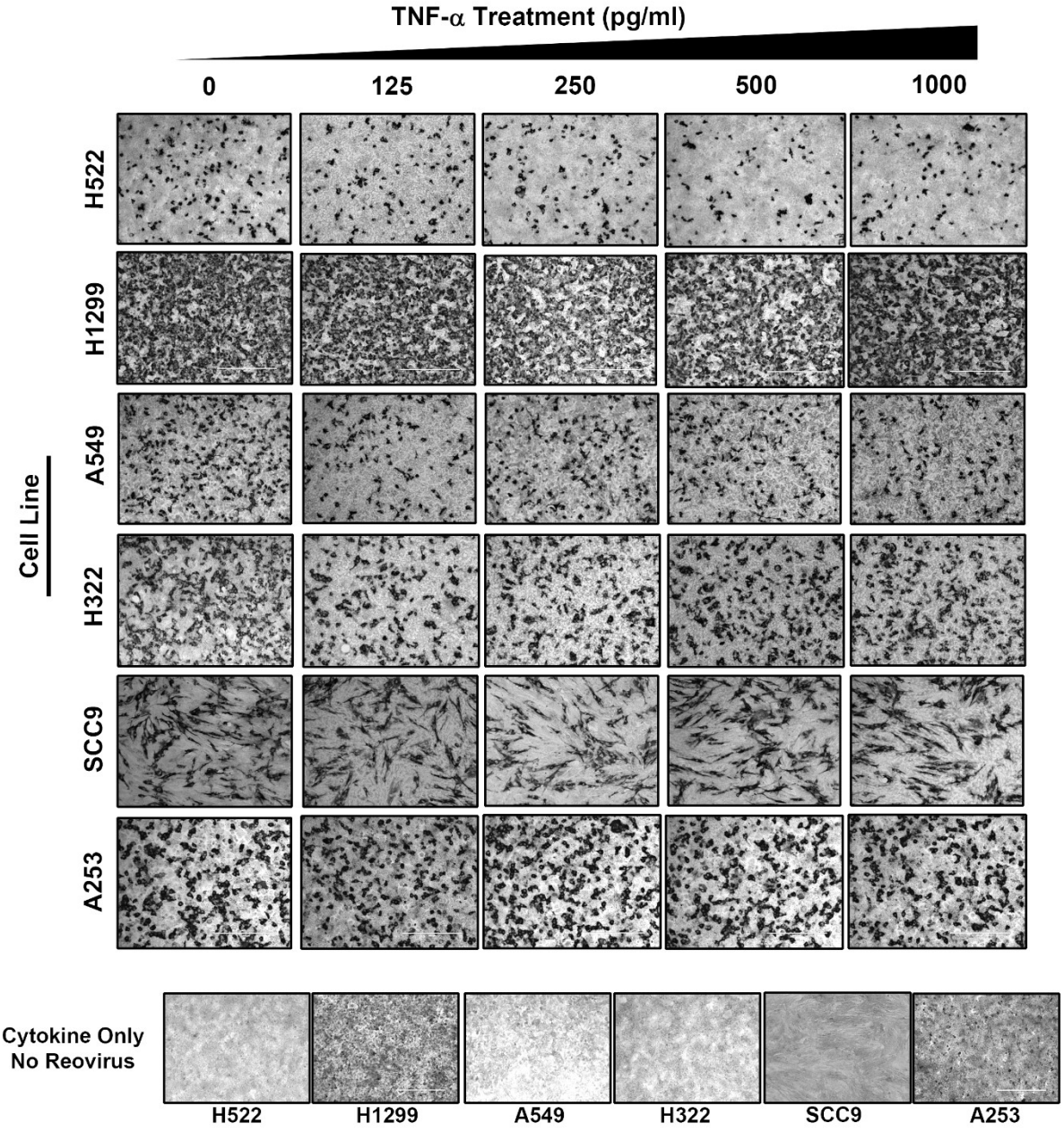

Figure 4.7.3. Pre-treatment of cells with TNF-α is insufficient to induce a protective effect against reovirus infection. All cells were seeded for confluency and then treated with ½ dilutions of recombinant TNF-α in media for 18 hrs. The media was then removed and cells were given an initial reovirus TCID of roughly 50%; H522 cells were under-infected and H1299 cells over-infected compared to the other cells. At 18 hpi, cells were fixed and stained for reovirus protein (black). None of the cell lines appeared to have a reduced level of reovirus infection as a result of the TNF-α stimulation.

example, SCC9 and A253 cells allow the least cell-to-cell spread (Results section 1.2) but they did not respond strongly to cytokine pre-treatments. On the other hand, susceptible H522 and H1299 cells did have some reductions in infection in response to the cytokines. In all cases a population of reovirus infected cells was present at 18 hpi despite treatment with the highest concentration of cytokine, with the exception of A549 cells treated with 3000 pg/ml of IFN-β which appeared to be uninfected.

A further interesting observation was that the reduction in reovirus infections were mostly not dose-dependent in nature. The lowest concentrations of cytokines used, corresponding to the amounts secreted by the reovirus susceptible cells, was often enough to bring about a reduction in infection compared to untreated cells. However, this response was saturated as reovirus infection would not decrease further as higher concentrations of the cytokines were added. An exception to this was the H1299 response to IFN-β.

7.2. Combination treatments of the various cytokines did not fully prevent reovirus infection in any of the cell lines, but highlighted the importance of IFN-β

To see if reovirus infection could be more drastically reduced or fully cleared in any of the cell lines, IFN-β, IFN-λ, and TNF-α were combined into treatments using them in pairs or as a treatment of all 3 cytokines together (**Figure 4.7.4**). However, for every cell line no noticeable additional reduction in infection was observed as a result of this combinatorial approach in comparison to treatment with individual cytokines. Reovirus infection was still always present even though infection was reduced by cytokine treatment in comparison to untreated cells. Interestingly, the combination treatments that included IFN-β with other cytokines appeared to have a greater protective effect, at least on A549 and A253 cells, in comparison to the treatment of IFN-λ and TNF-α together, but lacking IFN-β.

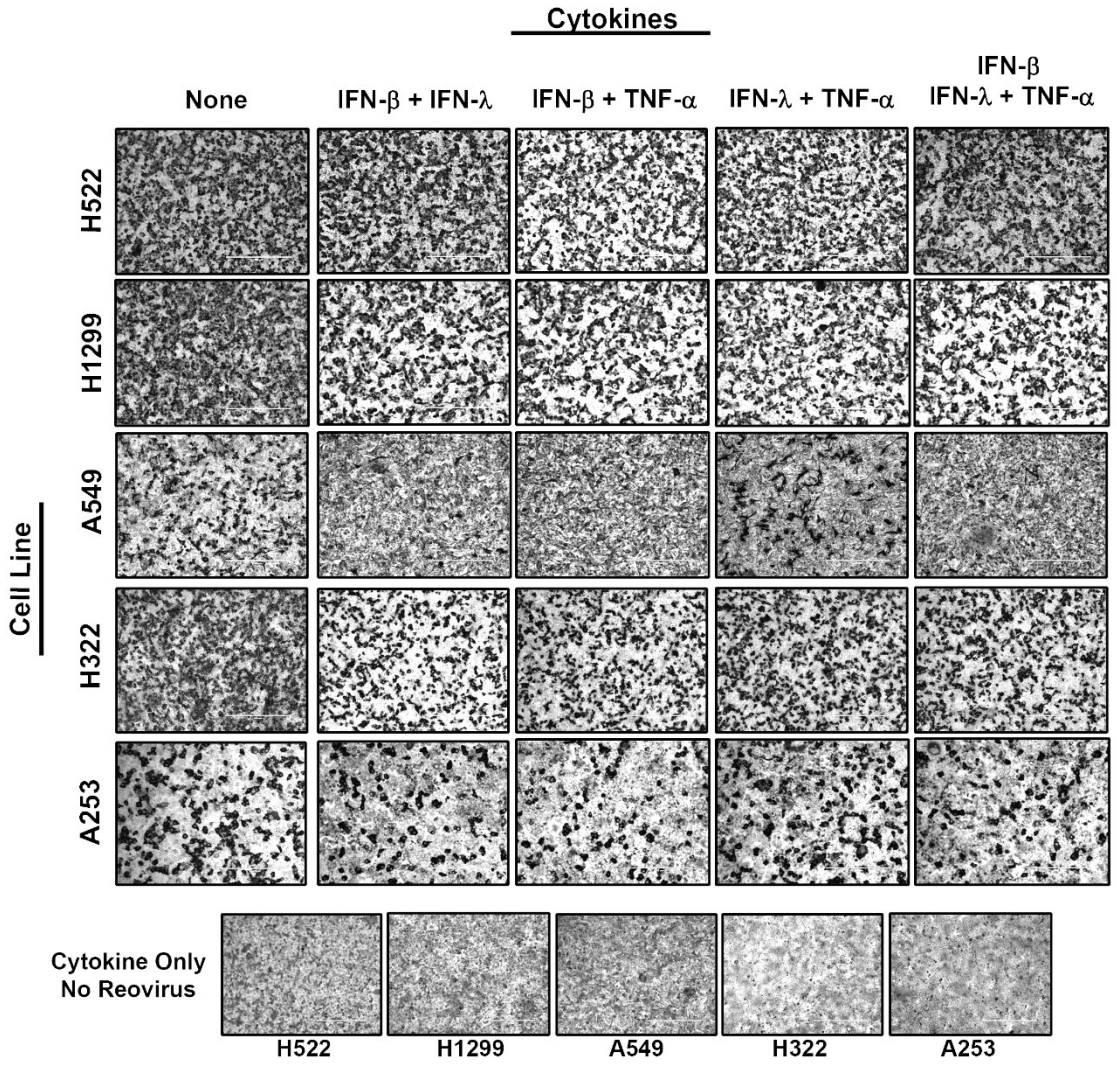

Figure 4.7.4. The combination of IFN-β, IFN-λ, and TNF-α cytokines into pre-treatments for cells had some protective effect against reovirus infection, but was insufficient to prevent reovirus infection. All cells were seeded for confluency and then treated with dilutions of recombinant cytokines (IFN-β 750 pg/ml, IFN-λ 3000 pg/ml, TNF-α 250 pg/ml) in media for 18 hrs. The media was then removed and cells were given an initial reovirus TCID of roughly 50%, although H522, H1299, and H322 cells appear over-infected. At 18 hpi, cells were fixed and stained for reovirus protein (black). A549 cells responded the most to the cytokine treatments, especially to the combinations that contained a dose of IFN-β. Infection was also reduced slightly in the H322 and H1299 cells, although the effect was not as strong as on A549 cells. A253 cells did not respond very strongly to treatment but also seem to share this response skewed towards IFN-β.

CHAPTER 5: DISCUSSION

My intention for this project was to decipher the mechanism(s) responsible for limiting the cell-cell spread of reovirus among a selection cancer cells. The variety of lung cancer and HNSCC cells that made up my cell panel were discovered to have a range of different susceptibilities for reovirus infection and the permissiveness of cell-to-cell virus spread (**Figures 4.1.1, 4.1.2**). The differing sensitivities of the cell lines was not a surprise as such a stratification was also observed in results obtained by other researchers in a variety of other cancer cell types.[30, 45, 58, 68, 180] Of the cell lines that I worked with, previous researchers had characterized L929 mouse fibroblasts and H1299 and H522 lung cancer cells as fairly permissive to reovirus spread, while A549, H322, and H23 lung cancer cells, as well as SCC9 HNSCC cells were comparatively more resistant to reovirus (personal communication, Dr. Shmulevitz).[58, 64, 180] These observations are similar to my results, although Sei *et al*. found H23 and A549 cells to have similar susceptibility while H322 cells were more resistant to cell death at 48 hpi.[58] I was examining a different metric, cell-cell reovirus spread from 18 hpi to 48 hpi, but I found it was A549 and H322 cells that had similar susceptibility, while H23 cells were ~2x more susceptible to reovirus. To the best of my knowledge the A253 cancer cell line had not been previously characterized with regards to its susceptibility to reovirus. Therefore, now that we know their phenotype for permissiveness to reovirus infection, we have new tools that can be used to analyze reovirus infection and replication.

Literature published prior to this research project indicated the importance of the IFN-β response as a determinant of cell susceptibility to reovirus infection. As described in my introduction, impaired IFN-β production and response increased susceptibility to reovirus in a model of Ras-transformed mouse fibroblast cells.[64] Other oncolytic RNA viruses had JAK/STAT signalling and the Type I IFN response implicated as the main determinant of cancer cell

susceptibility to virus infection as well.[156, 158, 159, 163, 167] Thus, since the IFN response was so heavily implicated with susceptibility of other oncolytic viruses and in mouse cells with reovirus, why wouldn't it also be the main determinant of human cancer cell susceptibility to reovirus too?

We had hypothesized that the IFN response would dictate cell susceptibility to reovirus. However, numerous experiments using shRNA knockdown of IFN receptors, IFN regulatory transcription factors, as well as the use of neutralizing IFN-β antibodies determined that this is likely not the case (**Figures 4.5.1, 4.5.2, 4.5.7, 4.6.3**). A549 cells, which resist reovirus cell-to-cell spread, did not become more noticeably more susceptible to infection due to any IFN pathway inhibition. Three possible explanations exist for why A549s remained resistant to reovirus spread despite the manipulations of IFN signalling:

1. The knockdowns and inhibition of signalling was not strong enough to block the full antiviral response
2. Overlap among the IFN signalling pathways rendered the inhibition insufficient
3. The presence of a different antiviral "Factor X" that is the effector of anti-reovirus function in the resistant cancer cell lines

Firstly, it could be possible that A549 cells were still resistant to reovirus spread because knockdown of the IFN receptors, or of IRF3 or IRF7, was insufficient to completely abrogate the signalling pathway (**Figures 4.5.4, 4.5.5, 4.6.1, 4.6.2**). Similarly, the neutralizing antibodies may not have fully blocked the IFN-β response. However, 600 NU/mL of the IFN-β neutralizing antibodies was more than enough to reduce recombinant IFN-β induced STAT1 signalling to basal levels (**Figure 4.5.1**). Contrastingly, in response to reovirus infection, residual P-STAT1 protein was still present despite shRNA knockdowns and IFN-β neutralization, suggesting that stimulation of STAT1 signalling was induced partly from an alternative pathway (**Figures 4.5.4, 4.5.5, 4.6.1, 4.6.2**). The clear solution to uncertainty of knockdown efficacy would be to generate stable cell

knockouts of these genes using the CRISPR/CAS9 system, as there would be no possibility of retained residual target protein that could be sufficient to induce an anti-reovirus state in the A549 cells.

A second possible explanation for why the A549 cells did not convert to a reovirus susceptible phenotype following all the IFN pathway inhibition could be due to the redundancy and crosstalk between all the components of the antiviral signaling pathways. The Type I and Type III IFN responses have been implicated in activating similar and overlapping responses to viral infections.[117] IRF3 and IRF7 are also frequently referred to in conjunction with each other for the same reason.[89, 90, 93] Therefore, knocking down these components in isolation may not be enough to block the anti-reovirus response. For example, knockdown of IRF3 will not induce susceptibility to reovirus if IRF7 activation is still functional and activating the same or similar antiviral response that IRF3 potentiates. This may explain why in **Figure 4.6.2**, knockdown of IRF7 occurs but there is still activation of antiviral ISG Mx1. Similar effects are observed in **Figure 4.6.1** where IRF3 knockdown does not effectively inhibit STAT1 signalling indicating alternative stimulation could be occurring. A logical method to reduce cross-activation of these important antiviral pathways would be to employ combination knockdowns or knockouts. A similar effect was attempted when combining the IFNλR1 knockdown with the IFN-β neutralizing antibodies to have inhibitory action against both the Type I and Type III IFN responses (**Figure 4.5.7**) however it was not sufficient to allow reovirus spread among A549 cells. I would try combinations such as IRF3/IRF7 and IFNAR/IFNλR1 shRNA knockdown or CRISPR knockouts.

A third possible explanation for why shRNA knockdowns and antibody inhibition failed to increase reovirus spread among A549 cells is the presence of another antiviral molecule that has not been tested on my cell panel yet. The 3 most prevalent cytokines produced by the resistant

cells were IFN-λ, IFN-β, and TNF-α (**Figure 4.4.1**) but the addition of these cytokines as a pre-treatment was insufficient to fully prevent cells from reovirus infection (**Figure 4.7.1, 4.7.2, 4.7.3, 4.7.4**). It's possible that a yet undefined antiviral factor (Factor X) remained in the cell media. In this case, Factor X would continually thwart cell-cell spread of reovirus despite my inhibition of IFN-β and IFN-λ. When the other analytes detected by multiplex ELISA are considered, such as IFN-α, IFN-ω or IFN-γ, it is unlikely that they are responsible for anti-reovirus effects due to their relatively low concentration or function (**Figure 4.4.1, Appendix A**). Therefore, I propose that the best way to isolate the soluble antiviral factor responsible for conferring resistance to reovirus infection (as seen in the media transfer assay, **Figure 4.3.1**) would be to fractionate infected cell media according to size. Harvesting infected cell media and performing a media transfer assay as done previously, but dividing up the fractions of media, would allow one to isolate the specific fraction of media that confers resistance to infection. This smaller fraction of media could then be analyzed by mass spectrometry to reveal what proteins are present, and this smaller pool of proteins could then be tested for their anti-reovirus properties.

Not all analysis of reovirus susceptibility focused on cytokine production and response, I also focused on comparisons of cell death between the various cell lines of my panel. Literature has reported on the importance of cell death for the spread of progeny virions to allow reovirus infection.[175] My experiments revealed some differences in cell death between my various cell lines. Namely the H322 and A253 cell lines released from 5-100 fold less of their progeny virus within the first 24 hpi (**Figure 4.2.1**). I am unsure why there are such differences between the cell lines, for example if it has to do with caspase expression, or the expression of Noxa or TRAIL. However, I did not investigate the mechanism because it was not found to be relevant to the differences in reovirus spread between the cell lines. For example, when additional reovirus was added to media

of infected cells to simulate a greater release of virions by the cells, there was no increase in infection that corresponded with the reovirus spike (**Figure 4.2.2**). So because the differences in cell death were not the sole determinant of limited spread of reovirus, the focus of my project was shifted to antiviral signalling.

My investigations into the antiviral signalling of my cell panel generated results which have led to new questions and insights. One insight was that receptors of Type I and Type III IFNs showed no correlation to the susceptibility of the cell line to reovirus (**Figure 4.4.3**). So while response to the production of IFNs could still be a reason for differing susceptibilities, the issue would likely be caused by a defect independent of the receptor. However, production of cytokines did show correlation with the ability of cells to limit reovirus spread, as 3 of 4 spread-limiting cell lines had much greater production of antiviral cytokines than the 2 susceptible cell lines (**Figure 4.4.1**). This leaves the H322 cells as an interesting case, as they are resistant to reovirus spread, yet produce low amounts of cytokines (IFN-λ, IFN-β, TNF-α) in a manner similar to susceptible H522 and H1299 cells. Since decreased cell death is also clearly not the reason for H322 reovirus resistance (**Figure 4.2.2**), there could be some undetected antiviral factor mediating the response against reovirus in those cells. The susceptible H1299 lung cancer cells also pose an interesting case study, as they have limited amounts of cytokines detected in media by the multiplex ELISA (**Figure 4.4.1**), yet induction of mRNA transcripts of Type I and Type III IFNs in response to reovirus infection is strong (**Figure 4.4.2**). H1299 cells have 128x greater IFN-β mRNA expression and 43x greater IFN-λ mRNA expression than H522 cells, in addition to high basal transcript levels of IFITM3 and PLEKHA4, and strong induction of Ifi44, OAS2, Viperin, TRIM22 and Mx1 (**Table 4.4.1, Figure 4.4.4**). Therefore, I speculate that there is some disconnect following the transcription step in H1299 cells, either resulting in defective protein translation, or

perhaps preventing cytokine secretion from the cell. Due to the heterogeneity of cancer cells, it wouldn't surprise me for many of the cell lines to have different defects.

A further avenue of investigation that could prove interesting would be to use the model system for this project, namely the lung cancer and HNSCC cell lines I evaluated, and test them with another oncolytic virus such as VSV (or the Measles Oncolytic Virus) instead of reovirus. These viruses have been known to have their replication inhibited by addition of exogenous IFN-β to cells.[156, 163, 167] If neutralizing the IFN-β response made the resistant cell lines from our model susceptible to infection with VSV, then we would know that reovirus is in some way stimulating a different antiviral response than VSV. On the other hand, if neutralizing IFN-β did not make our cells susceptible to VSV then we could conclude that our cell lines are utilising a different antiviral mechanism than the cells tested by the other researchers. Conversely, one could apply a similar approach and try to establish reovirus infection and spread on the different cancer cell lines used in the studies with VSV. If those cells, which were susceptible to VSV and sensitive to IFN-β, become resistant to reovirus with addition of exogenous IFN-β that would be an interesting result. Then we could assume there is something unique about the anti-reovirus response of the lung and HNSCC cell lines tested as part of our panel, since they do not have IFN-β as their determinant of reovirus susceptibility in the same way.

In conclusion, the panel of lung and HNSCC cancer cells tested conform to the results expected from the literature with a varied susceptibility to reovirus infection and spread. However, considering the prominence of the Type I IFN pathway as an innate antiviral response, and its importance as a determinant of susceptibility in model Ras-transformed mouse fibroblast cells and to other oncolytic viruses, it was a bit of a surprise that inhibition of the pathway did not confer susceptibility upon resistant cells. Since inhibition of the similar Type III IFN pathway was also

not able to induce a susceptible phenotype in reovirus spread-resistant A549 cells, so far no sole determinant of susceptibility vs resistance has been found. We are left with an unsolved puzzle requiring further experimentation to reveal whether other, untested antiviral mechanisms are responsible for the limitation of reovirus spread, or whether the crosstalk between the myriad antiviral pathways of a cell require a combination of complete knockouts to allow increased reovirus spread. Once a determinant of reovirus resistance in A549 cells has been identified, the final step would be to see if it applies to other cells in the panel and thus would make an effective biomarker for resistance to reovirus spread in cancer cells.

REFERENCES

1. LA, Schiff., ML, Nibert. & KL, Tyler. Reoviruses. In: Howley P.M., Knipe D.M. (ed). *Fields Virology*, 4th edn. Lippincott Williams & Wilkins: Philadelphia, 2006.

2. Shatkin, A.J., Sipe, J.D. & Loh, P. Separation of ten reovirus genome segments by polyacrylamide gel electrophoresis. *J Virol* **2**, 986-991 (1968).

3. Fajardo, E. & Shatkin, A.J. Expression of the two reovirus S1 gene products in transfected mammalian cells. *Virology* **178**, 223-231 (1990).

4. Antczak, J.B. & Joklik, W.K. Reovirus genome segment assortment into progeny genomes studied by the use of monoclonal antibodies directed against reovirus proteins. *Virology* **187**, 760-776 (1992).

5. Sabin, A.B. Reoviruses. A new group of respiratory and enteric viruses formerly classified as ECHO type 10 is described. *Science* **130**, 1387-1389 (1959).

6. Ramos-Alvarez, M. & Sabin, A.B. Characteristics of poliomyelitis and other enteric viruses recovered in tissue culture from healthy American children. *Proc Soc Exp Biol Med* **87**, 655-661 (1954).

7. Rosen, L. Serologic grouping of reoviruses by hemagglutination-inhibition. *Am J Hyg* **71**, 242-249 (1960).

8. Weiner, H.L. & Fields, B.N. Neutralization of reovirus: the gene responsible for the neutralization antigen. *J Exp Med* **146**, 1305-1310 (1977).

9. Weiner, H.L., Ramig, R.F., Mustoe, T.A. & Fields, B.N. Identification of the gene coding for the hemagglutinin of reovirus. *Virology* **86**, 581-584 (1978).

10. Joklik, W.K. Recent progress in reovirus research. *Annu Rev Genet* **19**, 537-575 (1985).

11. Rosen, L., Evans, H.E. & Spickard, A. Reovirus infections in human volunteers. *Am J Hyg* **77**, 29-37 (1963).

12. Jackson, G., Muldoon, R. & Cooper, G. Reovirus Type I As An Etiologic Agent Of Common Cold. *Journal of Clinical Investigation* **40**, 1051-& (1961).

13. Tai, J.H., Williams, J.V., Edwards, K.M., Wright, P.F., Crowe, J.E.& Dermody, T.S. Prevalence of reovirus-specific antibodies in young children in Nashville, Tennessee. *J Infect Dis* **191**, 1221-1224 (2005).

14. Selb, B. & Weber, B. A study of human reovirus IgG and IgA antibodies by ELISA and western blot. *J Virol Methods* **47**, 15-25 (1994).

15. Minuk, G.Y., Paul, R.W. & Lee, P.W. The prevalence of antibodies to reovirus type 3 in adults with idiopathic cholestatic liver disease. *J Med Virol* **16**, 55-60 (1985).

16. Grove, J. & Marsh, M. The cell biology of receptor-mediated virus entry. *J Cell Biol* **195**, 1071-1082 (2011).

17. Tsai, B. Penetration of nonenveloped viruses into the cytoplasm. *Annu Rev Cell Dev Biol* **23**, 23-43 (2007).

18. Barton, E.S., Forrest, J. C., Connolly, J. L., Chappell, J. D., Liu, Y., Schnell, F. J., Nusrat, A., Parkos, C. A. & Dermody, T. S. Junction adhesion molecule is a receptor for reovirus. *Cell* **104**, 441-451 (2001).

19. Maginnis, M.S., Forrest, J. C., Kopecky-Bromberg, S. A., Dickeson, S. K., Santoro, S. A., Zutter, M. M., Nemerow, G. R., Bergelson, J. M. & Dermody, T. S. Beta1 integrin mediates internalization of mammalian reovirus. *J Virol* **80**, 2760-2770 (2006).

20. Schulz, W.L., Haj, A.K. & Schiff, L.A. Reovirus uses multiple endocytic pathways for cell entry. *J Virol* **86**, 12665-12675 (2012).

21. Barton, E.S., Connolly, J.L., Forrest, J.C., Chappell, J.D. & Dermody, T.S. Utilization of sialic acid as a coreceptor enhances reovirus attachment by multistep adhesion strengthening. *J Biol Chem* **276**, 2200-2211 (2001).

22. Chappell, J.D., Duong, J.L., Wright, B.W. & Dermody, T.S. Identification of carbohydrate-binding domains in the attachment proteins of type 1 and type 3 reoviruses. *J Virol* **74**, 8472-8479 (2000).

23. Borsa, J., Copps, T.P., Sargent, M.D., Long, D.G. & Chapman, J.D. New intermediate subviral particles in the in vitro uncoating of reovirus virions by chymotrypsin. *J Virol* **11**, 552-564 (1973).

24. Sturzenbecker, L.J., Nibert, M., Furlong, D. & Fields, B.N. Intracellular digestion of reovirus particles requires a low pH and is an essential step in the viral infectious cycle. *J Virol* **61**, 2351-2361 (1987).

25. Ebert, D.H., Deussing, J., Peters, C. & Dermody, T.S. Cathepsin L and cathepsin B mediate reovirus disassembly in murine fibroblast cells. *J Biol Chem* **277**, 24609-24617 (2002).

26. Golden, J.W., Bahe, J.A., Lucas, W.T., Nibert, M.L. & Schiff, L.A. Cathepsin S supports acid-independent infection by some reoviruses. *J Biol Chem* **279**, 8547-8557 (2004).

27. Mason, S.D. & Joyce, J.A. Proteolytic networks in cancer. *Trends Cell Biol* **21**, 228-237 (2011).

28. Bodkin, D.K., Nibert, M.L. & Fields, B.N. Proteolytic digestion of reovirus in the intestinal lumens of neonatal mice. *J Virol* **63**, 4676-4681 (1989).

29. Sloane, B.F., Yan, S., Podgorski, I., Linebaugh, B. E., Cher, M. L., Mai, J., Cavallo-Medved, D., Sameni, M., Dosescu, J. & Moin, K. Cathepsin B and tumor proteolysis: contribution of the tumor microenvironment. *Semin Cancer Biol* **15**, 149-157 (2005).

30. Terasawa, Y., Hotani, T., Katayama, Y., Tachibana, M., Mizuguchi, H. & Sakurai, F. Activity levels of cathepsins B and L in tumor cells are a biomarker for efficacy of reovirus-mediated tumor cell killing. *Cancer Gene Ther* **22**, 188-197 (2015).

31. Zhang, L., Agosto, M. A., Ivanovic, T., King, D. S., Nibert, M. L. & Harrison, S. C. Requirements for the formation of membrane pores by the reovirus myristoylated micro1N peptide. *J Virol* **83**, 7004-7014 (2009).

32. Dryden, K.A., Wang, G., Yeager, M., Nibert, M. L., Coombs, K. M., Furlong, D. B., Fields, B. N. & Baker, T. S. Early steps in reovirus infection are associated with dramatic changes in supramolecular structure and protein conformation: analysis of virions and subviral particles by cryoelectron microscopy and image reconstruction. *J Cell Biol* **122**, 1023-1041 (1993).

33. Munemitsu, S.M. & Samuel, C.E. Biosynthesis of reovirus-specified polypeptides. Multiplication rate but not yield of reovirus serotypes 1 and 3 correlates with the level of virus-mediated inhibition of cellular protein synthesis. *Virology* **136**, 133-143 (1984).

34. Muñoz, A., Alonso, M.A. & Carrasco, L. The regulation of translation in reovirus-infected cells. *J Gen Virol* **66 (Pt 10)**, 2161-2170 (1985).

35. Mohamed, A., Johnston, R.N. & Shmulevitz, M. Potential for Improving Potency and Specificity of Reovirus Oncolysis with Next-Generation Reovirus Variants. *Viruses* **7**, 6251-6278 (2015).

36. Bennette, J.G. Isolation of a non-pathogenic tumour-destroying virus from mouse ascites. *Nature* **187**, 72-73 (1960).

37. Bennette, J.G., Bush, P.V. & Steele, R.D. Characteristics of a newborn runt disease induced by neonatal infection with an oncolytic strain of reovirus type 3 (REO3MH). I. Pathological investigations in rats and mice. *Br J Exp Pathol* **48**, 251-266 (1967).

38. Hashiro, G., Loh, P.C. & Yau, J.T. The preferential cytotoxicity of reovirus for certain transformed cell lines. *Arch Virol* **54**, 307-315 (1977).

39. Duncan, M.R., Stanish, S.M. & Cox, D.C. Differential sensitivity of normal and transformed human cells to reovirus infection. *J Virol* **28**, 444-449 (1978).

40. Strong, J.E., Tang, D. & Lee, P.W. Evidence that the epidermal growth factor receptor on host cells confers reovirus infection efficiency. *Virology* **197**, 405-411 (1993).

41. Strong, J.E. & Lee, P.W. The v-erbB oncogene confers enhanced cellular susceptibility to reovirus infection. *J Virol* **70**, 612-616 (1996).

42. Campbell, S.L., Khosravi-Far, R., Rossman, K.L., Clark, G.J. & Der, C.J. Increasing complexity of Ras signaling. *Oncogene* **17**, 1395-1413 (1998).

43. Strong, J.E., Coffey, M.C., Tang, D., Sabinin, P. & Lee, P.W. The molecular basis of viral oncolysis: usurpation of the Ras signaling pathway by reovirus. *EMBO J* **17**, 3351-3362 (1998).

44. Bos, J.L. ras oncogenes in human cancer: a review. *Cancer Res* **49**, 4682-4689 (1989).

45. Alain, T., Hirasawa, K., Pon, K. J., Nishikawa, S. G., Urbanski, S. J., Auer, Y., Luider, J., Martin, A., Johnston, R. N., Janowska-Wieczorek, A., Lee, P. W. & Kossakowska, A. E. Reovirus therapy of lymphoid malignancies. *Blood* **100**, 4146-4153 (2002).

46. Marcato, P., Shmulevitz, M. & Lee, P.W. Connecting reovirus oncolysis and Ras signaling. *Cell Cycle* **4**, 556-559 (2005).

47. What is Reolysin? 2016 [cited 2016 06 April]Available from: http://www.oncolyticsbiotech.com/reolysin/what-is-reolysin/

48. Chakrabarty, R., Tran, H., Fortin, Y., Yu, Z., Shen, S. H., Kolman, J., Onions, D., Voyer, R., Hagerman, A., Serl, S., Kamen, A., Thompson, B. & Coffey, M. Evaluation of homogeneity and genetic stability of REOLYSIN (pelareorep) by complete genome sequencing of reovirus after large scale production. *Appl Microbiol Biotechnol* **98**, 1763-1770 (2014).

49. Clinical Trials. 2016 [cited 2016 06 April]Available from: http://www.oncolyticsbiotech.com/reolysin/clinical-trials/

50. Thirukkumaran, C. & Morris, D.G. Oncolytic Viral Therapy Using Reovirus. *Methods Mol Biol* **1317**, 187-223 (2015).

51. Vidal, L., Pandha, H. S., Yap, T. A., White, C. L., Twigger, K., Vile, R. G., Melcher, A., Coffey, M., Harrington, K. J. & DeBono, J. S. A phase I study of intravenous oncolytic reovirus type 3 Dearing in patients with advanced cancer. *Clin Cancer Res* **14**, 7127-7137 (2008).

52. Morris, D.G., Feng, X., DiFrancesco, L. M., Fonseca, K., Forsyth, P. A., Paterson, A. H., Coffey, M. C. & Thompson, B. REO-001: A phase I trial of percutaneous intralesional administration of reovirus type 3 dearing (Reolysin®) in patients with advanced solid tumors. *Invest New Drugs* **31**, 696-706 (2013).

53. Galanis, E., Markovic, S. N., Suman, V. J., Nuovo, G. J., Vile, R. G., Kottke, T. J., Nevala, W. K., Thompson, M. A., Lewis, J. E., Rumilla, K. M., Roulstone, V., Harrington, K., Linette, G. P., Maples, W. J., Coffey, M., Zwiebel, J. & Kendra, K. Phase II trial of intravenous administration of Reolysin(®) (Reovirus Serotype-3-dearing Strain) in patients with metastatic melanoma. *Mol Ther* **20**, 1998-2003 (2012).

54. Gollamudi, R., Ghalib, M. H., Desai, K. K., Chaudhary, I., Wong, B., Einstein, M., Coffey, M., Gill, G. M., Mettinger, K., Mariadason, J. M., Mani, S. & Goel, S.

Intravenous administration of Reolysin, a live replication competent RNA virus is safe in patients with advanced solid tumors. *Invest New Drugs* **28**, 641-649 (2010).

55. Forsyth, P., Roldán, G., George, D., Wallace, C., Palmer, C. A., Morris, D., Cairncross, G., Matthews, M. V., Markert, J., Gillespie, Y., Coffey, M., Thompson, B. & Hamilton, M. A phase I trial of intratumoral administration of reovirus in patients with histologically confirmed recurrent malignant gliomas. *Mol Ther* **16**, 627-632 (2008).

56. Chiocca, E.A. The host response to cancer virotherapy. *Curr Opin Mol Ther* **10**, 38-45 (2008).

57. Sborov, D.W., Nuovo, G. J., Stiff, A., Mace, T., Lesinski, G. B., Benson, D. M., Efebera, Y. A., Rosko, A. E., Pichiorri, F., Grever, M. R., Hofmeister, C. C. A phase I trial of single-agent reolysin in patients with relapsed multiple myeloma. *Clin Cancer Res* **20**, 5946-5955 (2014).

58. Sei, S., Mussio, J. K., Yang, Q. E., Nagashima, K., Parchment, R. E., Coffey, M. C., Shoemaker, R. H. & Tomaszewski, J. E. Synergistic antitumor activity of oncolytic reovirus and chemotherapeutic agents in non-small cell lung cancer cells. *Mol Cancer* **8**, 47 (2009).

59. Heinemann, L., Simpson, G. R., Boxall, A., Kottke, T., Relph, K. L., Vile, R., Melcher, A., Prestwich, R., Harrington, K. J., Morgan, R. & Pandha, H. S. Synergistic effects of oncolytic reovirus and docetaxel chemotherapy in prostate cancer. *BMC Cancer* **11**, 221 (2011).

60. Gujar, S.A., Clements, D., Dielschneider, R., Helson, E., Marcato, P. & Lee, P. W. Gemcitabine enhances the efficacy of reovirus-based oncotherapy through anti-tumour immunological mechanisms. *Br J Cancer* **110**, 83-93 (2014).

61. Shmulevitz, M., Marcato, P. & Lee, P.W. Activated Ras signaling significantly enhances reovirus replication and spread. *Cancer Gene Ther* **17**, 69-70 (2010).

62. Shmulevitz, M. & Lee, P.W. Exploring host factors that impact reovirus replication, dissemination, and reovirus-induced cell death in cancer versus normal cells in culture. *Methods Mol Biol* **797**, 163-176 (2012).

63. Marcato, P., Shmulevitz, M., Pan, D., Stoltz, D. & Lee, P.W. Ras transformation mediates reovirus oncolysis by enhancing virus uncoating, particle infectivity, and apoptosis-dependent release. *Mol Ther* **15**, 1522-1530 (2007).

64. Shmulevitz, M., Pan, L.Z., Garant, K., Pan, D. & Lee, P.W. Oncogenic Ras promotes reovirus spread by suppressing IFN-beta production through negative regulation of RIG-I signaling. *Cancer Res* **70**, 4912-4921 (2010).

65. Garant, K.A., Shmulevitz, M., Pan, L., Daigle, R. M., Ahn, D. G., Gujar, S. A. & Lee, P. W. Oncolytic reovirus induces intracellular redistribution of Ras to promote apoptosis and progeny virus release. *Oncogene* **35**, 771-782 (2016).

66. Heinemann, L., Simpson, G. R., Annels, N. E., Vile, R., Melcher, A., Prestwich, R., Harrington, K. J. & Pandha, H. S. The effect of cell cycle synchronization on tumor sensitivity to reovirus oncolysis. *Mol Ther* **18**, 2085-2093 (2010).

67. Norman, K.L., Hirasawa, K., Yang, A.D., Shields, M.A. & Lee, P.W. Reovirus oncolysis: the Ras/RalGEF/p38 pathway dictates host cell permissiveness to reovirus infection. *Proc Natl Acad Sci U S A* **101**, 11099-11104 (2004).

68. Twigger, K., Roulstone, V., Kyula, J., Karapanagiotou, E. M., Syrigos, K. N., Morgan, R., White, C., Bhide, S., Nuovo, G., Coffey, M., Thompson, B., Jebar, A., Errington, F., Melcher, A. A., Vile, R. G., Pandha, H. S. & Harrington, K. J. Reovirus exerts potent oncolytic effects in head and neck cancer cell lines that are independent of signalling in the EGFR pathway. *BMC Cancer* **12**, 368 (2012).

69. Thirukkumaran, C.M., Luider, J. M., Stewart, D. A., Cheng, T., Lupichuk, S. M., Nodwell, M. J., Russell, J. A., Auer, I. A. & Morris, D. G. Reovirus oncolysis as a novel purging strategy for autologous stem cell transplantation. *Blood* **102**, 377-387 (2003).

70. Maitra, R., Seetharam, R., Tesfa, L., Augustine, T. A., Klampfer, L., Coffey, M. C., Mariadason, J. M. & Goel, S. Oncolytic reovirus preferentially induces apoptosis in KRAS mutant colorectal cancer cells, and synergizes with irinotecan. *Oncotarget* **5**, 2807-2819 (2014).

71. Hahn, W.C., Counter, C. M., Lundberg, A. S., Beijersbergen, R. L., Brooks, M. W., Weinberg, R. A. Creation of human tumour cells with defined genetic elements. *Nature* **400**, 464-468 (1999).

72. Errington, F., White, C. L., Twigger, K. R., Rose, A., Scott, K., Steele, L., Ilett, L. J., Prestwich, R., Pandha, H. S., Coffey, M., Selby, P., Vile, R., Harrington, K. J. & Melcher, A. A. Inflammatory tumour cell killing by oncolytic reovirus for the treatment of melanoma. *Gene Ther* **15**, 1257-1270 (2008).

73. Grandvaux, N., tenOever, B.R., Servant, M.J. & Hiscott, J. The interferon antiviral response: from viral invasion to evasion. *Curr Opin Infect Dis* **15**, 259-267 (2002).

74. Christian, S.L., Collier, T. W., Zu, D., Licursi, M., Hough, C. M. & Hirasawa, K. Activated Ras/MEK inhibits the antiviral response of alpha interferon by reducing STAT2 levels. *J Virol* **83**, 6717-6726 (2009).

75. Klampfer, L., Huang, J., Corner, G., Mariadason, J., Arango, D., Sasazuki, T., Shirasawa, S. & Augenlicht, L. Oncogenic Ki-ras inhibits the expression of interferon-responsive genes through inhibition of STAT1 and STAT2 expression. *J Biol Chem* **278**, 46278-46287 (2003).

76. Tian, J., Zhang, X., Wu, H., Liu, C., Li, Z., Hu, X., Su, S., Wang, L. F. & Qu, L. Blocking the PI3K/AKT pathway enhances mammalian reovirus replication by repressing IFN-stimulated genes. *Front Microbiol* **6**, 886 (2015).

77. Zhang, X., Wu, H., Liu, C., Tian, J. & Qu, L. PI3K/Akt/p53 pathway inhibits reovirus infection. *Infect Genet Evol* **34**, 415-422 (2015).

78. Ezell, S.A., Polytarchou, C., Hatziapostolou, M., Guo, A., Sanidas, I., Bihani, T., Comb, M. J., Sourvinos, G. & Tsichlis, P. N. The protein kinase Akt1 regulates the interferon response through phosphorylation of the transcriptional repressor EMSY. *Proc Natl Acad Sci U S A* **109**, E613-621 (2012).

79. Wilkins, C. & Gale, M. Recognition of viruses by cytoplasmic sensors. *Curr Opin Immunol* **22**, 41-47 (2010).

80. Furuichi, Y., Muthukrishnan, S. & Shatkin, A.J. 5'-Terminal m-7G(5')ppp(5')G-m-p in vivo: identification in reovirus genome RNA. *Proc Natl Acad Sci U S A* **72**, 742-745 (1975).

81. Kell, A.M. & Gale, M. RIG-I in RNA virus recognition. *Virology* **479-480**, 110-121 (2015).

82. Schlee, M. Master sensors of pathogenic RNA - RIG-I like receptors. *Immunobiology* **218**, 1322-1335 (2013).

83. Wies, E., Wang, M. K., Maharaj, N. P., Chen, K., Zhou, S., Finberg, R. W. & Gack, M. U. Dephosphorylation of the RNA sensors RIG-I and MDA5 by the phosphatase PP1 is essential for innate immune signaling. *Immunity* **38**, 437-449 (2013).

84. Meurs, E., Chong, K., Galabru, J., Thomas, N. S., Kerr, I. M., Williams, B. R. & Hovanessian, A. G. Molecular cloning and characterization of the human double-stranded RNA-activated protein kinase induced by interferon. *Cell* **62**, 379-390 (1990).

85. Hovanessian, A.G. The double stranded RNA-activated protein kinase induced by interferon: dsRNA-PK. *J Interferon Res* **9**, 641-647 (1989).

86. Williams, B.R. PKR; a sentinel kinase for cellular stress. *Oncogene* **18**, 6112-6120 (1999).

87. Kumar, A., Haque, J., Lacoste, J., Hiscott, J. & Williams, B.R. Double-stranded RNA-dependent protein kinase activates transcription factor NF-kappa B by phosphorylating I kappa B. *Proc Natl Acad Sci U S A* **91**, 6288-6292 (1994).

88. Cascalló, M., Capellà, G., Mazo, A. & Alemany, R. Ras-dependent oncolysis with an adenovirus VAI mutant. *Cancer Res* **63**, 5544-5550 (2003).

89. Paun, A. & Pitha, P.M. The IRF family, revisited. *Biochimie* **89**, 744-753 (2007).

90. Barnes, B., Lubyova, B. & Pitha, P.M. On the role of IRF in host defense. *J Interferon Cytokine Res* **22**, 59-71 (2002).

91. Nguyen, H., Hiscott, J. & Pitha, P.M. The growing family of interferon regulatory factors. *Cytokine Growth Factor Rev* **8**, 293-312 (1997).

92. Au, W.C., Moore, P.A., Lowther, W., Juang, Y.T. & Pitha, P.M. Identification of a member of the interferon regulatory factor family that binds to the interferon-stimulated response element and activates expression of interferon-induced genes. *Proc Natl Acad Sci U S A* **92**, 11657-11661 (1995).

93. Taniguchi, T., Ogasawara, K., Takaoka, A. & Tanaka, N. IRF family of transcription factors as regulators of host defense. *Annu Rev Immunol* **19**, 623-655 (2001).

94. Osterlund, P.I., Pietilä, T.E., Veckman, V., Kotenko, S.V. & Julkunen, I. IFN regulatory factor family members differentially regulate the expression of type III IFN (IFN-lambda) genes. *J Immunol* **179**, 3434-3442 (2007).

95. Raj, N.B., Engelhardt, J., Au, W.C., Levy, D.E. & Pitha, P.M. Virus infection and interferon can activate gene expression through a single synthetic element, but endogenous genes show distinct regulation. *J Biol Chem* **264**, 16658-16666 (1989).

96. Goodbourn, S. & Maniatis, T. Overlapping positive and negative regulatory domains of the human beta-interferon gene. *Proc Natl Acad Sci U S A* **85**, 1447-1451 (1988).

97. Fujita, T., Ohno, S., Yasumitsu, H. & Taniguchi, T. Delimitation and properties of DNA sequences required for the regulated expression of human interferon-beta gene. *Cell* **41**, 489-496 (1985).

98. Ryals, J., Dierks, P., Ragg, H. & Weissmann, C. A 46-nucleotide promoter segment from an IFN-alpha gene renders an unrelated promoter inducible by virus. *Cell* **41**, 497-507 (1985).

99. Kim, T.K. & Maniatis, T. The mechanism of transcriptional synergy of an in vitro assembled interferon-beta enhanceosome. *Mol Cell* **1**, 119-129 (1997).

100. Merika, M., Williams, A.J., Chen, G., Collins, T. & Thanos, D. Recruitment of CBP/p300 by the IFN beta enhanceosome is required for synergistic activation of transcription. *Mol Cell* **1**, 277-287 (1998).

101. Fujii, Y., Shimizu, T., Kusumoto, M., Kyogoku, Y., Taniguchi, T. & Hakoshima, T. Crystal structure of an IRF-DNA complex reveals novel DNA recognition and cooperative binding to a tandem repeat of core sequences. *EMBO J* **18**, 5028-5041 (1999).

102. Lin, R., Génin, P., Mamane, Y. & Hiscott, J. Selective DNA binding and association with the CREB binding protein coactivator contribute to differential activation of alpha/beta interferon genes by interferon regulatory factors 3 and 7. *Mol Cell Biol* **20**, 6342-6353 (2000).

103. Au, W.C., Yeow, W.S. & Pitha, P.M. Analysis of functional domains of interferon regulatory factor 7 and its association with IRF-3. *Virology* **280**, 273-282 (2001).

104. Onoguchi, K., Yoneyama, M., Takemura, A., Akira, S., Taniguchi, T., Namiki, H. & Fujita, T. Viral infections activate types I and III interferon genes through a common mechanism. *J Biol Chem* **282**, 7576-7581 (2007).

105. Kotenko, S.V. IFN-λs. *Curr Opin Immunol* **23**, 583-590 (2011).

106. Holm, G.H., Zurney, J., Tumilasci, V., Leveille, S., Danthi, P., Hiscott, J., Sherry, B. & Dermody, T. S. Retinoic acid-inducible gene-I and interferon-beta promoter stimulator-1 augment proapoptotic responses following mammalian reovirus infection via interferon regulatory factor-3. *J Biol Chem* **282**, 21953-21961 (2007).

107. Yoneyama, M., Kikuchi, M., Natsukawa, T., Shinobu, N., Imaizumi, T., Miyagishi, M., Taira, K., Akira, S. & Fujita, T. The RNA helicase RIG-I has an essential function in double-stranded RNA-induced innate antiviral responses. *Nat Immunol* **5**, 730-737 (2004).

108. Pestka, S., Krause, C.D. & Walter, M.R. Interferons, interferon-like cytokines, and their receptors. *Immunol Rev* **202**, 8-32 (2004).

109. Trinchieri, G. Type I interferon: friend or foe? *J Exp Med* **207**, 2053-2063 (2010).

110. Kawai, T. & Akira, S. Antiviral signaling through pattern recognition receptors. *J Biochem* **141**, 137-145 (2007).

111. de Weerd, N.A., Vivian, J. P., Nguyen, T. K., Mangan, N. E., Gould, J. A., Braniff, S. J., Zaker-Tabrizi, L., Fung, K. Y., Forster, S. C., Beddoe, T., Reid, H. H., Rossjohn, J. & Hertzog, P. J. Structural basis of a unique interferon-β signaling axis mediated via the receptor IFNAR1. *Nat Immunol* **14**, 901-907 (2013).

112. McNab, F., Mayer-Barber, K., Sher, A., Wack, A. & O'Garra, A. Type I interferons in infectious disease. *Nat Rev Immunol* **15**, 87-103 (2015).

113. Hervas-Stubbs, S., Perez-Gracia, J. L., Rouzaut, A., Sanmamed, M. F., Le Bon, A. & Melero, I. Direct effects of type I interferons on cells of the immune system. *Clin Cancer Res* **17**, 2619-2627 (2011).

114. Witte, K., Witte, E., Sabat, R. & Wolk, K. IL-28A, IL-28B, and IL-29: promising cytokines with type I interferon-like properties. *Cytokine Growth Factor Rev* **21**, 237-251 (2010).

115. Prokunina-Olsson, L., Muchmore, B., Tang, W., Pfeiffer, R. M., Park, H., Dickensheets, H., Hergott, D., Porter-Gill, P., Mumy, A., Kohaar, I., Chen, S., Brand, N., Tarway, M., Liu, L., Sheikh, F., Astemborski, J., Bonkovsky, H. L., Edlin, B. R., Howell, C. D., Morgan, T. R., Thomas, D. L., Rehermann, B., Donnelly, R. P. & O'Brien, T. R. A variant upstream of IFNL3 (IL28B) creating a new interferon gene IFNL4 is associated with impaired clearance of hepatitis C virus. *Nat Genet* **45**, 164-171 (2013).

116. Wack, A., Terczyńska-Dyla, E. & Hartmann, R. Guarding the frontiers: the biology of type III interferons. *Nat Immunol* **16**, 802-809 (2015).

117. Crotta, S., Davidson, S., Mahlakoiv, T., Desmet, C. J., Buckwalter, M. R., Albert, M. L., Staeheli, P. & Wack, A. Type I and type III interferons drive redundant amplification loops to induce a transcriptional signature in influenza-infected airway epithelia. *PLoS Pathog* **9**, e1003773 (2013).

118. Platanias, L.C. & Fish, E.N. Signaling pathways activated by interferons. *Exp Hematol* **27**, 1583-1592 (1999).

119. Uddin, S., Chamdin, A. & Platanias, L.C. Interaction of the transcriptional activator Stat-2 with the type I interferon receptor. *J Biol Chem* **270**, 24627-24630 (1995).

120. Colamonici, O., Yan, H., Domanski, P., Handa, R., Smalley, D., Mullersman, J., Witte, M., Krishnan, K. & Krolewski, J. Direct binding to and tyrosine phosphorylation of the alpha subunit of the type I interferon receptor by p135tyk2 tyrosine kinase. *Mol Cell Biol* **14**, 8133-8142 (1994).

121. Domanski, P., Fish, E., Nadeau, O. W., Witte, M., Platanias, L. C., Yan, H., Krolewski, J., Pitha, P. & Colamonici, O. R. A region of the beta subunit of the interferon alpha receptor different from box 1 interacts with Jak1 and is sufficient to activate the Jak-Stat pathway and induce an antiviral state. *J Biol Chem* **272**, 26388-26393 (1997).

122. Silvennoinen, O., Ihle, J.N., Schlessinger, J. & Levy, D.E. Interferon-induced nuclear signalling by Jak protein tyrosine kinases. *Nature* **366**, 583-585 (1993).

123. Müller, M., Briscoe, J., Laxton, C., Guschin, D., Ziemiecki, A., Silvennoinen, O., Harpur, A. G., Barbieri, G., Witthuhn, B. A. & Schindler, C. The protein tyrosine kinase JAK1 complements defects in interferon-alpha/beta and -gamma signal transduction. *Nature* **366**, 129-135 (1993).

124. Platanias, L.C. & Colamonici, O.R. Interferon alpha induces rapid tyrosine phosphorylation of the alpha subunit of its receptor. *J Biol Chem* **267**, 24053-24057 (1992).

125. Platanias, L.C., Uddin, S. & Colamonici, O.R. Tyrosine phosphorylation of the alpha and beta subunits of the type I interferon receptor. Interferon-beta selectively induces tyrosine phosphorylation of an alpha subunit-associated protein. *J Biol Chem* **269**, 17761-17764 (1994).

126. Schindler, C., Shuai, K., Prezioso, V.R. & Darnell, J.E. Interferon-dependent tyrosine phosphorylation of a latent cytoplasmic transcription factor. *Science* **257**, 809-813 (1992).

127. Fu, X.Y. A transcription factor with SH2 and SH3 domains is directly activated by an interferon alpha-induced cytoplasmic protein tyrosine kinase(s). *Cell* **70**, 323-335 (1992).

128. Abroun, S., Saki, N., Ahmadvand, M., Asghari, F., Salari, F. & Rahim, F. STATs: An Old Story, Yet Mesmerizing. *Cell J* **17**, 395-411 (2015).

129. Darnell, J.E. STATs and gene regulation. *Science* **277**, 1630-1635 (1997).

130. Darnell, J.E. Studies of IFN-induced transcriptional activation uncover the Jak-Stat pathway. *J Interferon Cytokine Res* **18**, 549-554 (1998).

131. Stark, G.R. How cells respond to interferons revisited: from early history to current complexity. *Cytokine Growth Factor Rev* **18**, 419-423 (2007).

132. Stark, G.R. & Darnell, J.E. The JAK-STAT pathway at twenty. *Immunity* **36**, 503-514 (2012).

133. Schneider, W.M., Chevillotte, M.D. & Rice, C.M. Interferon-stimulated genes: a complex web of host defenses. *Annu Rev Immunol* **32**, 513-545 (2014).

134. Schoggins, J.W. & Rice, C.M. Interferon-stimulated genes and their antiviral effector functions. *Curr Opin Virol* **1**, 519-525 (2011).

135. Mundt, E. Human MxA protein confers resistance to double-stranded RNA viruses of two virus families. *J Gen Virol* **88**, 1319-1323 (2007).

136. Stewart, M.J., Blum, M.A. & Sherry, B. PKR's protective role in viral myocarditis. *Virology* **314**, 92-100 (2003).

137. Nilsen, T.W., Maroney, P.A. & Baglioni, C. Inhibition of protein synthesis in reovirus-infected HeLa cells with elevated levels of interferon-induced protein kinase activity. *J Biol Chem* **257**, 14593-14596 (1982).

138. Anafu, A.A., Bowen, C.H., Chin, C.R., Brass, A.L. & Holm, G.H. Interferon-inducible transmembrane protein 3 (IFITM3) restricts reovirus cell entry. *J Biol Chem* **288**, 17261-17271 (2013).

139. Brass, A.L., Huang, I. C., Benita, Y., John, S. P., Krishnan, M. N., Feeley, E. M., Ryan, B. J., Weyer, J. L., van der Weyden, L., Fikrig, E., Adams, D. J., Xavier, R. J., Farzan, M. & Elledge, S. J. The IFITM proteins mediate cellular resistance to influenza A H1N1 virus, West Nile virus, and dengue virus. *Cell* **139**, 1243-1254 (2009).

140. Friedman, R.L., Manly, S.P., McMahon, M., Kerr, I.M. & Stark, G.R. Transcriptional and posttranscriptional regulation of interferon-induced gene expression in human cells. *Cell* **38**, 745-755 (1984).

141. Weidner, J.M., Jiang, D., Pan, X. B., Chang, J., Block, T. M. & Guo, J. T. Interferon-induced cell membrane proteins, IFITM3 and tetherin, inhibit vesicular stomatitis virus infection via distinct mechanisms. *J Virol* **84**, 12646-12657 (2010).

142. Locksley, R.M., Killeen, N. & Lenardo, M.J. The TNF and TNF receptor superfamilies: integrating mammalian biology. *Cell* **104**, 487-501 (2001).

143. Meusel, T.R., Kehoe, K.E. & Imani, F. Protein kinase R regulates double-stranded RNA induction of TNF-alpha but not IL-1 beta mRNA in human epithelial cells. *J Immunol* **168**, 6429-6435 (2002).

144. Fesik, S.W. Insights into programmed cell death through structural biology. *Cell* **103**, 273-282 (2000).

145. Inoue, J., Ishida, T., Tsukamoto, N., Kobayashi, N., Naito, A., Azuma, S. & Yamamoto, T. Tumor necrosis factor receptor-associated factor (TRAF) family: adapter proteins that mediate cytokine signaling. *Exp Cell Res* **254**, 14-24 (2000).

146. Wong, G.H. & Goeddel, D.V. Tumour necrosis factors alpha and beta inhibit virus replication and synergize with interferons. *Nature* **323**, 819-822 (1986).

147. Farone, A.L., O'Brien, P.C. & Cox, D.C. Tumor necrosis factor-alpha induction by reovirus serotype 3. *J Leukoc Biol* **53**, 133-137 (1993).

148. Sedger, L.M., Shows, D. M., Blanton, R. A., Peschon, J. J., Goodwin, R. G., Cosman, D. & Wiley, S. R. IFN-gamma mediates a novel antiviral activity through dynamic modulation of TRAIL and TRAIL receptor expression. *J Immunol* **163**, 920-926 (1999).

149. Pan, G., O'Rourke, K., Chinnaiyan, A. M., Gentz, R., Ebner, R., Ni, J. & Dixit, V. M. The receptor for the cytotoxic ligand TRAIL. *Science* **276**, 111-113 (1997).

150. Walczak, H., Degli-Esposti, M. A., Johnson, R. S., Smolak, P. J., Waugh, J. Y., Boiani, N., Timour, M. S., Gerhart, M. J., Schooley, K. A., Smith, C. A., Goodwin, R. G. & Rauch, C. T. TRAIL-R2: a novel apoptosis-mediating receptor for TRAIL. *EMBO J* **16**, 5386-5397 (1997).

151. Clarke, P., Meintzer, S. M., Gibson, S., Widmann, C., Garrington, T. P., Johnson, G. L. & Tyler, K. L. Reovirus-induced apoptosis is mediated by TRAIL. *J Virol* **74**, 8135-8139 (2000).

152. Clarke, P., Richardson-Burns, S.M., DeBiasi, R.L. & Tyler, K.L. Mechanisms of apoptosis during reovirus infection. *Curr Top Microbiol Immunol* **289**, 1-24 (2005).

153. Garber, K. China approves world's first oncolytic virus therapy for cancer treatment. *J Natl Cancer Inst* **98**, 298-300 (2006).

154. Miest, T.S. & Cattaneo, R. New viruses for cancer therapy: meeting clinical needs. *Nat Rev Microbiol* **12**, 23-34 (2014).

155. Stojdl, D.F., Lichty, B. D., tenOever, B. R., Paterson, J. M., Power, A. T., Knowles, S., Marius, R., Reynard, J., Poliquin, L., Atkins, H. , Brown, E. G., Durbin, R. K., Durbin, J. E., Hiscott, J. & Bell, J. C. VSV strains with defects in their ability to shutdown innate immunity are potent systemic anti-cancer agents. *Cancer Cell* **4**, 263-275 (2003).

156. Blackham, A.U., Northrup, S. A., Willingham, M., Sirintrapun, J., Russell, G. B., Lyles, D. S. & Stewart, J. H. Molecular determinants of susceptibility to oncolytic vesicular stomatitis virus in pancreatic adenocarcinoma. *J Surg Res* **187**, 412-426 (2014).

157. Murphy, A.M., Besmer, D. M., Moerdyk-Schauwecker, M., Moestl, N., Ornelles, D. A., Mukherjee, P. & Grdzelishvili, V. Z. Vesicular stomatitis virus as an oncolytic agent against pancreatic ductal adenocarcinoma. *J Virol* **86**, 3073-3087 (2012).

158. Moerdyk-Schauwecker, M., Shah, N. R., Murphy, A. M., Hastie, E., Mukherjee, P. & Grdzelishvili, V. Z. Resistance of pancreatic cancer cells to oncolytic vesicular stomatitis virus: role of type I interferon signaling. *Virology* **436**, 221-234 (2013).

159. Escobar-Zarate, D., Liu, Y.P., Suksanpaisan, L., Russell, S.J. & Peng, K.W. Overcoming cancer cell resistance to VSV oncolysis with JAK1/2 inhibitors. *Cancer Gene Ther* **20**, 582-589 (2013).

160. Westcott, M.M., Liu, J., Rajani, K., D'Agostino, R., Lyles, D. S. & Porosnicu, M. Interferon Beta and Interferon Alpha 2a Differentially Protect Head and Neck Cancer Cells from Vesicular Stomatitis Virus-Induced Oncolysis. *J Virol* **89**, 7944-7954 (2015).

161. Cataldi, M., Shah, N.R., Felt, S.A. & Grdzelishvili, V.Z. Breaking resistance of pancreatic cancer cells to an attenuated vesicular stomatitis virus through a novel activity of IKK inhibitor TPCA-1. *Virology* **485**, 340-354 (2015).

162. Msaouel, P., Iankov, I.D., Dispenzieri, A. & Galanis, E. Attenuated oncolytic measles virus strains as cancer therapeutics. *Curr Pharm Biotechnol* **13**, 1732-1741 (2012).

163. Achard, C., Boisgerault, N., Delaunay, T., Roulois, D., Nedellec, S., Royer, P. J., Pain, M., Combredet, C., Mesel-Lemoine, M., Cellerin, L., Magnan, A., Tangy, F., Grégoire, M. & Fonteneau, J. F. Sensitivity of human pleural mesothelioma to oncolytic measles virus depends on defects of the type I interferon response. *Oncotarget* **6**, 44892-44904 (2015).

164. Palosaari, H., Parisien, J.P., Rodriguez, J.J., Ulane, C.M. & Horvath, C.M. STAT protein interference and suppression of cytokine signal transduction by measles virus V protein. *J Virol* **77**, 7635-7644 (2003).

165. Shaffer, J.A., Bellini, W.J. & Rota, P.A. The C protein of measles virus inhibits the type I interferon response. *Virology* **315**, 389-397 (2003).

166. Takeuchi, K., Kadota, S.I., Takeda, M., Miyajima, N. & Nagata, K. Measles virus V protein blocks interferon (IFN)-alpha/beta but not IFN-gamma signaling by inhibiting STAT1 and STAT2 phosphorylation. *FEBS Lett* **545**, 177-182 (2003).

167. Berchtold, S., Lampe, J., Weiland, T., Smirnow, I., Schleicher, S., Handgretinger, R., Kopp, H. G., Reiser, J., Stubenrauch, F., Mayer, N., Malek, N. P., Bitzer, M. & Lauer, U. M. Innate immune defense defines susceptibility of sarcoma cells to measles vaccine virus-based oncolysis. *J Virol* **87**, 3484-3501 (2013).

168. Katze, M.G., DeCorato, D., Safer, B., Galabru, J. & Hovanessian, A.G. Adenovirus VAI RNA complexes with the 68 000 Mr protein kinase to regulate its autophosphorylation and activity. *EMBO J* **6**, 689-697 (1987).

169. Mundschau, L.J. & Faller, D.V. Oncogenic ras induces an inhibitor of double-stranded RNA-dependent eukaryotic initiation factor 2 alpha-kinase activation. *J Biol Chem* **267**, 23092-23098 (1992).

170. Coates, B.M., Staricha, K.L., Wiese, K.M. & Ridge, K.M. Influenza A Virus Infection, Innate Immunity, and Childhood. *JAMA Pediatr* **169**, 956-963 (2015).

171. García-Sastre, A., Egorov, A., Matassov, D., Brandt, S., Levy, D. E., Durbin, J. E., Palese, P. & Muster, T. Influenza A virus lacking the NS1 gene replicates in interferon-deficient systems. *Virology* **252**, 324-330 (1998).

172. Muster, T., Rajtarova, J., Sachet, M., Unger, H., Fleischhacker, R., Romirer, I., Grassauer, A., Url, A., García-Sastre, A., Wolff, K., Pehamberger, H. & Bergmann, M. Interferon resistance promotes oncolysis by influenza virus NS1-deletion mutants. *Int J Cancer* **110**, 15-21 (2004).

173. van Rikxoort, M., Michaelis, M., Wolschek, M., Muster, T., Egorov, A., Seipelt, J., Doerr, H. W. & Cinatl, J. Oncolytic effects of a novel influenza A virus expressing interleukin-15 from the NS reading frame. *PLoS One* **7**, e36506 (2012).

174. Mendez, I.I., Hermann, L.L., Hazelton, P.R. & Coombs, K.M. A comparative analysis of freon substitutes in the purification of reovirus and calicivirus. *J Virol Methods* **90**, 59-67 (2000).

175. Gong, J. & Mita, M.M. Activated ras signaling pathways and reovirus oncolysis: an update on the mechanism of preferential reovirus replication in cancer cells. *Front Oncol* **4**, 167 (2014).

176. Veckman, V., Osterlund, P., Fagerlund, R., Melén, K., Matikainen, S. & Julkunen, I. TNF-alpha and IFN-alpha enhance influenza-A-virus-induced chemokine gene expression in human A549 lung epithelial cells. *Virology* **345**, 96-104 (2006).

177. Buggele, W.A., Johnson, K.E. & Horvath, C.M. Influenza A virus infection of human respiratory cells induces primary microRNA expression. *J Biol Chem* **287**, 31027-31040 (2012).

178. Pauli, E.K., Schmolke, M., Wolff, T., Viemann, D., Roth, J., Bode, J. G. & Ludwig, S. Influenza A virus inhibits type I IFN signaling via NF-kappaB-dependent induction of SOCS-3 expression. *PLoS Pathog* **4**, e1000196 (2008).

179. Farrar, M.A. & Schreiber, R.D. The molecular cell biology of interferon-gamma and its receptor. *Annu Rev Immunol* **11**, 571-611 (1993).

180. Cooper, T., Biron, V. L., Fast, D., Tam, R., Carey, T., Shmulevitz, M. & Seikaly, H. Oncolytic activity of reovirus in HPV positive and negative head and neck squamous cell carcinoma. *J Otolaryngol Head Neck Surg* **44**, 8 (2015).

APPENDIX A: ADDITIONAL CYTOKINES DETECTED BY MULTIPLEX ELISA IN REOVIRUS INFECTED CULTURE MEDIA

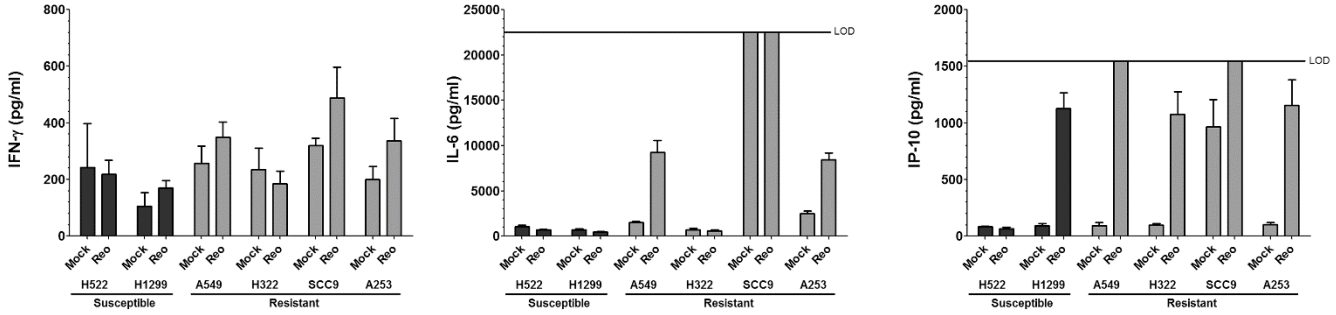

Appendix A. Additional cytokines quantified from reovirus infected cell media. Cell lines were infected with reovirus and culture media was collected 18 hpi for quantification of cytokine content by multiplex ELISA. Data are from 3 independent experiments, with samples tested in duplicate. Error bars represent SD; LOD stand for the limit of detection.